Context-Specific Ubiquitination of Ribosomes Regulates Translation Under Oxidative Stress

by

Shannon Elizabeth Dougherty

Department of Biology
Duke University

Defense Date: August 5, 2024

Approved:

Gustavo M. Silva, Advisor

Amy K. Schmid

Steven B. Haase

Jonathan C. Schisler

J. Will Thompson

Dissertation in partial fulfillment of the requirements for the degree of Doctor of Philosophy in
the Department of Biology in The Graduate School of
Duke University
2024

ABSTRACT

Context-Specific Ubiquitination of Ribosomes Regulates Translation Under Oxidative Stress

by

Shannon Elizabeth Dougherty

Department of Biology
Duke University

Defense Date: August 5, 2024

Approved:

Gustavo M. Silva, Advisor

Amy K. Schmid

Steven B. Haase

Jonathan C. Schisler

J. Will Thompson

An abstract of a dissertation submitted in partial fulfillment of the requirements for the degree of
Doctor of Philosophy in the Department of Biology in The Graduate School of
Duke University
2024

Abstract

Cellular exposure to oxidative stress is known to activate several translational control pathways through ribosome ubiquitination. Two such pathways, Redox-control of translation by ubiquitin (RTU) and Ribosome-associated protein quality control (RQC), modify the ribosome with K63-linked polyubiquitination but result in two different ribosome fates. The RTU responds to peroxide stress exposure by inducing a burst of ribosome polyubiquitination and subsequent pause of translation elongation. Alternatively, RQC leads to ubiquitination of already stalled ribosomes and mediates their clearance through subunit dissociation. Understanding how site-specific ribosome ubiquitination induces translational regulation is difficult due to the simultaneous occurrence of these distinct translational control pathways. Here, I develop a targeted proteomics approach to quantify site-specific ubiquitin modification across the ribosome in steady state and stress conditions. I found several sites to be differentially ubiquitinated due to stress, including sites known to be targeted by the RQC. Further results indicate that the RTU and RQC may target similar ribosome subpopulations within the cell but that they differentially contribute to the cellular stress response in an oxidative stressor-specific manner. These findings significantly contribute to the dissection of the complex coordination of translation in response to stress and shed light on the integration of important quality control pathways during the cellular stress response.

Dedication

This thesis is dedicated to my parents

Mr. and Mrs. Joseph and Sara Dougherty

Contents

Abstract ... iv

List of Tables ... x

List of Figures ... xi

Acknowledgments ... xiii

1. Introduction: ... 1

1.1 Review of Translation ... 5

1.1.1 Translation initiation ... 6

1.1.2 Translation elongation ... 8

1.1.3 Translation termination and ribosome recycling ... 10

1.2 Ubiquitin as a regulator of translation elongation ... 11

1.2.1 Ubiquitin (Ub)-modifications ... 12

1.2.2 Ubiquitinating enzyme cascade ... 14

1.2.3 Ubiquitin-mediated mechanisms of translation quality control (QC) ... 16

1.2.4 Ubiquitin-mediated mechanism of translation elongation regulation under oxidative stress ... 17

1.2.4.1 Site-specific K63 ubiquitination after peroxide stress ... 18

1.2.4.2 Structural impact of K63 ubiquitin on yeast translocating ribosomes under oxidative stress ... 19

1.3 Conclusion ... 21

2. Site-specific ubiquitinomics approach reveals the presence of ribosomal ubiquitin 'code' in hydrogen peroxide (H_2O_2) stress ... 23

2.1 Ubiquitinomics ... 24

2.1.1 Mass spectrometry-based proteomics ... 25

2.1.2 Mass-spectrometry identification of peptides derived from Ub-modified proteins ... 26

2.1.3 Ub-modified species enrichment ... 27

2.2 Site-Specific K63 Ubiquitinomics Provides Insights into Translation Regulation under Stress [141] ... 28

2.3 Design and optimization of Ribosome-target PRM (Rt-PRM) MS-based ubiquitinomics approach ... 30

2.3.1 Heavy peptide synthesis ... 30

2.3.2 Optimization of two-step enrichment of ribosomal K-GG peptides ... 31

2.4 Results ... 33

2.4.1 Implementation of Rt-PRM reveals 11 specific ribosome sites to be significantly ubiquitinated in response to hydrogen peroxide (H_2O_2) stress ... 33

2.4.2 Measurement of site-specific ribosome Ub reveals the two most abundant sites of modification are primarily dependent on the quality control ligase Hel2 in H_2O_2 stress ... 37

2.5 Methods ... 39

2.5.1 Heavy-labeled reference peptide synthesis and characterization ... 39

2.5.2 Yeast ribosomal peptide extraction and preparation ... 40

2.5.3 Targeted PRM Mass spectrometry analysis ... 41

2.5.4 Label Free Proteomics ... 41

2.5.5 Statistical Analysis ... 41

2.6 Conclusion ... 42

3. Examining the dynamics of ribosomal ubiquitination reveals that the ubiquitin 'code' is written by different E2-E3s in a stressor-specific manner ... 44

3.1 Ubiquitin-mediated translation quality control (QC) mechanisms ... 45

3.1.1 Ribosome-associated protein quality control (RQC) ... 46

3.1.2 No-go decay (NGD) ... 49

3.1.3 Non-functional rRNA decay (NRD) ... 50

3.1.4 Activation of quality control (QC) mechanisms under stress ... 51

3.2 Results ... 52

3.2.1 Investigation of Ub-modification dynamics reveals stressor-specific patterns of ribosomal protein ubiquitination 52

3.2.2 Measurement of RQC activity did not show evidence of increased RQC induction in oxidative stressors 58

3.2.3 The E2 conjugase, Rad6, antagonizes RQC pathway activity in steady-state conditions 61

3.3 Methods 63

3.3.1 Yeast growth conditions 63

3.3.2 Protein Extraction 64

3.3.3 Ribosome sucrose sedimentation 64

3.3.4 Western blot 65

3.3.5 Dual luciferase reporter 65

3.4 Conclusion 65

4. Stressor-specific contributions of the RTU and RQC pathways to the broader regulation of translation and the cellular stress response 67

4.1 Review of Integrated stress response (ISR) 68

4.1.1 Phosphorylation of eIF2α is the main driver of translation initiation inhibition and selective expression of stress response genes in the ISR 68

4.1.2 Regulation of Gcn2 by the RQC pathway 71

4.1.3 P-eIF2α-independent induction of Gcn4 translation in the absence of the RTU pathway 72

4.2 Results 73

4.2.1 Enzymes of the RQC and RTU pathways contribute to global translation regulation in an oxidative stressor-specific manner 73

4.2.2 The RQC and RTU pathways influence translational reprogramming in a stressor-specific manner 77

4.2.3 Stressor-specific contributions of the RQC and RTU to the ISR 81

4.3 Methods 85

4.3.1 Yeast strain generation, protein extraction, ribosome sucrose sedimentation, western blot........ 85

4.3.3 Translation rate assay........ 85

4.3.4 Gcn4 target mRNA-seq analysis........ 86

4.3.5 Gcn4-lacZ reporter assay........ 86

4.4 Conclusion........ 87

5. Conclusion........ 89

5.1 Summary of Findings........ 89

5.2 Future Directions........ 91

5.2.1 Elucidating the mechanistic details of how ribosomal K63 Ub pauses ribosomes in the RTU pathway........ 91

5.2.2 Dissecting the coordination of the RTU and RQC pathways and their contributions to the cellular response in oxidative stress conditions........ 92

5.3 Contributions to the field........ 93

Appendix........ 95

A.1 Supplemental Tables........ 95

A.2 Supplemental Figures........ 104

References........ 105

List of Tables

Table 1: Optimization of Rt-PRM biological K-GG peptide enrichment and MS quantification. 32

Table A1: Ribosome-target PRM (Rt-PRM) peptides and fold change (FC) of WT H_2O_2 Treated to Untreated........ 95

Table A2: *Saccharomyces cerevisiae* strains used in this study 100

Table A3: Plasmids used in this study 101

Table A4: Reagents........ 102

List of Figures

Figure 1: Structure of the 80S eukaryotic ribosome. 4

Figure 2: Diagram of translation initiation. 7

Figure 3: Diagram of translation elongation. 9

Figure 4: Diagram of translation termination and ribosome recycling. 11

Figure 5: Ubiquitin and linkages. 13

Figure 6: Ubiquitin Cascade. 15

Figure 7: Proposed mechanism of Redox control of translation by ubiquitin pathway (RTU). 18

Figure 8: K63 Ub ribosome trapped in pretranslocation stage of translation elongation. 20

Figure 9: Diagram of Liquid Chromatography coupled Tandem Mass Spectrometry. 26

Figure 10: K-GG remnant motif produced by trypsin digestion of Ub-modified proteins. 27

Figure 11: Ribosome-target Parallel Reaction Monitoring (Rt-PRM) detection of Ub linkages in H_2O_2 stress. 34

Figure 12: Ub-modified ribosome sites in H_2O_2 stress. 36

Figure 13: Hel2-indpendent Ub-modified ribosome sites in H_2O_2 stress. 38

Figure 14. Diagram of ubiquitin-mediated translation quality control (QC) pathways. 49

Figure 15: Ubiquitination of uS10 in stress conditions. 55

Figure 16: Dynamics of ribosome ubiquitination under stress conditions. 57

Figure 17: Recruitment of RQC factors to ribosome isolates. 58

Figure 18: Renilla-Firefly Luciferase RQC reporter. 60

Figure 19: GFP-X-FLAG-HIS3 RQC reporter in the absence of RTU enzymes. 62

Figure 20: GFP-X-FLAG-HIS3 RQC reporter upon expression of Rad6 mutants. 63

Figure 21: Diagram of Integrated stress response pathway (ISR). 70

Figure 22: Translation suppression in oxidative conditions. 75

Figure 23: Induction of the ISR in oxidative stressors. 80

Figure A1: uS5-3HA immunoblot. 104

Acknowledgments

First, I would like to thank my advisor, Dr. Gustavo Silva. His guidance, patience, and expertise have been invaluable throughout this process. His passion for research and dedication to diversity and inclusion in the field are inspiring. Thank you for giving me the space to grow as a scientist, an author, and as an individual.

To my committee: Dr. Amy Schmid, Dr. Steve Haase, Dr. Jonathan Schisler, and Dr. Will Thompson, your feedback has been instrumental in shaping this work, and I am so grateful for your time and support.

I would like to thank all of the present and past members of the Silva Lab. Each one of you has contributed to my growth as a researcher and as a person. To Dr. Nate Snyder, Dr. Andrew Gorman, Dr. Brian Gregory, and Vanessa Simões, thank you for your endless advice and support in my early years in the lab. To Dr. Ömür Kayikçi, Clara dos Santos, Blanche Cizubu, and Lana Harley, your support and kind words are very much appreciated. To Dr. Géssica Barros, your willingness to lend an ear, provide thoughtful advice and assistance has made the conclusion of this work possible. To Austin Maduka, your friendship throughout this journey has been a source of comfort and sanity.

My sincere thanks go to my collaborators, including Dr. Matthew Foster, Dr. Alberto Bartesaghi, Dr. Ye Zhou, Dr. Hyungwon Choi, and Dr. Guoshou Teo. Your contributions have been invaluable, and your patience in explaining computational and statistical analyses is deeply appreciated.

I am grateful for my undergraduate research advisor, Dr. Andrew VanDemark. His introduction to the field of oxidative stress and protein biochemistry sparked my curiosity and provided me with my first real research experience.

To my Biology cohort-mates, your friendship and support have made the ups and downs of grad school more bearable. Thank you.

To my friends, including Janani Perera, Kelly and Dylan Nessenson, Sarah Cummings, Matthew Russel, Andrew Becker, and Carson Miller, I am so grateful for you all. Thank you for always checking up on me, even when I forget to text.

Thank you to my parents for your unconditional love and unwavering support. You have always encouraged me to follow my dreams, and you are the reason I've accomplished so much. To my sister, thank you for always making me laugh.

Finally, to my partner Priyank, who has been my rock, my chief-of-staff, and my editor. I couldn't have completed this without you by my side. Thank you for believing in me even when I didn't believe in myself.

1. Introduction:

When we hear the word ‘stress,’ we often think of psychological stress, which denotes mental or emotional strain. Although this definition does not directly apply to cellular stress, it provides a fitting context to discuss and underscore the importance of the cellular stress response. Like psychological stress, cellular stress often arises due to external factors. However, rather than occurring in response to changing life circumstances, cellular stress occurs in response to environmental changes, such as fluctuations in temperature [1], nutrient availability [2, 3], or osmolarity [4, 5]. Both humans and cells must adapt to and mitigate sources of stress to ensure their safety and survival. Depending on the severity of the psychological stress, an individual may employ coping strategies such as meditation, seek professional help through therapy, or, in the most severe cases, seek inpatient care to alleviate their mental strain [6]. Similarly, cells have evolved a range of defense mechanisms to minimize the physical damage that arises from stress exposure. These mechanisms correspond to stress intensity and range from the expression of stress response genes in mild stress to programmed cell death in high-intensity stress [7, 8]. However, these innate defense responses are known to be dysregulated in disease states, including diabetes, Parkinson's, cardiovascular disease, and cancer [9, 10]. Just as successful treatment of psychological stress disorders has improved with increasing knowledge of intervention techniques [11, 12], understanding the innate mechanisms of the cellular stress response is crucial to identify opportunities and targets for medical intervention and mitigate the progression of associated disease states. Therefore, in this project, I sought to unravel the role and coordination of three regulatory mechanisms of protein expression that are vital for the innate cellular response to oxidative stress.

Oxidative stress is one of the most prevalent forms of cellular stress and arises from the accumulation of reactive oxygen species (ROS) within the cell [13]. ROS are free radicals that contain at least one oxygen atom and no less than one unpaired electron, making them highly reactive [14]. ROS, including hydrogen peroxide (H_2O_2), hydroxyl radicals (•OH), superoxide radicals ($O_2^{\bullet-}$), and singlet oxygen ($^1O_2$), are by-products of normal cellular metabolism [15]. In unstressed or steady-state conditions, ROS play an important role in cell signaling and homeostasis [16, 17] and are kept in check by antioxidants, compounds that can donate an electron to neutralize ROS in a process known as reduction [18, 19]. However, the dysregulation of cellular metabolism [20], as well as exposure to environmental factors such as UV radiation, pollution, pesticides, and toxic metals, is known to elevate ROS within the cell [21, 22]. When ROS is elevated beyond the cell's antioxidant capacity, the unstable species damage nucleic acids, proteins, and lipids [23-25].

Imbalance between ROS and antioxidants has major implications for human health and disease. For instance, oxidative damage of DNA is associated with the development of cancer [26], whereas oxidative damage of blood lipoproteins has been implicated in the progression of cardiovascular disease [24]. Furthermore, excessive ROS in neurons has been linked to neurological disorders, including Alzheimer's and Parkinson's [27]. Oxidative damage is theorized to be the main driver of human aging due to its implications in both disease and muscle deterioration [28, 29]. As oxidative damage is often irreversible [30], early and efficient intervention is crucial to mitigate the impairment of normal cellular function.

In addition to causing oxidative damage, excessive ROS induce several signaling pathways to reprogram gene expression and adapt to stress conditions [31-33]. In its simplest sense, gene expression is the process by which a gene encoded in the cell's DNA is transcribed into RNA and then translated into a protein [34]. Regulation of gene expression is crucial during oxidative stress, as cells must shut down this energetically costly process to allocate energy to survival [35-37]. At the same time, the expression of specific genes must be activated to address the excessive ROS and enable the cell to recover to homeostatic conditions [38, 39]. In recent decades, the study of gene expression regulation in response to stress has largely focused on changes in the expression of messenger RNA (mRNA) [40-43]. Much of this research has been conducted in baker's yeast (*Saccharomyces cerevisiae*) as many of the pathways important for the oxidative response are conserved between yeast and mammals [44, 45]. Studies of mRNA expression found that gene transcripts associated with translation and protein synthesis were repressed in oxidative stress [46], while those encoding antioxidant proteins are upregulated [47]. However, the temporal pattern of transcript expression in oxidative stress was found to be misaligned with changes in protein levels [34, 48]. This misalignment indicates the presence of further regulation of gene expression at the level of protein translation. Understanding how regulation of protein translation results in discrepancies between mRNA and protein levels is not only crucial to fully understand the innate cellular stress response but would offer new targets for therapeutic intervention to mitigate oxidative damage.

Regulation of translation, the process by which mRNA transcripts are decoded and used to produce functional proteins [49], is a growing field of study in both steady-state and stress conditions [50]. In response to oxidative stress, translation is globally suppressed to prevent damage to newly synthesized proteins, prevent toxic gain-of-functions, and minimize extraneous energy expenditure on non-essential proteins [10, 51, 52]. However, translation of stress-mitigating proteins must still occur to reduce cellular ROS and enable stress recovery [53, 54].

Achieving these opposing goals requires precise coordination of multiple regulatory mechanisms to ensure the proper proteins are expressed for the cell to adapt to and survive oxidative stress.

In this dissertation, I examine the role of three interconnected translation regulatory mechanisms that are crucial for the cellular response to specific oxidative stressors. This chapter begins with an overview of protein translation (Section 1.1) and an introduction to ubiquitin as a key regulator of translation (Section 1.2). In Section 1.2, I introduce two ubiquitin-mediated translation regulatory mechanisms: translational quality control (QC) (Section 1.2.3) and the Redox control of translation by ubiquitin (RTU) pathway (Section 1.2.4). Within Section 1.2.4, I emphasize the contributions of two key publications in delineating the mechanism of the RTU. The final part of this chapter (Section 1.3) summarizes the key findings and sets the stage for the experimental investigations detailed in the following chapters.

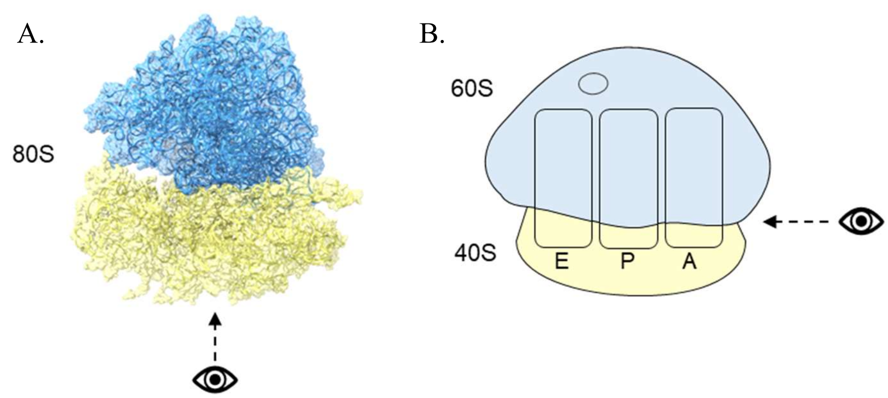

Figure 1: Structure of the 80S eukaryotic ribosome. A. 3D ribosome structure from side view (PDB 6XIR) [55, 56]. B. Model of the ribosome from front view featuring the 40S small ribosomal subunit, 60S large ribosomal subunit, and location of the aminoacyl site (A-site), peptidyl site (P-site), and tRNA exit site (E-site).

1.1 Review of Translation

To discuss the role of translation regulatory mechanisms in the cellular oxidative stress response, it is essential to first review the enzymes and stages of eukaryotic translation. In this section, I will discuss the key stages of translation, focusing on the structure of the ribosome and the translation factors that will be crucial for later discussion of the regulation of this process in oxidative stress.

Translation of mRNA into protein is facilitated by a large complex of RNA and proteins known as the ribosome (Fig 1A-B) [57, 58]. The eukaryotic *S. cerevisiae* ribosome (80S) is composed of two subunits: the small (40S) and large (60S) subunits (Fig 1B). The 40S contains the 18S ribosomal RNA (rRNA) and 33 ribosomal proteins (RPs), while the 60S contains the 25S, 5.8S, and 5S rRNA and 46 RPs [59, 60]. Translation occurs at the interface of these subunits, with the 40S responsible for reading the mRNA transcript 3-nucleotides (codon) at a time and the 60S catalyzing peptide bond formation [58]. Transfer RNAs (tRNAs) serve as an intermediary in this process, as they contain a complementary sequence (anti-codon) to the mRNA codon and carry the corresponding amino acid to the ribosome [61]. The ribosome contains three tRNA binding sites: the aminoacyl site (A-site), the peptidyl site (P-site), and the exit site (E-site) (Fig 1B) [62]. The A-site accepts the incoming aminoacyl-charged tRNA (aa-tRNA), the P-site holds the tRNA bound to the growing peptide chain, and the E-site releases the deacylated tRNA from the ribosome. Translation by the ribosome occurs in three stages: initiation, elongation, and termination (Figs 2-4) [57, 63-65], each providing unique opportunities for regulation in both steady-state and stress conditions.

1.1.1 Translation initiation

To begin translation, the 40S subunit associates with several eukaryotic initiation factors (eIFs) and a complex composed of the initiation factor eIF2, guanosine 5' triphosphate (GTP), and a methionine-charged tRNA (Met-tRNA$_i$) (Fig 2A) [63, 66]. This complex, known as the initiation ternary complex, binds to the tRNA P-site, and the methionine residue serves as the first amino acid in the newly synthesized (nascent) polypeptide chain (Fig 2A, C) [67, 68]. In canonical (cap-dependent) translation initiation, the small subunit is then recruited to eIF4-bound mRNA to form the 48S initiation complex (Fig 2B) [69]. The 48S then scans along the mRNA sequence in the 5' to 3' direction until encountering an AUG start codon, at which time binding of the 60S ribosomal subunit occurs, and initiation factors are released (Fig 2E) [68]. The assembled 80S ribosome is then ready to commence translation elongation.

As the rate-limiting step of translation, initiation is a prime target for regulation in response to cellular stress [66]. The most well-studied mechanism of translation initiation regulation is the Integrated stress response (ISR) (further discussed in Section 4.1) [70]. This mechanism is triggered by various cellular stresses including but not limited to, amino acid deprivation, , and oxidative stress [10]. The ISR functions to suppress initiation by disrupting the formation of the initiation ternary complex, while also promoting the expression of selective stress response proteins (further discussed in Section 4.1.1) (Fig 2A) [70]. While the ISR is an important translation regulator in response to cellular stress, it cannot regulate actively translating ribosomes. Thus, there is a growing focus on the regulation of translation elongation and its role in the cellular stress response.

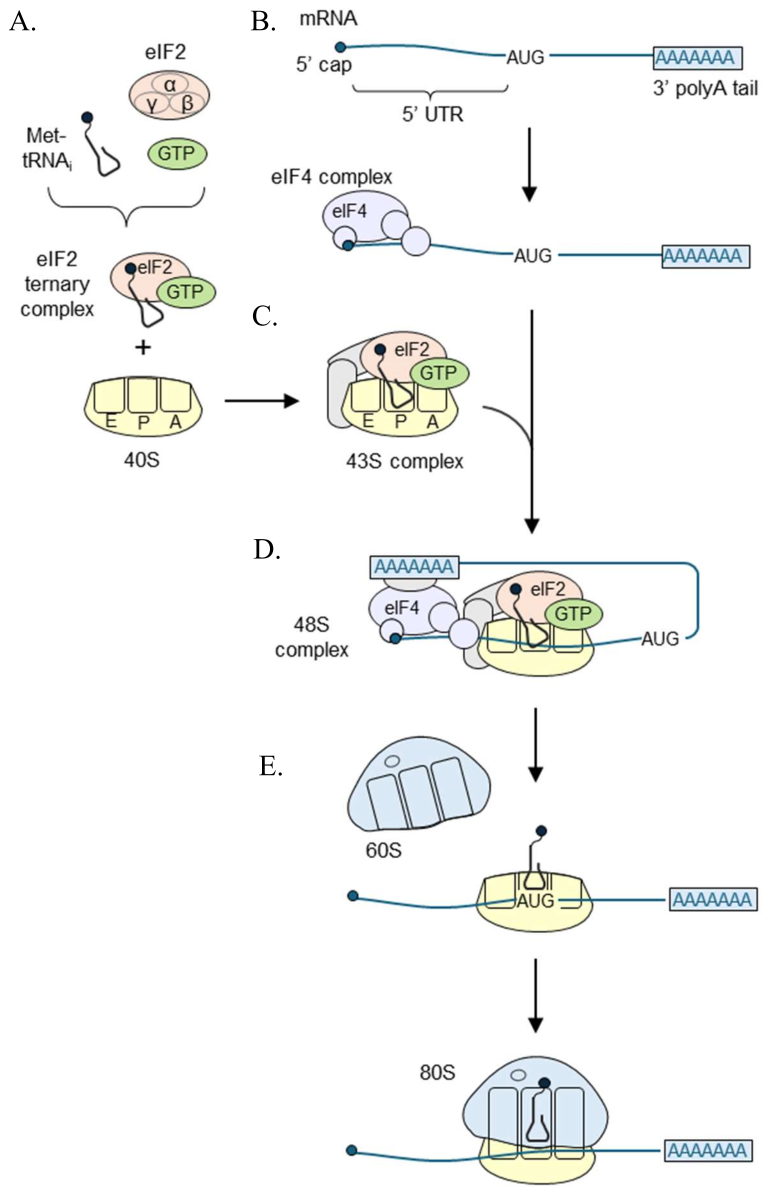

Figure 2: Diagram of translation initiation. A. Assembly of the initiation ternary complex composed of initiation factor eIF2, guanosine 5' triphosphate (GTP), and a methionine-charged tRNA (Met-tRNA$_i$). B. Binding of 5'cap mRNA by the eIF4 complex. C. Recruitment of ternary complex to 40S subunit to form the 43S complex. D. Recruitment of 43S complex to eIF4-bound mRNA to form 48S complex. E. 48S scans the mRNA for a start codon, at which time translation factors are released and the 60S subunit binds to small subunit. E. Complete assembly of the 80S ribosome.

1.1.2 Translation elongation

Translation elongation consists of a cycle of tRNA selection, peptide bond formation, and mRNA-tRNA complex translocation [57]. Following the assembly of the 80S ribosome, an aminoacyl-tRNA (aa-tRNA) with an anticodon corresponding to the next mRNA codon is delivered to the tRNA binding A-site (Fig 3A) [64]. The ribosome then catalyzes a peptide bond formation between the amino acid of the A-tRNA and that of the P-tRNA, transferring the peptide chain to the A-tRNA (Fig 3B-C) [58]. Concurrent with peptide bond formation, the 40S and 60S ribosomal subunits rotate with respect to one another, forcing the tRNAs into a hybrid position (Fig 3C) [71, 72]. In this position, the peptidyl acceptor end of the P- tRNA shifts to the E-site while the anticodon end remains in the P-site (P/E position), and the nascent peptide bond end of the A-tRNA shifts to the P-site while the anticodon remains in the A-site (A/P) position (Fig 3C)[56, 72]. This rotated ribosome conformation, known as the pretranslocation stage, immediately precedes the binding of the elongation factor eEF2 [72, 73]. eEF2 catalyzes the translocation of the mRNA-tRNA complex through the ribosome to the post-translocation conformation (Fig 3D) [73]. Finally, the deacetylated tRNA now occupying the E-site must be released from the ribosome. While the mechanisms underlying E-tRNA release are not well understood [74], several studies suggest that in *S.cerevisiae*, the elongation factor eEF3 promotes the release of deacylated E-tRNA through interactions with the ribosomal L1 stalk (Fig 3E) [75, 76], thus preparing the ribosome for another cycle of tRNA recruitment and peptide bond formation.

Control of translation elongation has been found to occur through several mechanisms, including the regulation of elongation factors, tRNA, and mRNA coding sequences [77]. These mechanisms are further bolstered by cellular stress with diminished availability of specific tRNAs, such as Trp, and inhibition of elongation factor eEF2 (Fig 3D) in stressed conditions [53, 78]. Disruption of proper mRNA decoding, tRNA recruitment, and elongation factor bindings can all lead to ribosome pausing and suspension of active translation elongation [79]. Additionally, post-translational modification of ribosomes by the small molecule ubiquitin has been implicated as both an inducer of ribosome pausing and a key signal for the clearance of ribosomes undergoing prolonged arrest in oxidative stress conditions [80, 81]. The role of ubiquitin in regulating translation elongation will be further detailed in the following section (Section 1.2).

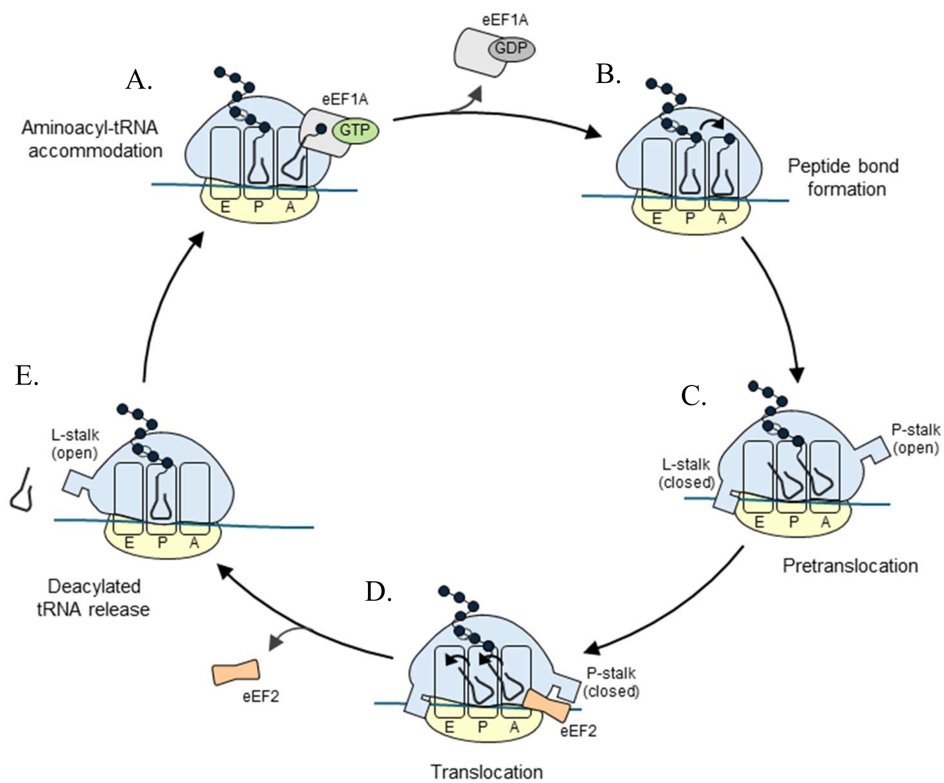

Figure 3: Diagram of translation elongation. A. Aminoacyl-tRNA is delivered to the empty A-site by elongation factor eEF1A. B. Peptide bond formation between amino acids of the A-tRNA and P-tRNA. C. With peptide bond formation, 40S and 60S subunits rotate and tRNAs occupy a hybrid A/P and P/E position. This orientation is known as the pretranslocation stage. D. the eEF2 elongation factor binds and promotes tRNA translocation. E. deacylated t-RNA is released from the E-site and a new round of elongation can occur.

1.1.3 Translation termination and ribosome recycling

The cycle of elongation continues until the ribosome encounters a stop codon, at which translational termination occurs [65, 82]. These codons, UAA, UAG, and UGA, are recognized by the eRF1 release factor, which promotes the release of the nascent polypeptide [83]. The 80S ribosome is then dissociated into its 40S and 60S subunits [65]. These subunits are recycled, and a new wave of translation can begin. A further understanding of translation termination is not required for this dissertation, but a more detailed discussion of this process and its control in cellular stress can be found in [65, 78, 82].

Each stage of translation provides unique targets for disruption and regulation of protein synthesis in response to stress [49, 64, 84]. As of now, several translation initiation regulatory mechanisms have been discovered, including disruption of eIF4 binding of mRNA by the mTOR signaling pathway (as reviewed in [66]), disruption of initiation ternary complex formation by the Integrated response pathway (ISR) (further discussed in Section 4.1) [70], and re-initiation events (further discussed in Section 4.1.3) [85-87]. Although initiation is the rate-limiting step of translation and a prime target for regulation [66], there is a growing focus on the regulation of translation elongation. The established mechanisms for the regulation of translation elongation include disruption of interactions between the ribosome and mRNA, tRNA, and elongation factors [53, 78]. Additionally, ubiquitin has emerged as another mechanism by which translation elongation is regulated in cellular stress [80]. In the following sections, I will introduce ubiquitin and two pathways of translation elongation regulation that employ ubiquitin in the cellular response to oxidative stress.

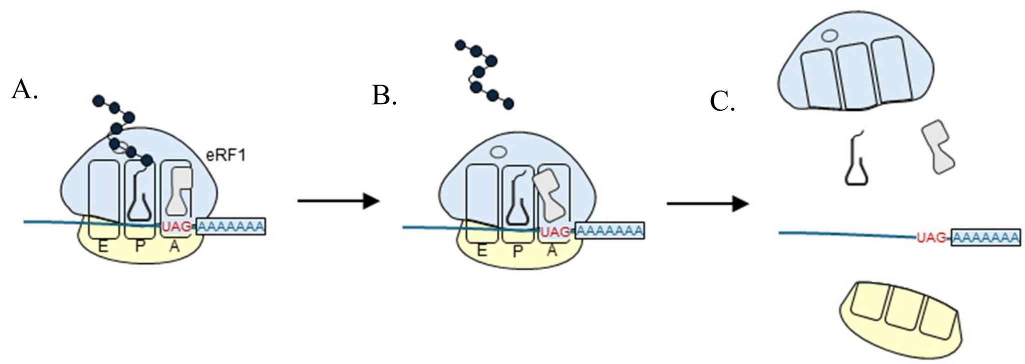

Figure 4: Diagram of translation termination and ribosome recycling. A. The ribosome encounters a stop codon and eRF1 release factor is recruited. B. eRF1 promotes the release of the nascent polypeptide. C. 80S ribosome dissociates into its subunits. These subunits are then recycled and available for new translation initiation.

1.2 Ubiquitin as a regulator of translation elongation

The ribosome is an ideal target for mechanisms of translation regulation as it mediates the interaction between mRNA, tRNA, and translation factors [58]. Post-translational modification of proteins (RPs) and rRNA that make up the ribosome provides a rapid and, in many instances, reversible way to modulate ribosome function [88]. Ubiquitin (Ub) is an evolutionarily conserved PTM that covalently attaches to the side chain of lysine (K) residues [89]. Ubiquitination of RPs is important for maintaining ribosome abundance throughout the cell, controlling both synthesis and degradation [80, 90, 91]. However, a growing body of literature has shown that ubiquitination of the ribosome is not only important for maintaining cellular ribosome levels but is also important for regulating ribosome function during translation[80, 92]. In this section, I will review the process of ubiquitination, highlight the role of ubiquitin in facilitating translational quality control (QC) mechanisms, and finally, discuss a ubiquitin-mediated mechanism of translational control that is distinct to oxidative stress conditions.

1.2.1 Ubiquitin (Ub)-modifications[1]

Ubiquitin is a small, 76 amino acid protein that forms an isopeptide bond with the ε-amino group (sidechain) of a lysine (K) residue or the N-terminus of a target protein (Fig 5A-B) [93]. The covalent attachment of a single ubiquitin is known as monoubiquitination (mono-Ub)(Fig 5C) [89]. Furthermore, ubiquitin itself can be modified at one of its 7 K residues or N-terminal methionine (M1) to create a polyubiquitin chain (Fig 5A-C) [94]. These different chain types, designated Ub linkages, dictate the signaling function of the modification [89, 95, 96]. Polyubiquitin linkages are classified into homotypic and heterotypic chains [97, 98]. Homotypic chains contain bonds at a single ubiquitin lysine position. In heterotypic chains, the bonds occur at several lysine positions and can be further distinguished as mixed or branched, the latter of which requires ubiquitination at more than two sites on a single ubiquitin molecule (Fig 5C) [97, 98]. These ubiquitin structures can be recognized and bound with linkage-specificity by 'readers,' proteins that contain tandem ubiquitin-binding domains [98]. These readers enable the cell to interpret the intricate ubiquitin code and perform diverse signaling functions, remarkably expanding upon the complexity encoded in eukaryotic genomes.

The possible functions of Ub-modification increase exponentially when the combinations of polyubiquitin linkages are considered. Homotypic chains, the more well-studied types of polyubiquitin chains, are designated by the K position through which the ubiquitin monomers are linked [99]. For example, K48-linked polyubiquitin chains (K48 Ub) are covalently attached through the 48 K residue of the preceding Ub molecule (Fig 5C) [100]. K48 Ub was quantified as the most abundant of the Ub linkages via mass spectrometry (MS)-based ubiquitinomics (further

---

[1] The text from this section was adapted from a review manuscript published in IJMS 80. Dougherty, S.E., et al., *Expanding Role of Ubiquitin in Translational Control.* Int J Mol Sci, 2020. **21**(3).. The included text was written by S.E.D. and revised for coherence and to include relevant updates.

discussed in Section 2.1)[101]. K48 Ub is known as the canonical signal for substrate degradation by the proteasome [99], a large protease complex responsible for breaking down proteins into smaller peptides [102]. This process, known as the ubiquitin-proteasome system (UPS) [103], plays a key role in the degradation of excess ribosomal proteins [104] and is known to be upregulated in response to oxidative stress to degrade damaged proteins [105].

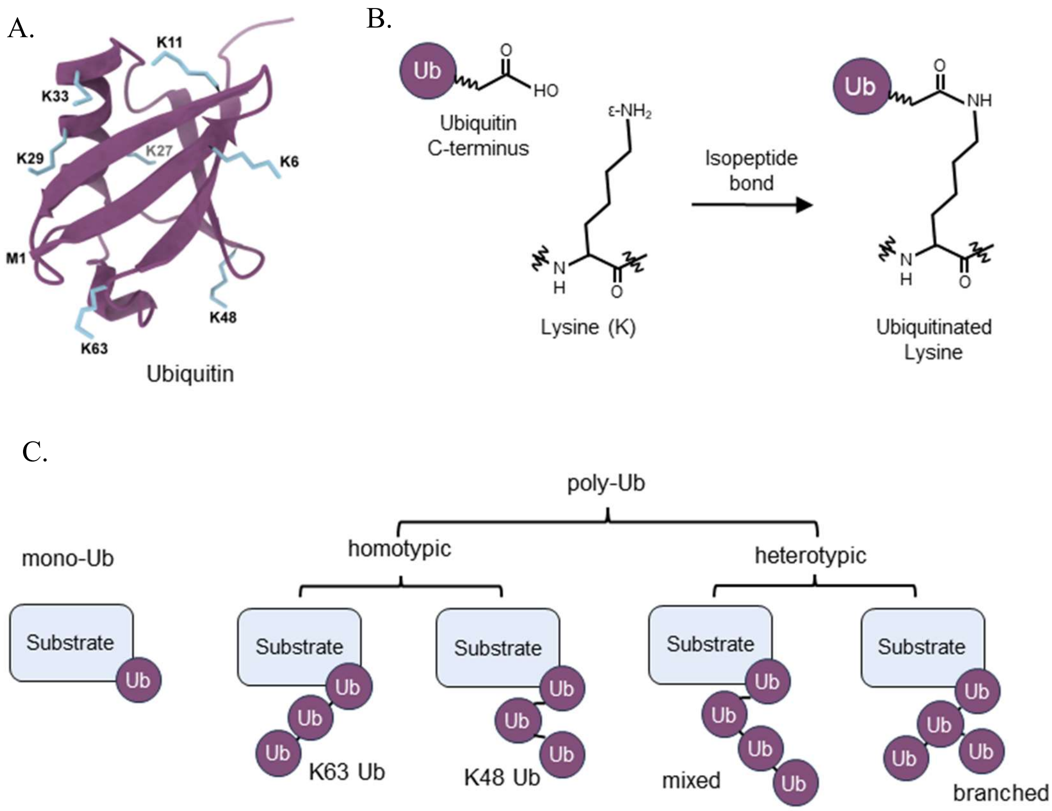

Figure 5: Ubiquitin and linkages. A. Structure of ubiquitin molecule and the position of its lysine (K) residues. B. Ubiquitination reaction in which the C-terminus of ubiquitin forms a covalent isopeptide bond with the amino group of the lysine (K) sidechain (ε-NH2). C. Common ubiquitin linkage types include mono ubiquitination (mono-Ub) and polyubiquitination (poly-Ub). Poly-Ub linkages can be broken down into homotypic and heterotypic chain types. Homotypic chains consist of ubiquitin monomers uniformly linked through a single lysine (K) position (i.e. K48 or K63). Alternatively, heterotypic chains contain links through multiple K residues. Heterotypic chains include mixed linkage types in which each ubiquitin monomer is modified at a single K residue and branched chains, in which a single ubiquitin molecule may be modified at multiple K residues [106].

K63-linked polyubiquitin (K63 Ub) (Fig 5C), another well-studied homotypic Ub linkage, is implicated in cellular signaling rather than UPS function [107]. K63 Ub has been quantified as the second most abundant cellular Ub linkage by MS [101] and is the only linkage that does not accumulate upon proteasome inhibition [108]. Rather, K63 Ub has been found to play a role in immune signaling [109], protein trafficking [110], and kinase activation [111]. While K63 Ub has been identified as a marker for autosomal degradation of ribosomes by the lysosome [104, 112], it is also known to regulate several aspects of translation itself, including quality control (highlighted in Section 1.2.3) [113, 114], and regulation in oxidative stress (highlighted in Section 1.2.4) [115, 116].

1.2.2 Ubiquitinating enzyme cascade[2]

The addition of ubiquitin chains to a target protein requires a cascade of increasingly specific enzymes, including an activating enzyme (E1), conjugating enzyme (E2), and a ligase (E3) (Fig 6). The ubiquitin activating enzyme (E1) binds free ubiquitin in an ATP-dependent reaction in the initial step of the enzyme cascade [80]. E1s are the least specific of the ubiquitinating enzymes, with only one enzyme encoded in yeast (UBA1) [117]. Following activation by an E1, ubiquitin is transferred to a ubiquitin conjugating enzyme (E2) (Fig 6) [118]. E2s are more diverse than E1s, with 11 enzymes found to be encoded in the yeast genome [119].

Despite the increased diversity of E2s, it is the distinct combination of E2-E3 pairs that recognize and ubiquitinate specific targets. Ubiquitin ligases (E3s) are the largest class of the ubiquitin enzyme cascade, numbering around 60–100 in yeast [119]. Although E2s are often responsible for Ub conjugation and defining linkage specificity, E3s recognize both the target and

---

[2] The text from this section was adapted from a review manuscript published in IJMS 80. Ibid.. The included text was written by S.E.D. and revised for coherence and to include relevant updates.

the E2 and catalyze the transfer of ubiquitin to the substrate (Fig 6) [120]. As an E2 can often pair with several E3s, distinct E2-E3 pairing is crucial for proper protein targeting and formation of specific ubiquitin chain types [121].

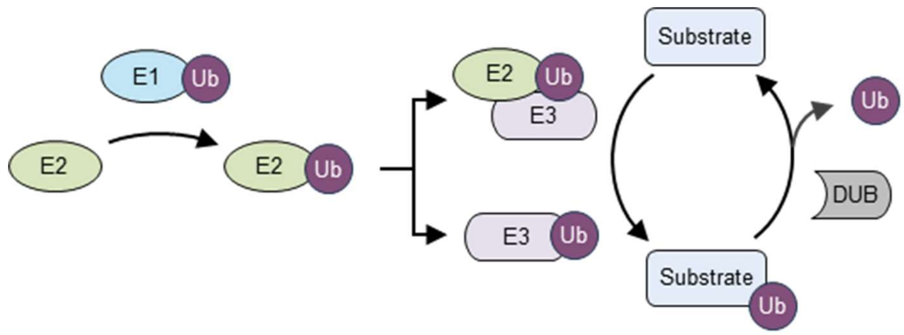

Figure 6: Ubiquitin Cascade. E1 ubiquitin activating enzyme transfers Ub to E2 ubiquitin conjugase. E3 ubiquitin ligase catalyzes the transfer of Ub to substrate by either bringing the E2 and substrate together or transferring Ub from the E2 to E3 and E3 to the substrate. Deubiquitinating enzymes (DUB) remove Ub from the substrate.

The last class in the ubiquitin enzymatic cascade is the deubiquitinating enzymes (DUBs). DUBs play a crucial role in maintaining global levels of protein ubiquitination through the removal of ubiquitin from the target or by breaking up polyubiquitin chains into free monomers (Fig 6) [122]. It is estimated that there are around 20 DUBs in yeast [123-125], which target specific proteins and ubiquitin chain types [126].

The E2–E3 pair and DUB create an antagonistic system that can strictly control the level of target ubiquitination. As such, the identities of the E2, E3, DUB, and Ub-linkage types are all pivotal for distinguishing the role of Ub-modification and the fate of the targeted protein [80, 98]. For the remainder of this section, I will highlight two processes of translation elongation control mediated by ubiquitination of the ribosome. While both processes use K63 Ub, they utilize different E2 and E3 enzymes to modify the ribosome in specific cellular contexts, leading to distinct ribosome fates.

1.2.3 Ubiquitin-mediated mechanisms of translation quality control (QC)

As the ribosome completes the cycles of translation elongation, it progresses across the mRNA transcript. This progression may be interrupted by a multitude of factors, including poly-basic amino acid encoding sequences, rare codon sequences, tRNA availability, and mRNA and rRNA integrity, leading to ribosome arrest [90, 127-130]. While a temporary arrest is not a problem, prolonged ribosome arrest may result in a collision by the following translating ribosome [131]. The collided ribosomes, also known as a disome, are recognized by quality control (QC) mechanisms, including Ribosome-associated protein quality control (RQC) (further reviewed in Section 3.1.1), No-go-decay (NGD)(further reviewed in Section 3.1.2), and Non-functional rRNA decay (NRD) (further reviewed in Section 3.1.3) [81, 114, 132]. In each of these pathways, the ubiquitin ligase Hel2 (ZNF598 in humans) mediates the K63 Ub of the ribosome [127, 133]. This K63 Ub occurs at specific ribosomal lysine residues (hereafter referenced as Ub-modified sites) and acts as a signal to recruit specific downstream factors responsible for dissociating the stalled ribosome, degrading problematic RNA and proteins, and recycling ribosome subunits [81, 90]. These ubiquitin-mediated mechanisms are active in steady-state conditions but have also been found to be upregulated in stress [134, 135]. Oxidatively damaged mRNA has been proposed to induce ribosome stalling, disome formation, and induce translation QC pathways [135, 136]. While the connection between oxidative stress and QC pathway induction remains unresolved, the RQC, NGD, and NRD are not the only pathways known to control translation through ubiquitination of the ribosome in stress.

1.2.4 Ubiquitin-mediated mechanism of translation elongation regulation under oxidative stress

It is well-established that there is an increase in global ubiquitination in response to oxidative stress [137]. K48 Ub, which is linked to the degradation of oxidatively damaged proteins by the ubiquitin-proteasome system (UPS) [138], is extensively upregulated in oxidative stress [105]. However, investigation of the other Ub linkages has revealed that K63 Ub also rapidly accumulates in response to oxidative stress in yeast [116]. This burst of K63 Ub was found to largely occur on ribosomes but was independent of the E3 Hel2 [116]. Rather, this ribosomal K63 Ub accumulation was found to be dependent on the E2-E3 pair Rad6 and Bre1 and antagonized by the deubiquitinase Ubp2 (Fig 7) [116, 139, 140], suggesting this ubiquitination was distinct from the translation QC mechanisms discussed in Section 1.2.3. This mechanism, dubbed the Redox control of translation by ubiquitin (RTU) [80], was further identified to be specific to peroxide stress [116]. The current model of RTU activation suggests that cellular exposure to peroxide inactivates Ubp2, enabling the accumulation of ribosome ubiquitination and stabilization of the 80S ribosome (Fig 7) [116, 140]. However, the role of ribosomal K63 Ub-modification in regulating translation and conferring resistance to oxidative stress [116] remained unknown.

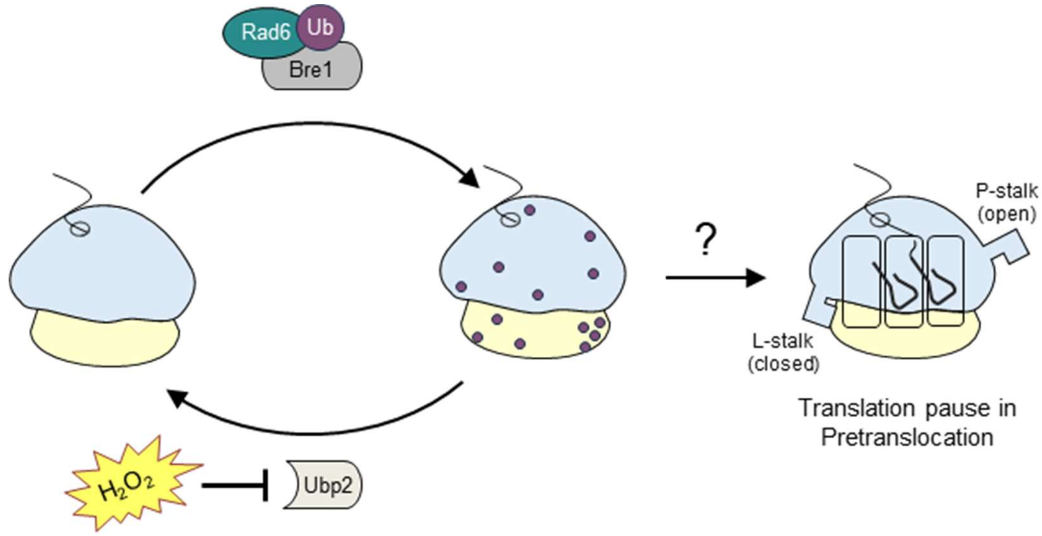

Figure 7: Proposed mechanism of Redox control of translation by ubiquitin pathway (RTU). The ribosome is modified with K63 Ub by the E2-E3 pair Rad6-Bre1, and deubiquitinated by the DUB, Ubp2. In peroxide stress, Ubp2 is inhibited, enabling the accumulation of K63 Ub on the ribosome. K63 Ub ribosomes are trapped in the pretranslocation stage of elongation in peroxide stress through an unknown mechanism.

1.2.4.1 Site-specific K63 ubiquitination after peroxide stress

In an effort to elucidate the role of ribosomal K63 Ub in regulating translation in oxidative stress, the Silva lab sought to identify the precise sites of K63 Ub-modification in peroxide stress [141]. Using a novel mass spectrometry (MS)-based technique involving a sequential enrichment strategy for K63 Ub (further discussed in Section 2.2), they identified ~1100 K63 Ub-modified lysine residues across the proteome after exposure to hydrogen peroxide (H_2O_2) [141]. Among these sites, 78 were mapped to 37 RPs [141], affirming previous findings that the ribosome is a target of K63 Ub in oxidative stress [116]. However, identification of these Ub-modified sites was done in comparison to a *K63R* strain also exposed to H_2O_2 [116]. In *K63R*, K63 of ubiquitin is mutated to arginine (R), thus hindering the formation of K63 Ub chains [142]. As such, it is difficult to distinguish which of the identified sites are modified by K63 Ub in response to H_2O_2 exposure from those that are modified independently of peroxide stress. Furthermore, it remains unknown which of the 78 ribosomal sites are targets of the RTU pathway, as several of these sites are also known targets of translational QC mechanisms [80, 114].

1.2.4.2 Structural impact of K63 ubiquitin on yeast translocating ribosomes under oxidative stress

This work is adapted from a manuscript published in PNAS [56]. Gustavo M. Silva designed the project, supervised experimental and structural work, and wrote the manuscript. Shannon E. Dougherty prepared control samples and contributed to the interpretation of structural results.

As the ribosome was identified as a target of K63 Ub-modification in peroxide stress, we hypothesized that this ubiquitination served to regulate translation in oxidative stress. To investigate the impact of K63 Ub on translation, we utilized single-particle cryo-electron microscopy (cryo-EM) to determine its impact on ribosome structure [56]. In cryo-EM, images of individual macromolecules, such as the ribosome, are computationally combined to generate high-resolution reconstructions of the molecular 3D structure [143]. Our study determined the structure of K63 Ub-modified ribosomes in comparison to ribosomes isolated from the *K63R* strain upon H_2O_2 exposure [56, 116, 144]. This analysis revealed K63 Ub-modified ribosomes to be trapped in the pretranslocation stage of elongation (Fig 3C, 8A), the stage preceding elongation factor eEF2 binding (Fig 3D) [56, 145]. This trapped configuration was not observed for ribosomes isolated from the *K63R* strain [56], indicating that it was a result of ribosome modification with K63-linked ubiquitin.

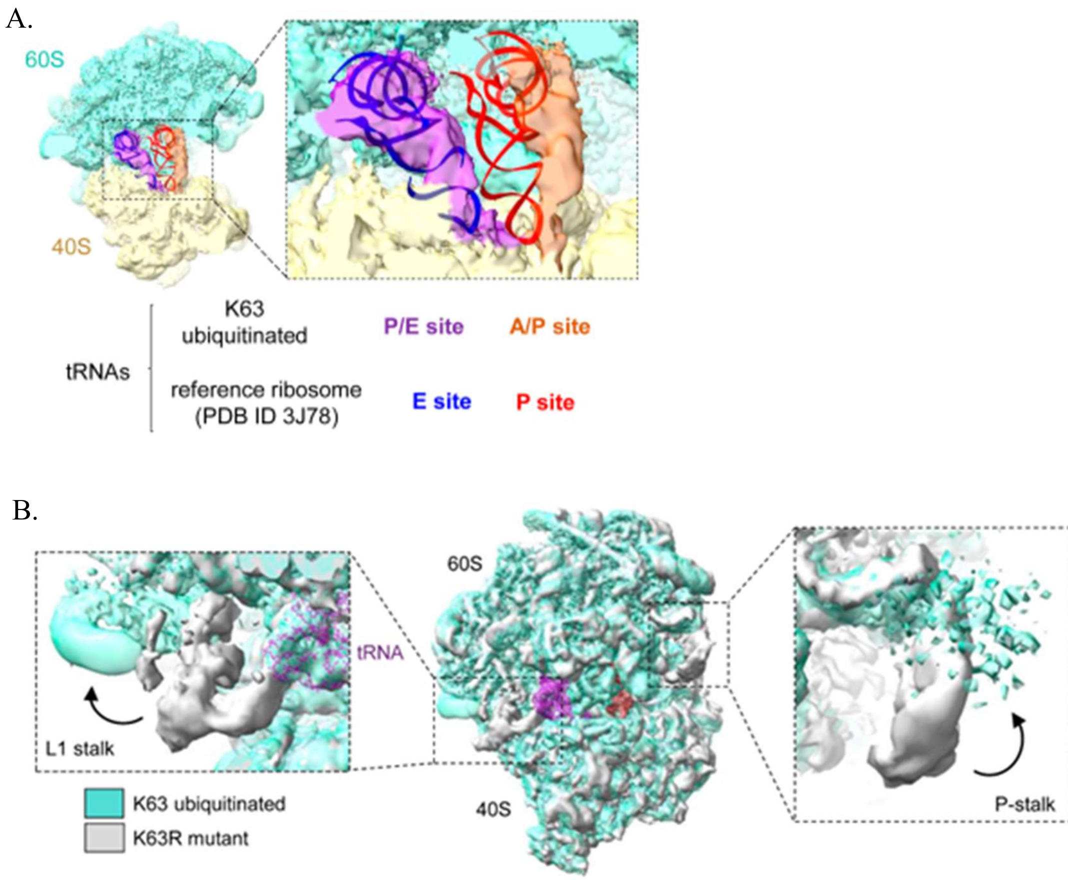

Figure 8: K63 Ub ribosome trapped in pretranslocation stage of translation elongation. Figures from [56] and not generated by S.E.D. A. Structure of trapped K63 Ub ribosomes in the pretranslocation stage with tRNAs occupying a P/E and A/P hybrid position. B. Structure of K63 Ub trapped ribosomes compared to *K63R* mutant. Insets highlight open conformation of L1 stalk and disordered P-stalk in K63 Ub ribosomes.

In the pretranslocation structure, the ribosome was found to occupy a rotated orientation, with 2 tRNAs occupying the A/P and P/E hybrid binding sites (Fig 8A) (see Section 1.1.2 for a more detailed explanation). Among these ribosomes, 3 subclasses were identified, 2 of which adopted a structure with an open L1 stalk (Fig 8B) [56]. The ribosomal L1 stalk is a structure known to interact with and facilitate the release of deacylated tRNA from the ribosome [146, 147], suggesting that K63 Ub may disrupt the release of tRNA from the E-site. Furthermore, the proteins comprising a structure known as the ribosomal P stalk (Fig 8B) were found to be highly flexible, suggesting K63 Ub may also disrupt this region of the ribosome and inhibit eEF2 binding (Fig 3C-D) [56, 148, 149].

From this work, it is evident that peroxide-induced K63 Ub-modification of the ribosome functions to trap ribosomes in a pretranslocation orientation, thereby pausing translation elongation. While this structural analysis highlighted several regions that are disrupted in K63 Ub-modified ribosomes, how K63 Ub induces these structural changes and prevents ribosome translocation remains undefined. Furthermore, whether the structural changes are a direct effect of K63 Ub accumulation or an indirect effect arising from altered ribosome orientation or interactions with translation factors remains undetermined.

1.3 Conclusion

In this introductory chapter, I have highlighted the importance of translational regulation in response to oxidative stress, discussed ubiquitin as a post-translational modification, and discussed two K63 Ub-mediated mechanisms of translational control that are thought to be induced in oxidative stress conditions. The remainder of this dissertation is dedicated to decoding the complex pattern of ribosome ubiquitination in oxidative stress and its ramifications for the broader cellular stress response. In Chapter 2, I employ a novel mass spectrometry (MS)-based approach to identify and quantify ribosomal ubiquitination at 11 specific sites in response to H_2O_2 exposure. In Chapter 3, I establish the stressor-specific contributions of the RTU and QC pathways in writing the ribosomal ubiquitin ‘code’. In Chapter 4, I investigate the stressor-specific contributions of both the RTU and QC pathways to the broader regulation of translation and the cellular stress response. Finally, Chapter 5 contains a summary of the key findings from this investigation of three interconnected translation regulatory mechanisms and discusses their relevance in the broader context of ubiquitinomics and stress-induced regulation of translation. This dissertation, therefore, offers valuable insights into the intricate role of context-specific ribosome ubiquitination in the regulation of translation under oxidative stress conditions.

2. Site-specific ubiquitinomics approach reveals the presence of ribosomal ubiquitin 'code' in hydrogen peroxide (H_2O_2) stress

Chapter 2 is modified from a manuscript in preparation for publication. The pre-print version is available on BioRxiv [150]. The authors are Shannon E. Dougherty, Géssica C. Barros, Matthew W. Foster, Guoshou Teo, Hyungwon Choi, and Gustavo M. Silva. S.E.D. devised the project, completed sample preparation, and wrote the manuscript under the supervision of G.M.S. S.E.D. All mass spectrometry analysis was completed at the Duke Proteomics and Metabolomics Core Facility by M.W.F. G.T. and H.C. assisted with computational data analysis.

Early studies characterizing ubiquitin (Ub) were dependent on biochemical approaches [151-153] and had identified a small number of modified targets, such as cell cycle and transcriptional regulators [154, 155]. However, these biochemical approaches were limited in throughput, and thus, new methods to identify ubiquitinated substrates on a large scale were required [154]. In 2003, Peng et al. utilized a mass spectrometry (MS)-based approach to detect 110 precise sites of protein ubiquitination across the yeast proteome, thereby establishing MS as a leading technique for detecting and quantifying protein ubiquitination [101]. Since then, the utilization of MS-based approaches for the study of ubiquitination, known as ubiquitinomics, has continued to evolve and advance [156, 157].

MS-based ubiquitinomics analysis has led to the determination of over 1,100 sites of K63 ubiquitination in peroxide stress, including 78 ribosomal sites [141]. However, whether Ub-modification of these sites is induced by peroxide stress, and whether they function in the regulation of translation by the RTU remains unclear. In this chapter, I develop and optimize a novel targeted MS-based proteomics technique to quantify site-specific Ub-modification of the ribosome in response to peroxide stress. This is an essential first step to determine the arrangement, or ‘code’, of ribosome ubiquitination that functions to pause elongating ribosomes [56]. In the following sections, I will introduce the field of MS-based ubiquitinomics (Section 2.1) and discuss the identification of 78 Ub-modified ribosome sites in peroxide stress (Section 2.2). In Section 2.3, I will describe the development and optimization of a novel targeted MS-based ubiquitinomics approach to quantify site-specific ribosome ubiquitination. This targeted approach was employed to detect and quantify site-specific ubiquitination induced by peroxide stress, the results of which are discussed in Section 2.4. Section 2.5 includes a detailed description of the methods used in this chapter’s analysis, and Section 2.6 contains concluding remarks.

2.1 Ubiquitinomics

Mass spectrometry (MS) is an analytical technique that separates and measures ions based on their mass-to-charge ratio (m/z) [158, 159]. Originally used to measure mass on an atomic scale [160], through advancements in instrumentation, including the coupling of multiple mass spectrometers [161-163], MS has evolved as a leading method for protein identification and quantification (proteomics). As ubiquitin is covalently attached to its substrate protein, the specific location of Ub-modified lysine (K) residues (hereafter referenced as Ub-modified sites) can be detected, and their occurrence quantified by MS-based proteomics [101, 164]. However, the detection of Ub-modified substrates by MS, a methodology dubbed ubiquitinomics, remained limited due to the low stoichiometric ratio of ubiquitinated to non-ubiquitinated substrates [156].

In this section, I will review the basics of MS-based proteomics (2.1.1), highlight how Ub-modified sites are identified by MS (2.1.2), and finally, discuss methods of ubiquitinated substrate enrichment required for the detection of the stoichiometrically low modification (2.1.3). These foundations are important to discuss the identification of 78 ribosomal Ub-modified sites

[141] and the development of a novel targeted MS-based ubiquitinomics approach needed to decipher the code of ribosomal Ub-modification in peroxide stress.

2.1.1 Mass spectrometry-based proteomics

The most prominent approach for MS-based proteomics, known as “bottom-up” proteomics, requires the breakdown of proteins into smaller peptides that can be readily detected and measured by mass spectrometry [165]. To accomplish this, proteins are enzymatically digested with trypsin protease to produce short peptide segments that fall within the ideal mass range for MS analysis [166, 167]. These peptides are then separated by liquid chromatography (LC) based on their hydrophobicity [168]. The LC columns contain long carbon chains (C18) that create a hydrophobic environment ideal for binding peptides [169]. Once peptides are loaded onto the LC column, a liquid gradient with increasing hydrophobicity, such as increasing concentrations of acetonitrile (ACN), is added to the column [170]. As such, peptides remain bound to the column for a distinct and predictable amount of time, known as peptide retention time (RT) [171], before eluting off the column (Fig 9).

As peptides elute from the LC column, they are aerosolized and ionized [172]. These ionized peptides, known as precursors, are then directed into the first mass analyzer (MS1), which separates and selects precursors based on their mass-to-charge ratio (m/z) [173, 174]. Selected precursors are then directed to a collision chamber in which they are fragmented into product ions [171]. These product ions often derive from a single peptide bond break within the precursor. The product ions are then directed to a second mass analyzer (MS2), in which their abundance is measured to generate a mass spectrum [158, 171]. The mass difference between these ions can be compared to the known mass of amino acids to determine the sequence of the original peptide [175].

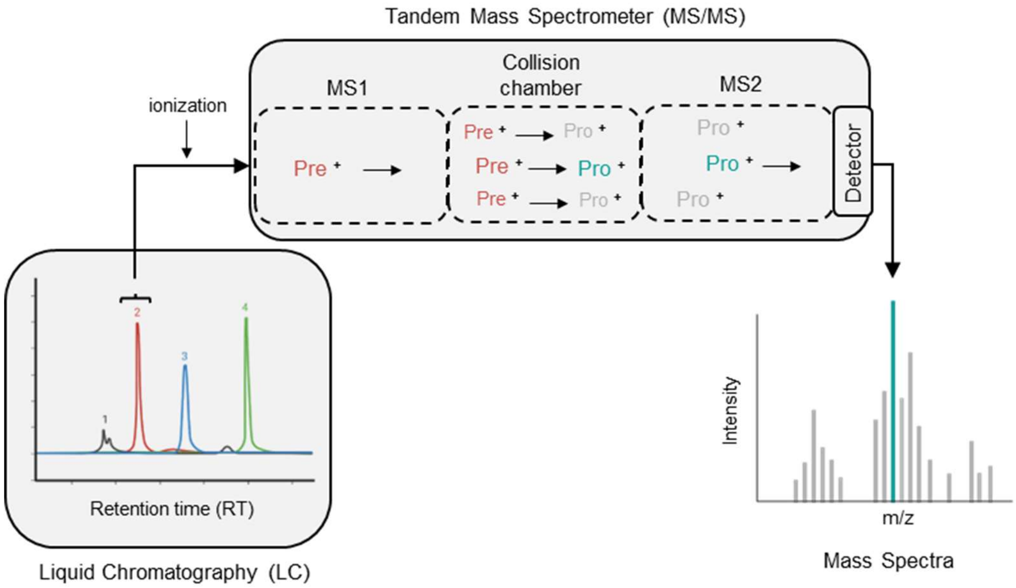

Figure 9: Diagram of Liquid Chromatography coupled Tandem Mass Spectrometry.

2.1.2 Mass-spectrometry identification of peptides derived from Ub-modified proteins

Identification of Ub-modified proteins via MS does not differ from the previously outlined method and is dependent upon the unique nature of the peptide derived from trypsin digestion of the modified protein [156]. Trypsin typically cleaves at the C-terminus of arginine (R) and lysine (K) residues; however, it is unable to cleave after a Ub-modified lysine (K) [164]. Furthermore, the covalently bonded Ub is a target for trypsin digestion, resulting in a di-glycine (GG) signature, which remains attached to the modified K residue (Fig 10) [164, 176]. These di-Gly remnant (K-GG) peptides contain both a missed trypsin cleavage and a mass shift of 114.1 Da (GG) [101]. The increased length from the missed cleavage alters the peptide's hydrophobicity, thus enabling the K-GG peptide to be separated from its non-modified counterpart during liquid chromatography (LC) [177]. Furthermore, the increased mass from both the missed cleavage and additional GG remnant alters the mass-to-charge ratio (m/z) of the K-GG peptide, allowing the modified peptide to be separated in MS1 [101, 177]. Finally, the difference between the ions in the mass spectrum generated from MS2 measurements can be used to determine the precise site of ubiquitination, as the mass difference between the sequential ions will be equivalent to that of a K residue with an additional mass of 114.1 Da (GG).

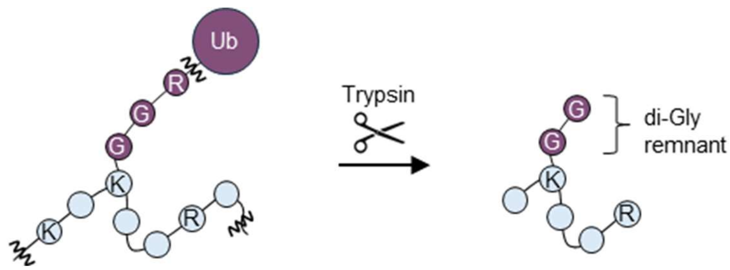

Figure 10: K-GG remnant motif produced by trypsin digestion of Ub-modified proteins.

It is evident that peptides derived from Ub-modified proteins can be distinguished from their non-modified counterparts, but whether K-GG peptides are detected is dependent on their abundance. While mass spectrometers are increasing in sensitivity [178], the ion chambers within the instrument have limits [174]. As Ub-modified proteins are stoichiometrically low, non-modified peptides will outnumber those containing a K-GG remnant and thus obstruct their detection [156, 164]. Therefore, the enrichment of Ub-modified substrates is crucial for the detection and quantification of the K-GG peptides via MS.

2.1.3 Ub-modified species enrichment

As Ub-modified proteins are stoichiometrically low, an additional step to enrich these species has proven crucial to improve MS-based detection and quantification [157, 164]. There are several methods of Ub-modified protein enrichment, including affinity enrichment of His-tagged ubiquitin and enrichment with Ub and linkage-specific antibodies [156]. Alternatively, tandem ubiquitin binding entities (TUBEs) contain several ubiquitin-binding domains and are more selective than linkage-specific antibodies [179]. While these enrichment methods have improved the identification of ubiquitinated protein targets, their application in determining the specific sites of Ub-modification is limited [157].

Upon trypsin digestion of Ub-modified proteins, most of the peptides are non-modified, which may hinder MS-detection of the K-GG peptide. To overcome this limitation, peptide-centric methods of enrichment, such as the PTMScan Motif antibody (Cell Signaling), have evolved to isolate only those peptides that contain a K-GG [156, 164]. Thus, interference from non-modified peptides is minimized while the resolution of site-specific modifications improves. While protein-centric Ub enrichment methods have successfully been used to identify 100s of Ub-modified sites across the yeast genome [157], sites identified following K-GG peptide enrichment methods number in the 1000s [164, 177]. However, K-GG enrichment occurs after protein digestion, and therefore, the knowledge of the Ub linkage associated with Ub-modified sites is lost.

2.2 Site-Specific K63 Ubiquitinomics Provides Insights into Translation Regulation under Stress [141]

While K63 Ub was found to accumulate on the ribosome in peroxide stress [116], how this modification regulated translation remained unknown. To determine the role of K63 Ub, the Silva lab first sought to determine the precise sites of ribosomal ubiquitination [141]. As structural studies of the ribosome have revealed much about the mechanisms underlying translation [60], mapping the precise sites of Ub modification provides crucial insights into how K63 Ub regulates this process. MS-based ubiquitinomics was deemed an ideal method to identify the K63 Ub-modified sites as it is both sensitive and high-throughput [157]. As discussed in Section 1.2.4.1, the Silva lab developed a new mass spectrometry (MS) methodology to determine the specific sites of K63 Ub [141]. To maintain knowledge of the Ub linkage identity while also benefiting from the increased sensitivity of peptide-centric enrichment methods, the Silva lab developed a sequential K63 Ub enrichment strategy. K63 Ub-modified proteins were first isolated with K63 TUBE and then enriched with a K-GG-specific antibody following digestion [141]. These enriched samples were then analyzed by MS using a data-dependent approach (DDA) in which the most abundant precursors detected by MS1 are selected for fragmentation and further analysis by MS2 [180].

MS analysis of these enriched samples revealed 78 Ub-modified sites across 37 ribosomal proteins after exposure to hydrogen peroxide (H_2O_2)[141]. Over half of these sites are localized to the head of the 40S ribosome, an important region for translational regulation [58, 181]. The presence of ubiquitin sites on the surface of the 40S head may disrupt the binding of translational regulators such as initiation and elongation factors, as well as mRNA and tRNA molecules [182], thus providing potential mechanisms for regulation of translation. However, as these 78 ribosomal sites were identified in comparison to those enriched from a *K63R* strain incapable of forming K63-linked polyubiquitin chains [142], whether modification of these sites occurred in a stress-responsive manner is unclear. Furthermore, the untargeted MS approach employed was not sensitive enough to quantify the abundance of site-specific ubiquitination due to the low stoichiometric ratio of modified to unmodified species. While the work from this study was crucial for mapping the potential sites of K63 Ub modification, it remained unclear which sites are targets of the RTU pathway.

2.3 Design and optimization of Ribosome-target PRM (Rt-PRM)[3] MS-based ubiquitinomics approach

To understand the role of K63 Ub in regulating translation elongation in the RTU pathway, it it was crucial to delineate those ribosomal sites that were ubiquitinated in response to H_2O_2 stress and quantify the extent of their modification. As ribosome structure and configuration is so critical for progression through the steps of translation elongation (Fig 3) [58], determining those sites that are ubiquitinated in response to H_2O_2 would provide key insights into how these modifications trap ribosomes in the pretranslocation orientation (Figs 7-8)[56] and disrupt normal function. As an untargeted MS approach was not sensitive enough for absolute quantification of site-specific Ub-modification [141], I utilized the previously mapped 78 sites to develop a targeted MS-based approach using Parallel Reaction Monitoring MS (PRM). PRM overcomes the bias toward the most abundant peptides seen in untargeted approaches, such as DDA, as the m/z window of MS1 is pre-specified to match the desired peptide [183]. As a result, PRM minimizes interference from non-targets and has increased sensitivity toward targeted peptides [184]. This targeted MS approach has already been successfully employed to quantify PARKIN-dependent ubiquitination in human cell lines [185], highlighting its utility in ubiquitinomics. Therefore, I developed a two-step protocol for the enrichment of ribosomal K-GG peptides and targeted MS approach dubbed Ribosome-target PRM (Rt-PRM).

2.3.1 Heavy peptide synthesis

Implementation of PRM requires knowledge of the retention time (RT) and the m/z ratio of desired peptides to properly schedule MS1 filtering [186]. Therefore, to employ PRM to

[3] All mass spectrometry analysis was completed at the Duke Proteomics and Metabolomics Core Facility by M.W.F.

measure site-specific ubiquitination of the ribosome, we first had to determine the RT and m/z ratios of peptides corresponding to the previously identified 78 Ub-modified sites [141]. To do so, G.M.S. and I designed a set of 103 heavy-labeled (C-terminal Lysine ($^{13}C_6$,$^{15}N_2$) or Arginine($^{13}C_6$,$^{15}N_4$)) reference K-GG peptides corresponding to those arising from trypsin digestion of the 78 Ub-modified sites (Table A1). This heavy peptide pool also included reference peptides corresponding to each possible Ub linkage (Table A1). Of the 103 peptides, 78 were successfully detected via data-dependent acquisition (DDA) mass spectrometry by M.W.F. and were used to build a spectral library in Skyline software [187] to schedule PRM m/z filtering and target the biologically derived peptides (Table A1).

2.3.2 Optimization of two-step enrichment of ribosomal K-GG peptides

In addition to designing the pool of heavy reference peptides, I had to develop and optimize a method for enriching ribosomal K-GG peptides (as discussed in Sections 2.1.2- 2.1.3). In my first attempt, I employed the PTMScan Motif antibody (Cell Signaling) to enrich K-GG peptides from trypsin digestion of whole cell lysate. I also spiked in the heavy peptide pool at a concentration of 10 fmol per peptide post-K-GG enrichment to serve as a guide for PRM scheduling and as an internal standard for the absolute quantification of biological peptide abundance. However, this preliminary attempt only yielded the detection of 15 of the 78 target peptides (Table 1, Stage 1), likely due to interference from non-ribosomal K-GG peptides.

Table 1: Optimization of Rt-PRM biological K-GG peptide enrichment and MS quantification.

Optimization stage	Yeast culture size (mL)	First enrichment step	Heavy peptide (fmol/peptide)	Pre or post K-GG spike	K-GG enrichment incubation	Biological peptides quantified (out of 78)
1	250	Cell lysate	10	post	Agarose	15
2	500	Ribosome isolation	10	pre	Agarose	46
3	500	Ribosome isolation	10	pre	Agarose	55 detected
4	500	Ribosome isolation	1 (new pool)	pre	Agarose	63
5	500	Ribosome isolation	1 (new pool)	pre	Magnetic	68

To reduce this interference, I added a ribosome enrichment step preceding K-GG enrichment. The initial cell culture volume was doubled to account for the loss of material expected upon sucrose sedimentation of the ribosomes from the cell lysate. Additionally, the heavy reference peptide spike was completed prior to K-GG enrichment to account for the bias of the PTMScan antibody. The addition of the ribosome isolation step increased the detection of biological peptides to number 46 out of 78 (Table 1, Stage 2), indicating that a sequential enrichment would be necessary to quantify ribosome Ub-modification at the site-specific level. While replication of this sequential enrichment continued to yield similar detection of biological peptides (Table 1, Stage 3), the detection of heavy reference peptides decreased. Troubleshooting the diminishing heavy peptide signal led to the discovery that the synthetic peptides had degraded over the course of several years.

After reordering the synthetic heavy peptides and generating a new heavy peptide pool, I repeated the sequential ubiquitination. I reduced the heavy peptide spike to 1 fmol per peptide to more closely match the concentration range expected for the biological peptides. In the presence of the new heavy peptide pool, 63 of the 78 peptides were successfully detected and quantified (Table 1, Stage 4). However, there appeared to be a significant variance in the intensity of heavy peptides between replicates, which was hypothesized to arise due to variation in the K-GG antibody enrichment step. A switch from protein A agarose bead conjugated antibody (#5562) to magnetic bead conjugated antibody (#59322) allowed for more consistent immunoaffinity purification and resulted in reproducible detection and quantification of 68 of the 78 targeted peptides (Table 1, Stage 5).

2.4 Results

2.4.1 Implementation of Rt-PRM reveals 11 specific ribosome sites to be significantly ubiquitinated in response to hydrogen peroxide (H_2O_2) stress

To investigate Ub-modified ribosome sites under stress, I collected log-phase yeast cells before and after treatment with 0.6 mM H_2O_2 and analyzed these samples via the optimized Rt-PRM protocol (as discussed in Section 2.3) (Fig 11A). In order to assess the efficiency of Rt-PRM, I tested its capacity to detect the accumulation of K63 Ub induced by H_2O_2 (Fig 11B) [116]. I measured the abundance of the K63-linked signature ubiquitin peptide (Ub.K63) in both H_2O_2-treated and untreated conditions (Fig 11C) and observed a more than 4-fold increase in treated conditions. I also found that the abundance of K48-linked ubiquitin (Ub.K48) increased in response to peroxide treatment, while Ub.K11 showed no significant increase (Fig 11C). These results are consistent with previously published trends for Ub linkages in peroxide stress [116, 188], confirming that Rt-PRM can be reliably used to measure stress-induced changes in protein ubiquitination.

A.

B.

C.

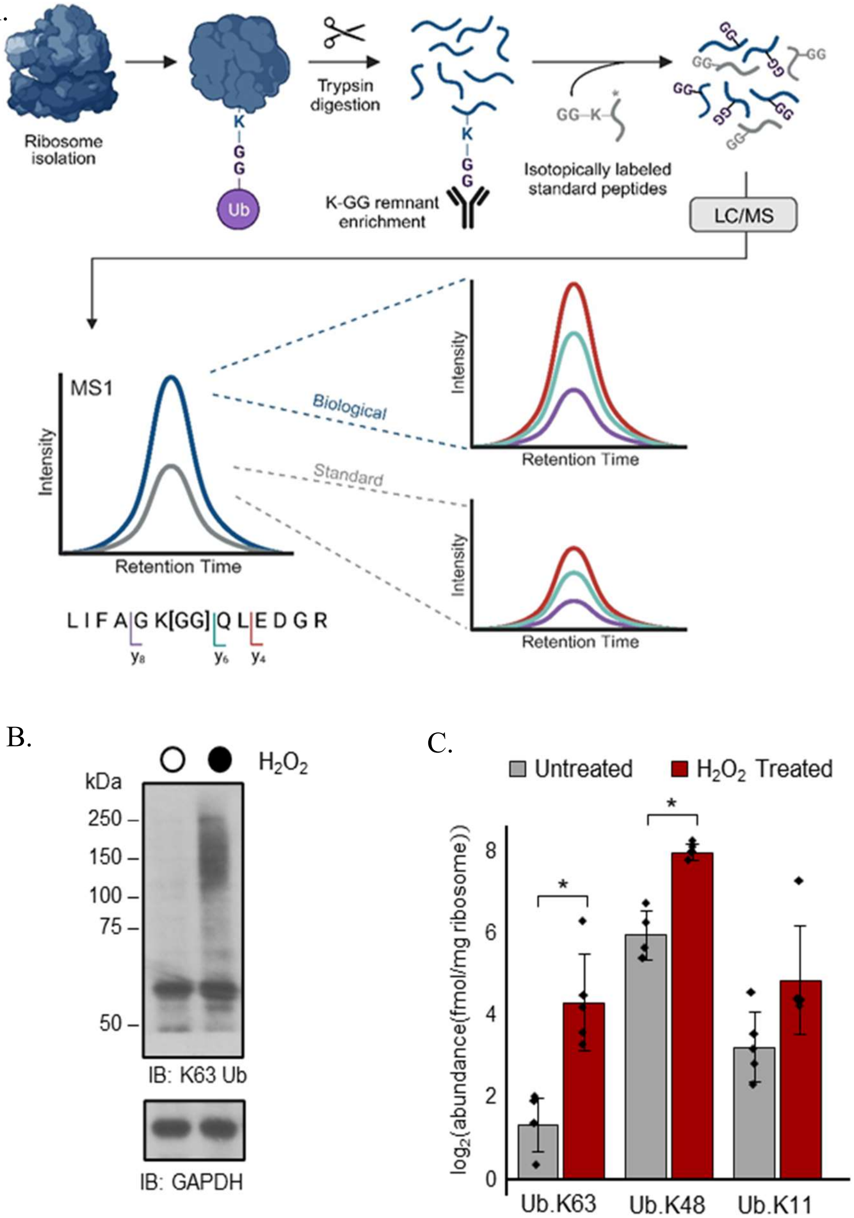

Figure 11: Ribosome-target Parallel Reaction Monitoring (Rt-PRM) detection of Ub linkages in H_2O_2 stress.A. Rt-PRM two-step enrichment for K-GG containing ribosome peptides. Heavy-labeled reference peptides were spiked in before enrichment with K-GG antibody. Peptides were analyzed by LC-MS/MS. B. Western blot of K63 polyubiquitin chains from cells treated in the presence or absence of 0.6 mM H_2O_2 for 30 minutes. anti-GAPDH was used as a lysate loading control. C. Cells were treated in the presence or absence of 0.6 mM H_2O_2 and K-GG containing ribosome peptides were isolated and subject to PRM analysis. The abundance (fmol) of K-GG per mg of ribosome for ubiquitin linkage types is shown. Error bars represent SD (n=5). (*pvalue <0.05 by student's paired t-test).

Of the 78 detected K-GG peptides, 15 peptides, including Ub.K63, Ub.K48, and 13 ribosome Ub-modified sites, were found to significantly increase in response to H_2O_2 treatment compared to untreated conditions (Fig 12A). Among these significant Ub-modified sites, 11 demonstrated a more than 2-fold increase due to H_2O_2 treatment, with 2 sites, uS10.K8 and uS8.K88, showing more than a 4-fold increase (Fig 2A). As specific sites are observed to undergo differential Ub-modification, this finding suggests that a site-specific arrangement of Ub-modification, or ubiquitin 'code', arises in response to peroxide stress and is responsible for changes in translation progression.

While increases in the fold change (FC) of Ub-modification provide important information on site-specific sensitivity to H_2O_2, it does not adequately reflect the frequency at which the modification occurs. However, the Rt-PRM method not only quantifies the increase of Ub-modified sites under stress but also allows quantification of their absolute abundance. This quantification was achieved by normalizing the biological peptide intensity with the intensity of the heavy reference peptide spiked-in. I observed that 9 of the Ub-modified peptides were measured in the range of 0.1-1 fmol per mg of isolated ribosome (Fig 12B). Two of the 11 sites, uS10.K8 and uS5.K33, were measured at more than 50 fmol per mg of isolated ribosome (Fig 12B). These 2 Ub-modified sites are both located on the beak of the 40S ribosomal subunit, a region well-established as a hub of translational regulation (Fig 12C) (PDB 6XIR) [55, 56, 58, 181]. Interestingly, uS10.K8 and uS5.K33 are also reported as target sites for Ub-modification by the Ribosome-associated protein quality control pathway (RQC) [135, 189, 190], raising questions as to whether the RQC-associated E3 ligase, Hel2, is responsible for the site-specific Ub-modification observed under H_2O_2 stress.

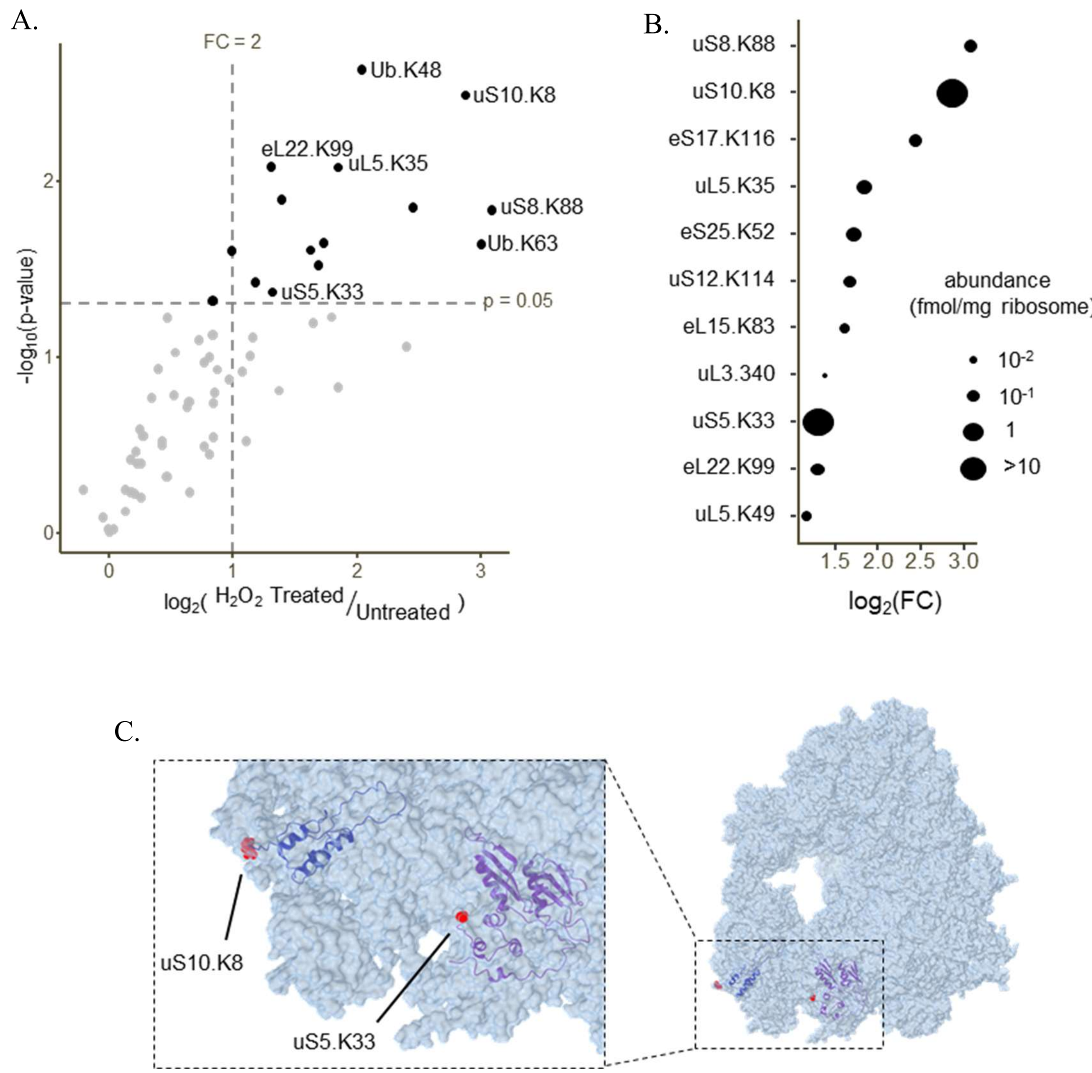

Figure 12: Ub-modified ribosome sites in H_2O_2 stress. A. Volcano plot of log$_2$(fold change (FC)) of Ub-modified ribosome sites in H_2O_2 Treated and Untreated conditions. p-values calculated by student's paired t-test (n=5). B. Plot of log2(FC) Ub-modified ribosome sites found to significantly increase from Untreated to H_2O_2 Treated conditions ($p<0.05$) vs peptide abundance (fmol/mg of ribosome) calculated by normalization to Ub-modified ribosome site-specific heavy-peptide. C. Mapping of most abundant uS10.K8 and uS5.K33 K-GG containing peptides to the 3D ribosome (PDB 6XIR) [55, 56].

2.4.2 Measurement of site-specific ribosome Ub reveals the two most abundant sites of modification are primarily dependent on the quality control ligase Hel2 in H_2O_2 stress

In accordance with previous studies [116, 139], the burst of H_2O_2-induced K63 Ub occurs even in the absence of the RQC ubiquitin ligase (E3), Hel2 (Fig 13A). This suggests that Hel2 is not the primary mediator of K63 Ub accumulation in peroxide stress. To determine if site-specific Ub-modification detected in H_2O_2 is also independent of Hel2, I enriched K-GG peptides from ribosome isolates of *hel2Δ* cells. Mass spectrometry analysis of these peptides confirmed the H_2O_2-induced increases in Ub linkages to be independent of Hel2 (Fig 13B). Ub.K63, Ub.K48, and Ub.K11 peptides exhibited similar fold-changes (FC) in *hel2Δ* cells (Fig 13B), as was seen for wild-type (WT) upon H_2O_2 treatment (Fig 11C). However, I observed that the Ub-modification of uS10.K8 increased by an average of 1.5-fold and the Ub-modification of uS5.K33 decreased by half in response to H_2O_2 in *hel2Δ* (Fig 13C). The decrease of Ub-modified uS5.K33 in H_2O_2 indicates that this site is, in fact, dependent on Hel2 [135, 189]. While I observed an increase in Ub-modified uS10.K8 in *hel2Δ*, this increase was only 20% of that observed in wild-type (Fig 13C), indicating that much of uS10.K8 ubiquitination in H_2O_2 stress is mediated by Hel2. Despite not being statistically significant, the slight increase in ubiquitinated uS10.K8 in response to H_2O_2 indicates that there is some Ub-modification of this site independent of Hel2. This finding suggests a novel role for uS10.K8 ubiquitination independent of its established role in the RQC pathway.

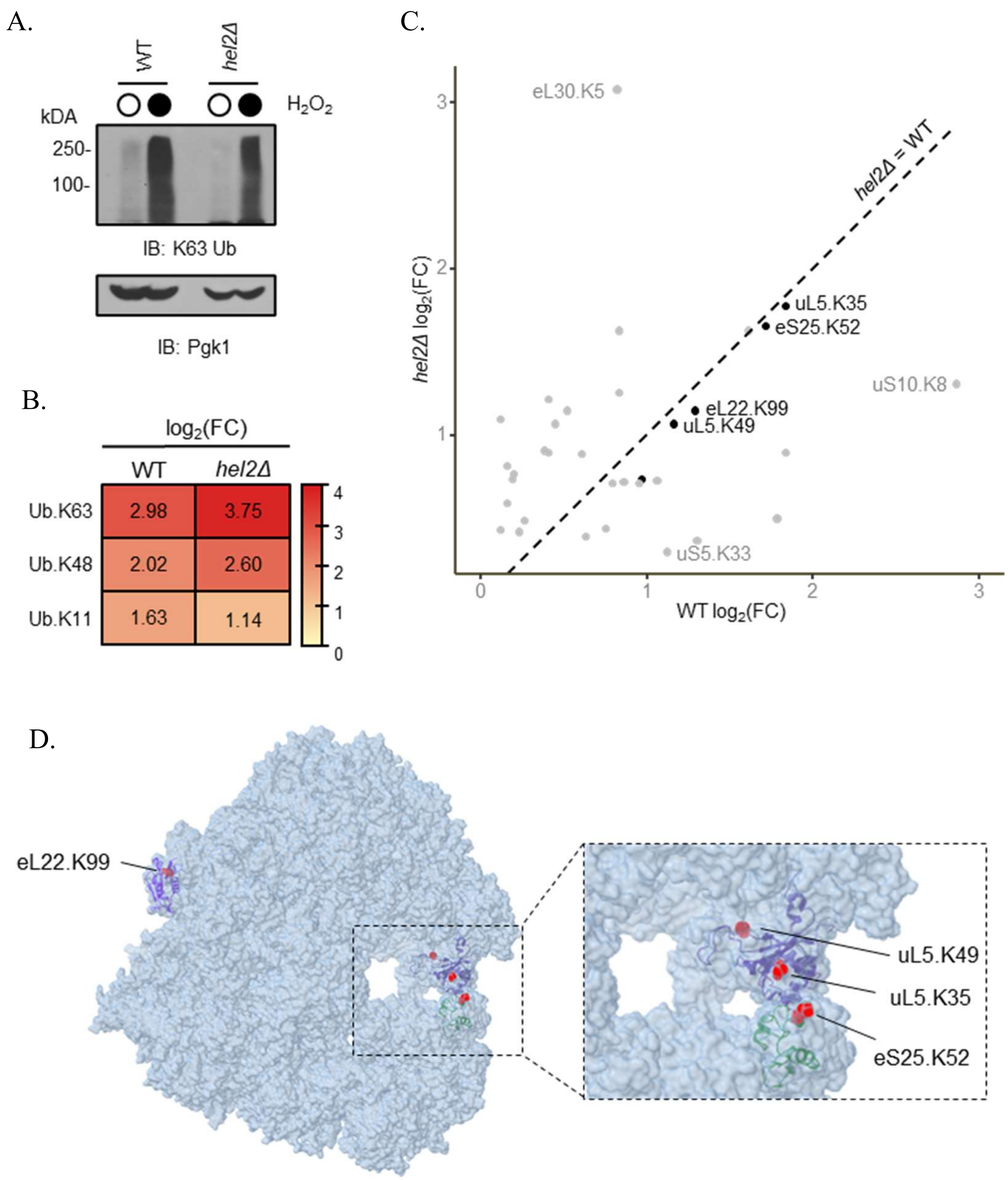

Figure 13: Hel2-indpendent Ub-modified ribosome sites in H_2O_2 stress. A. Western blot of K63 polyubiquitin chains from WT and *hel2Δ* cells treated in the presence or absence of 0.6 mM H_2O_2 for 30 minutes. anti-GAPDH was used as a lysate loading control. B. Heatmap comparing log2(Fold Change (FC)) of ubiquitin linkage peptides quantified before and after H_2O_2 treatment between wild-type (WT) and *hel2Δ* samples. C. Plot of Ub-modified ribosome site-specific H_2O_2-induced fold change in WT (x-axis) to *hel2Δ* (y-axis). Sites found to undergo statistically significant FC in *hel2Δ* (student's paired t-test, $p < 0.05$) are shown in black. D. Mapping of statistically significant, Hel2-independent and H_2O_2-induced Ub-modified ribosome sites to the 3D ribosome (PDB 6XIR) [55, 56].

Further investigation of the Ub-modified sites in *hel2Δ* revealed 4 sites, uL5.K35, eS25.K52, eL22.K99, and uL5.K49, to significantly increase from untreated to H_2O_2-treated conditions regardless of Hel2 expression (Fig 13C). While eL22.K99 is located on the large ribosomal subunit far from the decoding center, uL5.K35, eS25.K52, and uL5.K49 are adjacent to the tRNA exit, and modification of these sites could interfere with translational elongation (Fig 13D) (PDB 6XIR) [55, 56, 58]. For example, eS25 has been proposed to stabilize the closed conformation of the ribosomal L1 stalk [191]. Ub-modification could disrupt this stabilization and lead to the open L1 stalk observed in the trapped K63 Ub ribosome (Fig 8B) [56]. Additionally, uL5 has been identified to interact with the P-site occupying tRNA when the ribosome is in the rotated state [62]. This interaction could be disrupted upon Ub-modification of uL5 and prevent ribosome translocation.

2.5 Methods

2.5.1 Heavy-labeled reference peptide synthesis and characterization

Heavy labeled reference peptides for PRM containing isotopically labeled C-terminal Lysine ($^{13}C_6$,$^{15}N_2$) or Arginine($^{13}C_6$,$^{15}N_4$) residues were synthesized by JPT Peptide Technologies (Table A1). Heavy labeled reference peptides were reconstituted in 100 mM Ammonium Bicarbonate (ACN) to a final concentration of 100 pmol/μL.

To generate a spectral library, 200 fmol of stable isotope-labeled peptides were analyzed by LC-MS/MS using a Waters M-Class interfaced to a Thermo Fusion Lumos MS/MS (ThermoFisher) Liquid chromatography utilized a trap-elute configuration and 90 min gradient. MS/MS used data-dependent acquisition with an orbitrap MS2 resolution of 30,000, AGC target of 5E4, max injection time (IT) of 54 ms and stepped normalized collision energy (NCE) of 30 -

/+ 5%. Mass spectra were imported to Skyline [187] to build a spectral library using the MS-Amanda search engine.

2.5.2 Yeast ribosomal peptide extraction and preparation

SUB280 or SUB280 *hel2Δ* yeast were grown to mid-log phase in SD medium. Half of the sample was collected, while the remaining sample was treated with 0.6 mM H2O2 for 30 minutes at 30°C and 200 rpm agitation. Cells were lysed by glass bead disruption agitation at 4°C in lysis buffer containing 50 mM Tris-acetate pH 7, 100 mM NaCl, 30 mM MgCl2, 20 mM iodoacetamide (IAM), and 1x complete mini EDTA-free protease inhibitor cocktail (Roche #04693159001). Cell extracts were clarified by centrifugation and were sedimented by ultracentrifugation for 120 min at 70,000 rpm (Beckman Optima Max-TL, TLA-110 rotor) at 4°C in a 50% sucrose cushion buffered in 50 mM Tris-acetate, pH 7.0, 150 mM NaCl, and 15 mM MgCl2. Ribosome pellets were resuspended in 250 µL digestion buffer (50 mM ACN pH 8, 50 mM NaCl, 8M Urea). Samples were diluted to < 1 M Urea with 50 mM ACN pH8, and protein concentration was determined by Bradford Assay (Bio-Rad, #5000205). 25 mg of resuspended ribosome pellet was digested with trypsin at a [20:1] protein: protease (w/w) ratio for 4 hours at 32°C. Digests were acidified to a final concentration of 1% FA for at least 15 minutes, clarified by centrifugation, and desalted by Sep-Pak C18 Cartridges (Waters #WAT051910). Samples were dried by lyophilization and resuspended in IAP buffer from PTMScan HS Ubiquitin/SUMO Remnant Motif (K-ε-GG) Kit (Cell Signaling #59322). K-GG containing heavy reference peptides were pooled and diluted into the IAP buffer resuspension at a final concentration of 1 fmol per peptide. Samples were incubated for 2 hours at 4°C with K-GG antibody beads and eluted with IAP Elution buffer (0.15% TFA) in accordance with the manufacturer's protocol.

Samples were again desalted by C18 Stage Tip cleanup prior to sample resuspension and targeted PRM or LC-MS/MS analysis.

2.5.3 Targeted PRM Mass spectrometry analysis

The samples of K-GG-enriched peptides were reconstituted in 12 µL, and 3 µL of each was analyzed by LC-MS/MS using a Waters M-Class interfaced to a Thermo Exploris 480 MS/MS (ThermoFisher) (n=5). Liquid chromatography utilized a trap-elute configuration and 90 min gradient. MS/MS used parallel reaction monitoring (targeted MS2) with a resolution of 30,000, AGC target of 200%, max IT of 200 ms and NCE of 30. The scheduled inclusion list used 4 min wide windows and a 3 s cycle time. Mass Spectra were imported to PRMkit for ion chromatogram extraction, peptide transition identification, and peak area calculations.

2.5.4 Label Free Proteomics

The samples of K-GG-enriched peptides were analyzed by LC-MS/MS using a Waters M-Class interfaced to a Thermo Exploris 480 MS/MS (ThermoFisher) (n=5). Liquid chromatography utilized a trap-elute configuration and 90 min gradient. MS/MS used data-independent acquisition (DIA) with a 120,000 resolution precursor scan from 375-1600 m/z, AGC target of 300% and max IT of 45 ms. DIA used 30,000 resolution, AGC target of 1000% and max IT of 60 ms a NCE of 30. DIA windows (20 total) spanned 400-1000 m/z with a window width of 30 m/z and window overlap of 1 m/z. Mass spectra were matched to the previously built spectral library in Skyline [187] and quantified.

2.5.5 Statistical Analysis

Statistical analysis of peptide fold-change (FC) statistical significance was computed by student's pair t-test, and multiple testing correction was performed with the Benjamini-Hochberg procedure. Pairwise comparisons were considered to be statistically significant if FC (fold-change) > 1.5 and p-value < 0.05.

2.6 Conclusion

Previous work established 78 ribosome sites to be modified by K63 Ub after exposure to H_2O_2 stress [141]. However, it was unclear whether Ub-modification of these ribosomal sites occurred in response to stress. By employing Rt-PRM (Fig 11A), I identified 11 ribosomal sites that showed a more than 2-fold increase in Ub-modification in response to H_2O_2 treatment (Fig 12A). Among these sites, I identified 2 known targets of the RQC pathway (Fig 12A-C), which were found to be dependent upon the E3 Hel2 (Fig 13C). However, 4 ribosomal sites (uL5.K35, uL5.K49, eS25.K52, and eL22.K99) were identified to be ubiquitinated in the absence of Hel2 (Fig 13C-D). Notably, 3 of these sites (uL5.K35, uL5.K49, and eS25.K52) are located near the tRNA exit site (E-site) (Fig 13D) and may be important for ribosome pausing by the RTU pathway.

Overall, the quantification of ribosomal ubiquitination has revealed a complex code of site-specific Ub modification. These sites vary in sensitivity to peroxide stress, the abundance of their modification, and their dependency on the E3 ligase, Hel2. While further investigation of peroxide-sensitive and Hel2-independent sites is required to determine their role in inducing ribosomal pausing [56], this analysis was a crucial first step in determining the ubiquitin code of the RTU pathway. Furthermore, this MS analysis revealed an increase in Hel2-dependent ubiquitination of sites known to be targets of the RQC and other quality control pathways in H_2O_2 stress. While this is not the first report of increased ubiquitination associated with the RQC in oxidative conditions [135], it remains unclear to what extent this site-specific Ub-modification correlates with the induction of QC pathways. Therefore, I next sought to determine the extent to which known RQC targets were ubiquitinated in H_2O_2 compared to stressors known to induce ubiquitination by Hel2 and measure the impact of these stress conditions on RQC pathway activity.

3. Examining the dynamics of ribosomal ubiquitination reveals that the ubiquitin ‘code’ is written by different E2-E3s in a stressor-specific manner

Chapter 3 is modified from a manuscript in preparation for publication. The pre-print version is available on BioRxiv [150]. The authors are Shannon E. Dougherty, Géssica C. Barros, Matthew W. Foster, Guoshou Teo, Hyungwon Choi, and Gustavo M. Silva. S.E.D. devised the project and wrote the manuscript under the supervision of G.M.S. S.E.D. and G.C.B. carried out experimental work. Data analysis was completed by S.E.D. under the supervision of G.M.S.

The ribosome is a central hub of translational control by an increasing number of ubiquitin-mediated pathways [80, 91, 113]. Among these pathways are several that control ribosome abundance through biogenesis or degradation [104], those specific to endoplasmic reticulum bound ribosomes [192], and those responsive to stress, such as the Redox control of translation by ubiquitin pathway (RTU) [116, 141]. Among the most prominent ubiquitin-mediated translational control pathways are quality control (QC) mechanisms that ensure the production of toxic protein products is minimized [90]. As aberrant translation is a hallmark of cellular stress and related damage, the overlap of these QC mechanisms and stress response mechanisms is likely. However, how the induction and activity of these Ub-mediated pathways are coordinated to ensure cell survival is unclear.

In addition to the identification of novel ribosomal sites of Ub-modification that may function in the Redox control of translation by ubiquitin (RTU) pathway, MS-based ubiquitinomics revealed ubiquitination of known QC-pathway sites to also increase in peroxide stress (Fig 12A-B) [190, 193, 194]. While Ub-modification of uS10.K8 and uS5.K33 were predominantly dependent on the E3 ligase Hel2, ubiquitination of uS10.K8 was not completely abolished in *hel2Δ* (Fig 13C), suggesting that this site may also serve an independent function from its established role in quality control. However, how ribosomal Ub-modification serves as a signal for two different mechanisms and whether it leads to distinct outcomes remains unknown.

In the following section (Section 3.1), I will review the mechanisms of ubiquitin-mediated translation quality control (QC) pathways and discuss what is known about their induction in cellular stress. In Section 3.2, I will investigate the dynamics of stressor-specific ribosome ubiquitination and the interplay between QC pathways and the RTU. Section 3.3 contains a detailed description of the methods used in this chapter's analysis, and Section 3.4 contains concluding remarks.

3.1 Ubiquitin-mediated translation quality control (QC) mechanisms

Ubiquitination of the ribosome by Hel2 is a key feature of several QC pathways, including the Ribosome-associated protein quality control pathway (RQC) [132, 190], No-go decay (NGD) [195, 196], and Non-functional rRNA decay (NRD) [197, 198]. Each of these pathways serves as a surveillance mechanism for aberrant translation elongation, typically through the detection of stalled and collided ribosomes [196, 199, 200]. These QC pathways result in translation abortion and the degradation of associated polypeptides, mRNA, and rRNA [127, 201]. While oxidative and alkylative mRNA damage has been proposed to induce ribosome stalling [135, 202], the extent to which QC pathways are induced under stress remains unclear.

To discern the possible QC-independent role of ribosome Ub-modification in peroxide stress, it is essential to first establish what is known about the ribosomal sites targeted by Hel2 and how their ubiquitination results in translation abortion. In this section, I will review the established mechanisms of stalled ribosome clearance by the RQC and the associated quality control mechanisms of No-go decay (NGD) and Non-functional rRNA decay (NRD), highlighting the known sites of ribosomal Ub-modification and the fate of translation machinery. I will also discuss what is known about the induction of these QC pathways in stress conditions.

3.1.1 Ribosome-associated protein quality control (RQC)

The RQC pathway was initially discovered as a fail-safe mechanism for ribosomes that bypassed the stop codon and continued translating the poly-A tail of the mRNA 3' UTR [203]. It was hypothesized that the poly-basic K sequence encoded by the poly-A tail interacted with the residues within the ribosomal nascent peptide exit tunnel and caused ribosome stalling [204, 205]. Ribosome stalling presents a risk to the cell as it is often a sign of aberrant translation, the products of which may aggregate and become toxic to the cell [206]. The nascent peptide associated with the stalled ribosome was found to be modified with K48 Ub by the E3 ligase Ltn1 (Listerin in mammals) and shuttled to the proteasome for degradation [203, 207]. Since the pathway's initial discovery, our understanding of the mechanisms underlying the RQC pathway has greatly expanded. Further work found that in addition to poly-A tails, poly-arginine (R) encoding sequences, rare codons, and mRNA damage, all induced ribosome stalling [127-130]. However, the RQC does not target lone stalled ribosomes but targets collided ribosomes (also known as disomes) [132]. When a ribosome stalls for a prolonged period of time, the following ribosome continues through the process of translational elongation until it collides with the stalled ribosome. The collided ribosome interface is recognized by the E3 ligase, Hel2, which, in tandem with the E2 conjugase, Ubc4, is known to modify the small ribosomal protein (RP) uS10 at K6 and/or K8 with K63 Ub [132, 190]. This K63 Ub is required for recruitment of the RQT complex, which facilitates dissociation of the 80S ribosome into its subunits [208, 209]. The RQT complex consists of three enzymes: Cue3, which binds ubiquitin; Slh1, an RNA helicase with ATPase activity; and Rqt4, an enzyme with yet unknown function [190].

Much of what is known about the RQC pathway post-dissociation of the 80S by the RQT complex centers around the processing of the large 60S subunit. The 60S subunit is bound by Rqc2, which recruits the E3, Ltn1 which modifies the still bound nascent peptide chain with K48 Ub (Fig 14A) [203, 210, 211]. If the nascent chain contains no available K residues for modification, Rqc2 extends the nascent chain through the addition of alanine (A) and threonine (T) amino acids to the C-terminus, in a process known as CAT-tailing [212]. The addition of these residues either exposes K residues previously present in the ribosome exit tunnel for Ltn1 ubiquitination or acts as a degron, a sequence that serves as a mark for proteasome degradation [213, 214]. The K48 Ub-modified nascent peptide is recognized and extracted from the 60S by a complex of CDC48, Ufd1, and Npl4 and transported to the 26S proteasome [207, 215]. The protein Vms1 has been implicated in cleaving the nascent peptide from tRNA prior to nascent peptide degradation, but the importance of this step remains unclear [216]. Upon completion of RQC-mediated ribosome dissociation and nascent peptide degradation, the 40S and 60S ribosomal subunits are recycled and able to participate in a new cycle of translation initiation [217].

In summary, in the RQC pathway, Hel2 recognizes the disome interface and ubiquitinates ribosomal protein uS10 at the K6 or K8 position. Through the recruitment of downstream factors, this Ub-modification ultimately results in translation abortion, the dissociation of the ribosomal subunits, and degradation of the nascent peptide. Establishing the conventional role of Ub-modified uS10 in the RQC pathway provides opportunities to determine whether Ub-modified uS10 deviates from this function in peroxide stress.

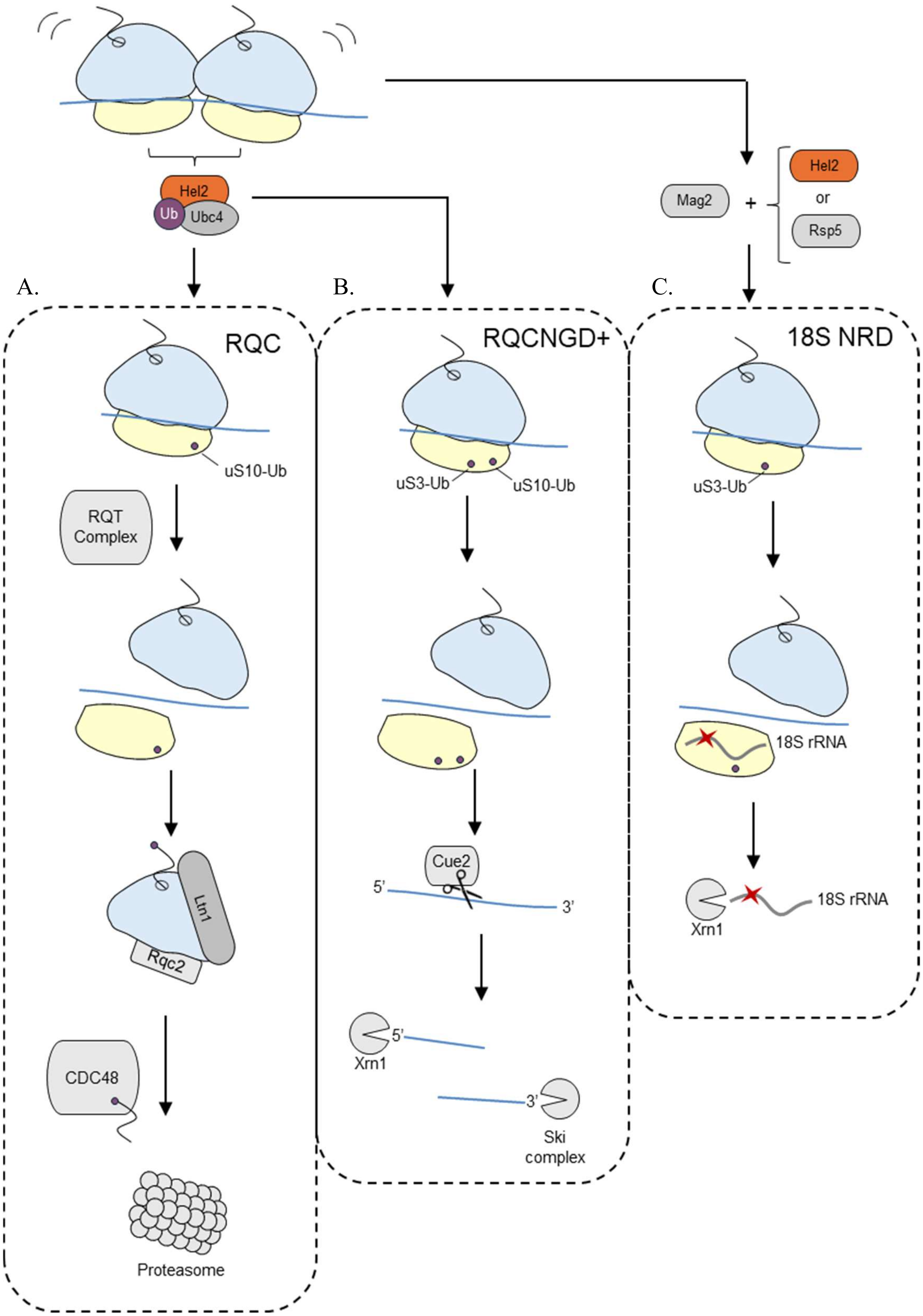
Hel2
Ub
Ubc4
Mag2
+
Hel2
or
Rsp5
A.
B.
C.
RQC
uS10-Ub
RQT Complex
Ltn1
Rqc2
CDC48
Proteasome
RQCNGD+
uS3-Ub
uS10-Ub
Cue2
5'
3'
Xrn1
5'
3'
Ski complex
18S NRD
uS3-Ub
18S rRNA
Xrn1
18S rRNA

Figure 14. Diagram of ubiquitin-mediated translation quality control (QC) pathways. Known mechanism of the Ribosome-associated protein quality control pathway (RQC). Collided ribosomes are recognized by the E3 ligase, Hel2, which modifies uS10 of the stalled ribosome with K63 Ub. K63 Ub promotes the recruitment of the RQT complex to dissociate the ribosomal subunits. The large 60S subunit is bound by Rqc2 and Ltn1, which modifies the nascent peptide with K48 Ub. The nascent peptide is then shuttled to the proteasome for degradation. B. Known mechanism of the RQC-associated No-go-decay pathway (RQCNGD+). Collided ribosomes are recognized by Hel2, which modifies uS3 and uS10 with K63 Ub. After ribosomal subunit dissociation, the mRNA transcript is cleaved by the Cue2 endonuclease. The 5' end of the mRNA is degraded by Xrn1, while the 3' end is degraded by the Ski complex. C. Known mechanism of 18S Non-functional rRNA decay (18S NRD). Mutations in the small subunit 18S rRNA cause ribosome stalling. Ribosomal protein uS3 is first monoubiquitinated by Mag2, and the K63 chain is extended by either Hel2 or Rsp5. Ribosomal subunits are dissociated, and the 18S rRNA is degraded by Xrn1.

3.1.2 No-go decay (NGD)

The no-go decay pathway (NGD) is a surveillance mechanism that targets the mRNAs that cause ribosome stalling during translation elongation [218, 219]. Among these problematic mRNAs are those with RNA secondary structures, rare codons, poly-basic encoding sequences, and mRNA damage [220]. Although NGD was initially discovered independently of the RQC [218], two mechanisms of NGD, RQC-associated (NGDRQC+) and RQC-independent (NGDRQC-) [114, 221], have now been established. In NGDRQC+, mRNA degradation is triggered by ribosome collision, requires Hel2 ubiquitination of uS10 (Fig 14B), and depends on Slh1, a component of the RQT complex [114, 132]. While some work has implicated the ubiquitination of ribosomal protein uS3 at K212 by Hel2 in the NGD (Fig 14B) [195, 196], other work has found this site-specific modification to be non-essential for either RQC or NGD function [90]. NGDRQC-, which occurs when the RQC is defective, occurs upstream of collided ribosomes and requires ubiquitination of ribosomal protein eS7 [132, 222]. The E3 ligase, Not4, mediates the monoubiquitination of eS7, and Hel2 functions to extend the modification to a K63 Ub chain [223]. Both RQC+ and RQC- NGD employ the endonuclease Cue2 to cleave the problematic mRNA transcript [221, 224]. Once the transcript is cleaved, the 5' mRNA fragment is degraded by Xrn1, and the 3' mRNA fragment is degraded by the Ski complex [225, 226].

In summary, in the NGDRQC+ pathway, Hel2 Ub-modification of uS10, and potentially uS3, is required for translation abortion by the RQC and degradation of the mRNA transcript. As NGDRQC+ was found to be required for clearance of oxidatively damaged mRNAs *in vitro* [136], establishing the ribosomal sites expected to be modified by Hel2 is important to determine whether H_2O_2-induced Ub-modification is also associated with the NGDRQC+ pathway.

3.1.3 Non-functional rRNA decay (NRD)

In addition to protein and mRNA quality control, the non-functional rRNA decay pathway (NRD) serves as a surveillance mechanism for rRNA integrity, even within fully assembled ribosomes [90, 227]. While NRD of the 25S rRNA, or 25S NRD, occurs in the cytoplasm independently of translation, 18S NRD that targets the 18S rRNA occurs in tandem with translation [114]. Mutations in 18S rRNA are proposed to cause ribosome stalling and induce ubiquitination of ribosomal protein uS3 at K212 (Fig 14C) [198]. Monoubiquitination of uS3.K212 is dependent on the E3, Mag2, and the chain is then extended by the E3s: Hel2 or Rsp5 [198, 228]. While the exact mechanisms are unknown, it is known that Slh1 is required to stimulate subunit dissociation for 18S NRD, and the non-functional 18S rRNA is degraded by Xrn1 [198].

In summary, 18S NRD leads to translation abortion and ribosomal subunit dissociation through a yet undiscovered mechanism. However, Ub-modification of uS3, mediated in part by Hel2, has been proposed to promote this process. As ubiquitination of uS3 is also involved in the function of the NGD pathway (Section 3.1.2), it seems that Ub-modified uS3 has two distinct roles. Although both the 18S NRD and NGD pathways are associated with translation abortion and subunit dissociation, each pathway results in distinct outcomes—degradation of rRNA and mRNA, respectively[90, 114]. The dual consequences of uS3 ubiquitination emphasize the complexity of cellular signals encoded in ribosome ubiquitination and underscore the need for precise coordination of the associated QC pathways. For example, inducing degradation of 18S rRNA is pointless if problematic mRNA was the cause of ribosome stalling. While investigation of the coordination of the QC pathway and the role of site-specific ribosome modification is ongoing, limited effort has been devoted to studying these pathways in stress conditions. To fully understand how the ribosome ubiquitin code regulates translation elongation, it is essential to determine the involvement of QC pathways and distinguish their role from that of other mechanisms, including the Redox control of translation by ubiquitin pathway (RTU), under stress.

3.1.4 Activation of quality control (QC) mechanisms under stress

As mentioned above, the RQC, NGD, and NRD pathways are important regulators of translational control in steady-state conditions [81, 90], but investigation into their role in stress conditions is limited. In mammalian cell lines, exposure to stressors, including nitric oxide [229], arsenite [230], and elongation inhibitors [231], have been found to increase ribosome collisions and subsequently activate QC pathways. A study of stress-induced QC in yeast has suggested that exposure to the alkylating agent methyl methanesulfonate (MMS) and the oxidizing agent 4-nitroquinoline 1-oxide (4-NQO) activates the RQC and NGD pathways through targeted RNA damage [135]. MS-based ubiquitinomics analysis (see Section 2.1 for review) revealed several ribosomal sites, including uS3.K212, uS10.K8, and uS5.K33, to be Ub-modified upon 4-NQO stress [135]. However, a direct connection between the increase in site-specific Ub-modification and an increase in QC-mediated translation abortion has yet to be established under 4-NQO stress

[135, 202, 232]. As I also observed an increase of uS10.K8 and uS5.K33 Ub-modification in H_2O_2 stress (Fig 12A-C), these findings suggest that peroxide stress may induce site-specific ubiquitination similar to 4-NQO stress.

3.2 Results

3.2.1 Investigation of Ub-modification dynamics reveals stressor-specific patterns of ribosomal protein ubiquitination

To determine whether ribosomal ubiquitination observed in response to H_2O_2 mirrored that observed upon treatment with 4-NQO, I first sought to characterize the dynamics and abundance of ribosomal protein (RP) ubiquitination in response to each stressor. To determine whether the abundance of protein ubiquitination in H_2O_2 stress equaled the amount in 4-NQO stress, I measured the amount of Ub-modified endogenously expressed 3HA-tagged uS5 or uS10 using exposure to MMS as a positive control [195, 202]. While I was not able to distinguish the abundance of polyubiquitinated (poly-Ub) uS5-3HA in any stress conditions (Fig A1), I did detect polyubiquitinated forms of uS10-3HA in H_2O_2 (0.6 mM, 5 mM), 4-NQO (1 µg/mL, 5 µg/mL) and MMS (0.1%, 0.33%) (Fig 15A). The presence of ubiquitinated uS10-3HA corroborates the proteomics findings that H_2O_2 stress induces uS10 ubiquitination (Fig 13C). Moreover, the amount of Ub-modified uS10-3HA was similar between H_2O_2 and 4-NQO, indicating that the lower and higher concentrations of these stressors have a comparable impact on the abundance of uS10 ubiquitination. Finally, the level of uS10 ubiquitination corresponded to the concentration of stressor for both H_2O_2 and 4-NQO, but not in MMS stress (Fig 15A). Although prior work has equated the impact of 4-NQO and MMS stress due to their propensity to damage nucleotides and disrupt codon-anticodon base pairing [135], this finding indicates that there may be more dissimilarities between the two stress conditions than initially anticipated. For example, while oxidatively damaged nucleotides were reported to induce ribosome stalling regardless of position within the codon, alkylated nucleotides were only found to cause ribosome stalling when located in the second codon position [233]. The different rates of ribosome stalls induced by nucleotide oxidation and alkylation could explain why an increase in MMS concentration does not equate to a significant increase in uS10 ubiquitination. Overall, these findings confirm that the Ub-modification of the QC target uS10 does occur in response to H_2O_2 stress. Additionally, the amount of Ub-modification occurs at a similar abundance to that induced by 4-NQO stress, suggesting that these oxidative conditions may be more comparable than 4-NQO and MMS stress conditions.

I next asked whether ubiquitination of uS10-3HA occurred independently of Hel2 as found in the proteomics analysis. I deleted *HEL2* from the genome of the uS10-3HA strain and confirmed its deletion using an established RQC GFP-FLAG-HIS3 reporter (Fig 15B) [190]. This reporter is constitutively expressed and contains either a No-Stall control or a 6xCGA stall sequence inserted between GFP and FLAG. As RQC-mediated clearance of 6xCGA stalled ribosomes culminates in translation abortion and nascent peptide degradation, its inefficiency can be measured by translational bypass and synthesis of the full-length (FL) reporter. Synthesis of the No-Stall reporter is used as a control for differences due to strain background. While the amount of No-Stall reporter was similar between the WT and *hel2Δ* uS10-3HA strains (Fig 15 C, lanes 1&3), the full-length 6xCGA reporter was only detected upon *HEL2* deletion (Fig 15C, lanes 2&4), confirming that *HEL2* was in fact deleted and RQC efficiency reduced in its absence.

To determine whether uS10 was ubiquitinated independently of Hel2, I measured ubiquitination of the 3HA-tagged uS10 from *hel2Δ* in untreated, H_2O_2 (0.6 mM, 5 mM), 4-NQO (1 µg/mL, 5 µg/mL) and MMS (0.1%, 0.33%) stress (Fig 15D). Polyubiquitinated uS10-3HA was detected in all conditions, although at a lower amount than the WT strain (Fig 15D). Furthermore, the accumulation of poly-Ub increased in the higher concentrations of H_2O_2 and 4-NQO but not in MMS (Fig 13D). While it cannot be discounted that this ubiquitination is still linked to the induction of the RQC pathway, these findings indicate that there are, as yet undiscovered, Hel2-independent pathways of uS10 ubiquitination that are upregulated in response to oxidative stressors. Rather than acting as a signal for the recruitment of RQC factors for the dissociation of stalled ribosomes, this Hel2-independent ubiquitination of uS10 may play a role in ribosome pausing in the RTU pathway [56, 141]. Alternatively, as uS10 is located in the head region of the 40S [58], it is central to many interactions between the ribosome and associated proteins. As such, ubiquitination of uS10 could be related to several processes other than the RQC pathway, including the recruitment of translation factors and binding of Tsa1, a thioredoxin peroxidase that acts as an antioxidant [234].

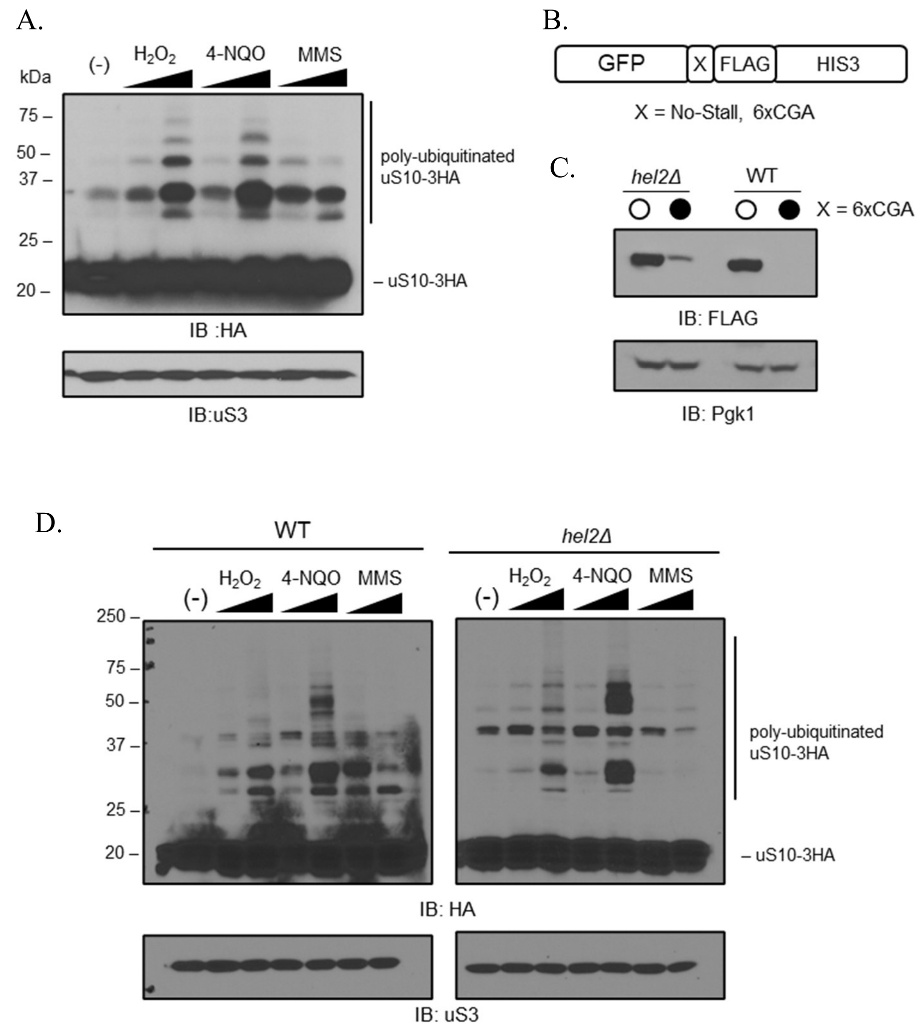

Figure 15: Ubiquitination of uS10 in stress conditions. A. Western blot of ribosomes isolated from untreated and H_2O_2 (0.6 mM, 5mM), 4-NQO (1 µg/mL, 5 µg/mL), and MMS (0.1%, 0.33%) treated cells with 3HA tagged uS10 probed with anti-HA. Anti-uS3 was used as a loading control. B. Schematic for the GFP-X-FLAG-HIS3 reporter construct. C. Western blot for full-length GFP-X-FLAG-HIS3 reporter expression for the No-Stall and 6xCGA reporter in *hel2Δ* and WT cells expressing uS10-3HA with anti-FLAG. Anti-Pgk1 was used as a loading control. D. Western blot of ribosomes isolated from WT and *hel2Δ* uS10-3HA expressing cells in untreated and H_2O_2 (0.6 mM, 5mM), 4-NQO (1 µg/mL, 5 µg/mL), and MMS (0.1%, 0.33%) uS10-3HA was probed with anti-HA and anti-uS3 was used as a loading control.

My results with uS10 motivated me to investigate whether the ubiquitination of uS3 observed in 4-NQO was similarly induced by H_2O_2 stress. In addition to the observation of site-specific Ub-modification of uS3.K212 in 4-NQO via MS, monoubiquitinated (mono-Ub) uS3 was also detected via immunoblot upon exposure to both 4-NQO and MMS [195]. Although the Ub-modified uS3.K212 reference peptide was not captured by Rt-PRM (Table A1), I probed uS3 modifications on isolated ribosomes via immunoblotting (Fig 16A). Mono-Ub uS3 (uS3-Ub_1) was detected in 4-NQO and MMS stress conditions but not in H_2O_2. Ubiquitination of uS3 under 4-NQO and MMS stress was previously determined to be dependent on the E3 Hel2 [190, 198]. Consistent with these reports, I observed a total loss of uS3-Ub_1 in MMS stress in *hel2Δ* (Fig 16A). However, I only observed a partial loss of uS3-Ub_1 in 4-NQO stress, indicating that some modification of uS3 occurs independently of Hel2 in this stress condition. Furthermore, the uS3 ubiquitination in 4-NQO was not dependent on the redox-regulated E2, Rad6 (Fig 16A). In all, these findings indicate that the ubiquitination of uS3 is both stressor and enzyme-dependent and does not occur in response to H_2O_2 stress.

While H_2O_2 stress showed similar levels of uS10 Ub-modification to that of 4-NQO, the differences in uS3 ubiquitination led me to hypothesize that although both H_2O_2 and 4-NQO are oxidative stressors, they promote different patterns of ubiquitination. To evaluate my hypothesis, I measured the amount of K63 Ub accumulation induced by H_2O_2 and 4-NQO stresses, using MMS as a control for non-oxidative stress. I found that the burst of K63 Ub observed in 0.6 mM H_2O_2 did not occur in 4-NQO nor MMS stress (Fig 16B). Consistent with previous findings, K63 Ub accumulation in H_2O_2 was found to be dependent on Rad6 [116, 139] but I observed no change in ubiquitin accumulation in 4-NQO or MMS upon deletion of either *RAD6* or *HEL2* (Fig 16B).

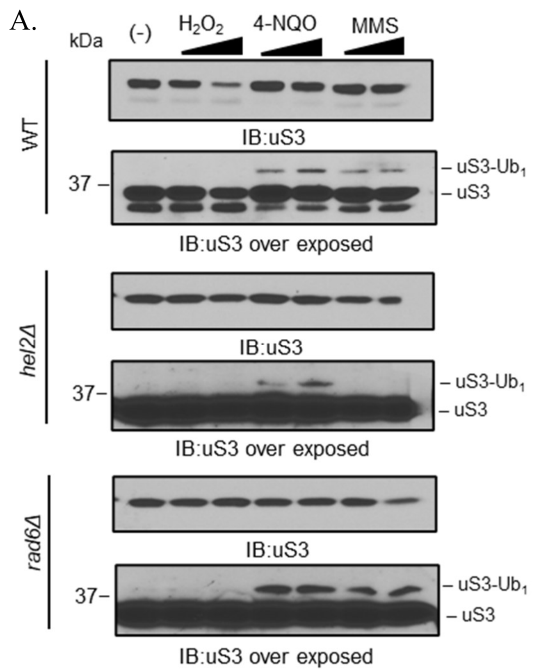

Figure 16: Dynamics of ribosome ubiquitination under stress conditions. A. Western blot of ribosomes isolated from untreated and H_2O_2 (0.6 mM, 5mM), 4-NQO (1 µg/mL, 5 µg/mL), and MMS (0.1%, 0.33%) treated WT, *hel2Δ*, and *rad6Δ* cells probed with anti-uS3. B. Western blot of K63 polyubiquitination from WT, *hel2Δ*, and *rad6Δ* cells treated with H_2O_2 (0.6 mM, 5mM), 4-NQO (1 µg/mL, 5 µg/mL), and MMS (0.1%, 0.33%). anti-Pgk1 was used as a loading control.

Overall, these findings demonstrate that the pattern of ribosome ubiquitination differs based on stressor identity and severity. While H_2O_2 and 4-NQO stress may induce Ub-modification of uS10 to similar amounts, the larger context in which this modification occurs is distinct. This supports the existence of a complex ubiquitin code, which varies in composition depending on conditions within the cell. How this code is read by cellular machinery and induces distinct translational control pathways remains to be elucidated.

3.2.2 Measurement of RQC activity did not show evidence of increased RQC induction in oxidative stressors

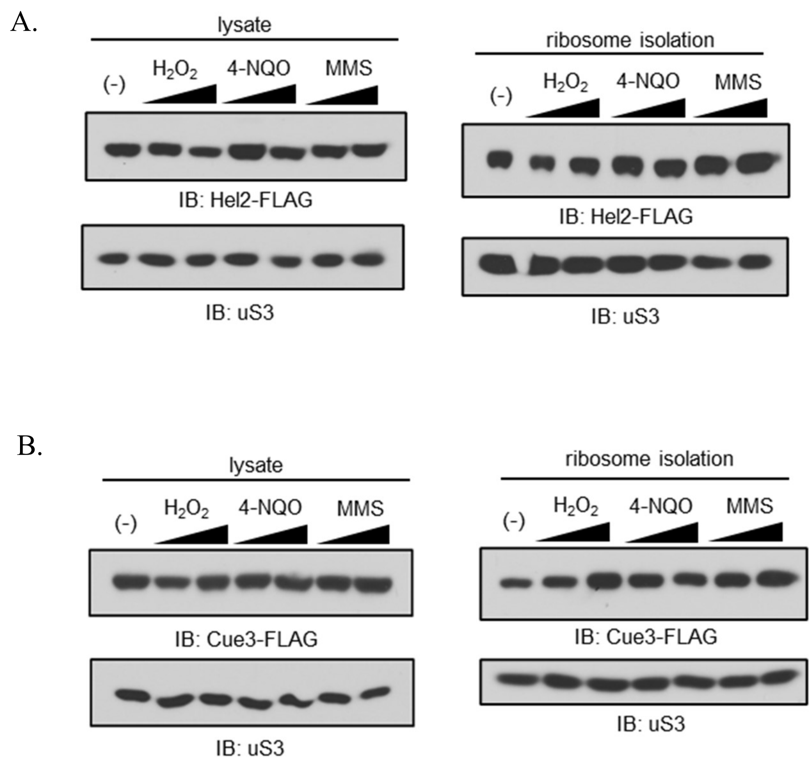

Figure 17: Recruitment of RQC factors to ribosome isolates. A. Western blot of cell lysates and ribosome isolations from untreated and H_2O_2 (0.6 mM, 5mM), 4-NQO (1 μg/mL, 5 μg/mL), and MMS (0.1%, 0.33%) treated in cells expressing FLAG-tagged Hel2. anti-uS3 was used as a loading control. B. Western blot of cell lysates and ribosome isolations from untreated and H_2O_2 (0.6 mM, 5mM), 4-NQO (1 μg/mL, 5 μg/mL), and MMS (0.1%, 0.33%) treated in cells expressing FLAG-tagged Cue3. anti-uS3 was used as a loading control.

I previously showed that Ub-modification of uS10 occurs in H_2O_2 at similar levels to 4-NQO and still occurs in the absence of Hel2, but whether this ubiquitination equates to induction of the RQC pathway in these conditions remains unclear. To test whether the RQC pathway is induced by peroxide stress, I investigated the impact of H_2O_2 on the recruitment of key RQC factors to the ribosome. Measurement of exogenous FLAG-tagged RQC factors Hel2 and Cue3 revealed no significant differences in enzyme recruitment to sucrose-sedimented ribosomes following exposure to H_2O_2 stress (Fig 17 A-B). I also observed no significant change in enzyme recruitment upon exposure to 4-NQO or MMS stress (Fig 17A-B). This finding suggests that exposure to any of these stressors does not discernably induce the RQC by altering the recruitment of pathway enzymes. However, levels of endogenous Hel2 have been estimated to be around 1% of the number of ribosomes [235]. As the expression of the Flag-tagged Hel2 (and Cue3) increases the enzyme-to-ribosome ratio, it is possible that the use of exogenous constructs results in saturated ribosome recruitment before any stress is introduced to the system.

To investigate whether the RQC is induced in H_2O_2 stress through alternative means, we next measured the efficiency of stalled ribosome clearance using an established RQC reporter system[4]. The inducible dual-luciferase reporter contains either a No-Stall control or 6xCGA polyarginine sequence inserted between Renilla luciferase (Rluc) and Firefly luciferase (Fluc) encoding regions (Fig 18A) [236]. As RQC-mediated clearance of 6xCGA stalled ribosomes culminates in translation abortion and nascent peptide degradation, the efficiency of arrested ribosome clearance can be quantified from the ratio of Fluc to Rluc. While we observed 90% translation arrest in wild-type (WT), we only observed a 75% arrest in *hel2Δ* (Fig 18B). This data indicates that in the absence of Hel2, arrested ribosomes are not efficiently cleared, enabling a fraction of ribosomes to bypass this arresting sequence and continue translating.

[4] The experiments and analysis using the inducible dual-luciferase RQC reporter were conducted by Géssica C. Barros. Data visualization and contextualization were performed by S.E.D.

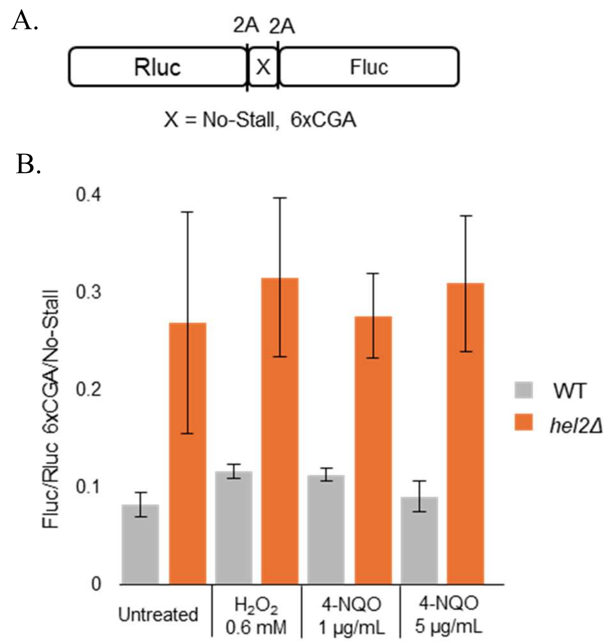

Figure 18: Renilla-Firefly Luciferase RQC reporter. A. Schematic for the Renilla-Firefly luciferase reporter construct. B. The Ratio of Fluc/Rluc for the 6xCGA reporter compared with a No-Stall reporter in WT and *hel2Δ* in H_2O_2 (0.6 mM) and 4-NQO (1 μg/mL, 5 μg/mL) stress.

If the RQC is induced in H_2O_2, one would expect to observe more translation arrest upon stress exposure. Surprisingly, we did not observe a significant difference in translation arrest upon treatment with H_2O_2 in either wild-type or *hel2Δ* (Fig 18B). Moreover, no change in translation arrest was observed in response to 4-NQO stress (Fig 18B). Upon first glance, this data appears to indicate that ribosome stalling is not exacerbated in either tested oxidative stressor. However, this interpretation only considers the effects of stress on translation elongation. Exposure to oxidative stress is also known to suppress global translation initiation [10]. Suppression of translation initiation in H_2O_2 or 4-NQO would also result in no observable difference in the ratio of Fluc/Rluc compared to untreated amounts. This scenario illustrates the challenge of distinguishing the role of translational regulatory pathways, such as the RQC, from the broader control of translation in cellular stress conditions, a topic that is further explored in Chapter 4. However, as the increase of Ub-modified uS10 in H_2O_2 and 4-NQO (Fig 13C, 17D) does not appear to equate to increased RQC clearance of stalled ribosomes, these findings further support an RQC-independent role of uS10 ubiquitination.

3.2.3 The E2 conjugase, Rad6, antagonizes RQC pathway activity in steady-state conditions

My findings suggest that uS10 Ub-modification can occur independently of Hel2 and may serve a role other than RQC induction. As the E2-E2 pair Rad6-Bre is responsible for the accumulation of ribosomal ubiquitination in peroxide stress (Fig 7) [116], I questioned whether these enzymes might also target uS10 for ubiquitination. I hypothesized that if uS10 were a target for the RTU ubiquitinating enzymes, Rad6 and Bre1 would compete with Hel2 and the RQC for targets. To evaluate this hypothesis, I utilized the GFP-FLAG-HIS3 reporter system (Fig 19A) as a readout of RQC efficiency in steady-state conditions. If Rad6 and/or Bre1 competed with Hel2 for ribosome targets, I would expect to see an increase in RQC clearance of 6xCGA stalled ribosomes upon their deletion, represented by less synthesis of full-length (FL) construct.

I measured translational bypass of the 6xCGA stalling sequence in wild-type (WT), *hel2Δ*, *rad6Δ,* and *bre1Δ* cells (Fig 19B-C). The No-Stall containing reporter served as a control for expression differences due to strain background. In wild-type, we observed a 15% bypass of the 6xCGA sequence compared to the No-Stall control (Fig 19B-C). Upon deletion of *HEL2*, we observed a 50% 6xCGA bypass (Fig 19B-C), confirming that RQC is less efficient in the absence of Hel2. While deletion of *BRE1* had little effect, upon deletion of *RAD6*, we observed less than 10% bypass of 6xCGA (Fig 19B-C), suggesting that Rad6 antagonizes the RQC pathway.

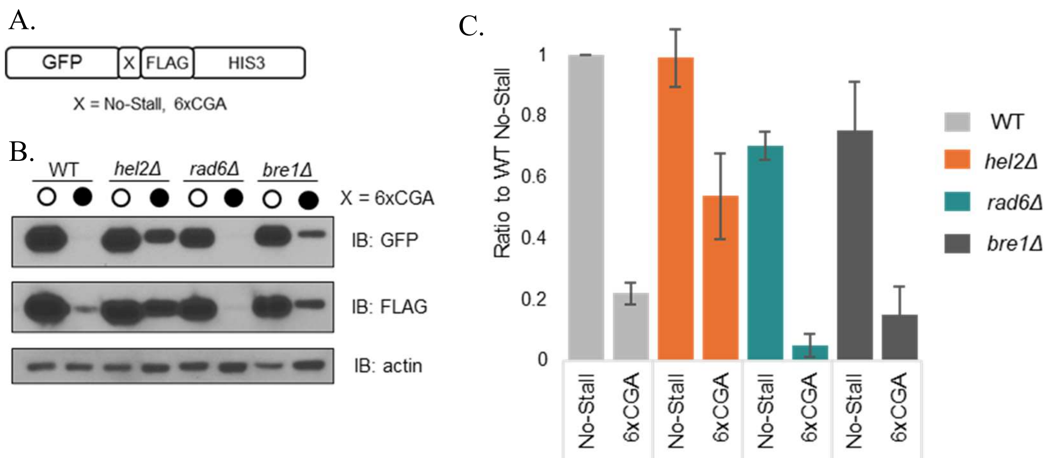

Figure 19: GFP-X-FLAG-HIS3 RQC reporter in the absence of RTU enzymes. A. Schematic for the GFP-X-FLAG-HIS3 reporter construct. B. Western blot for full-length GFP-X-FLAG-HIS3 reporter expression for the No-Stall and 6xCGA reporter in WT, *hel2Δ, rad6Δ*, and *bre1Δ* with anti-GFP and anti-FLAG. Anti-actin was used as a loading control. C. Quantification of full-length GFP-X-FLAG-HIS3 for the 6xCGA reporter detected with anti-FLAG normalized to No-Stall expression (n=3).

To confirm the antagonistic relationship between the E2 Rad6 and RQC, I employed the GFP-FLAG-HIS3 reporter to measure RQC efficiency upon overexpression of exogenously expressed HA-tagged Rad6, and several Rad6 mutants (Fig 20A)[139]. Immunoblot revealed that overexpression of Rad6 not only restored RQC efficiency to WT levels but further inhibited it (Fig 20B). This inhibition was not dependent on Rad6's ubiquitinating activity, as the catalytically dead Rad6^{C88S} mutant produced similar results as wild-type Rad6 (Fig 20B). Moreover, the expression of two Rad6 constructs known to have increased (Rad6^{LLL}) and decreased (Rad6$^{1\text{-}149}$) ribosome affinity [139] did not differ from wild-type Rad6. However, as Rad6 constitutively interacts with ribosomes, even in the absence of peroxide stress [139], the overexpression of Rad6 may be enough to negate the effects of low ribosome affinity. These findings support a model in which the intrinsic interaction between Rad6 and the ribosome hinders RQC pathway activity. As Rad6 levels increase, more ribosomes are occupied, leaving fewer available for the RQC pathway.

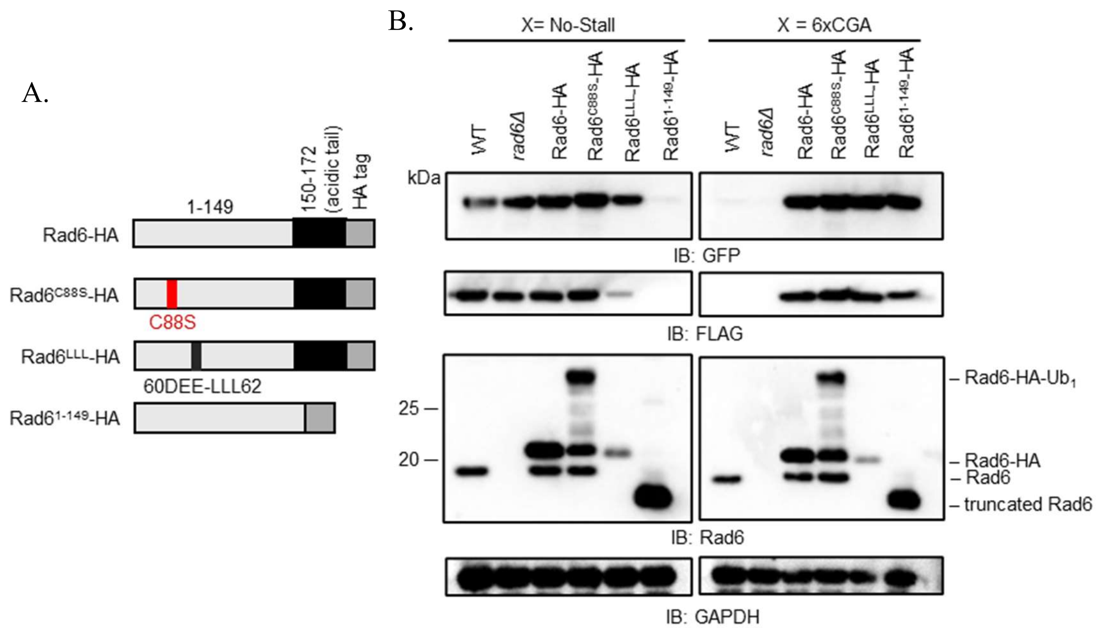

Figure 20: GFP-X-FLAG-HIS3 RQC reporter upon expression of Rad6 mutants. A. Schematic for HA-tagged exogenously expressed Rad6 mutant constructs. B. Western blot for full-length GFP-X-FLAG-HIS3 reporter expression of the No-Stall and 6xCGA constructs in WT, *rad6Δ,* and strains expressing exogenous HA-tagged Rad6 and Rad6 mutants.

3.3 Methods

3.3.1 Yeast growth conditions

Standard recombination methods were used to delete and tag genes and were confirmed by PCR. Plasmids were constructed using either T4 ligation (New England Biolabs #M0202L) or HiFi DNA Assembly methods (New England Biolabs, #E2621S). All plasmids used in this study are listed in Table A3.

SUB280 and W303 yeast derivatives were grown in SD complete media using dropout amino acid supplements without Ura (Sigma, #Y0751) and supplementing back with Uracil (Sigma, #U0750). SUB62 strain derivatives were grown in (SD) medium composed of D-Glucose (BD Difco, #215510), yeast nitrogen base (BD Difco, #291940) and drop-out amino acid medium without Ura (Sigma, #U0750). Unless specified, yeast cells were cultivated at 30°C at 200 rpm agitation to mid-log phase. Unless otherwise stated, yeast cells were treated for 30 minutes with the following stressors/concentrations: freshly diluted H_2O_2 (peroxide) (Sigma, #216763) was added to a concentration of 0.6 mM or 5 mM, 4-nitroquinoline 1-oxide (4-NQO) (Sigma-Aldrich #N8141) was added to a concentration of 1 μg/mL or 5 μg/mL, Methyl methanesulfonate (MMS) (Sigma-Aldrich #129925) was added to a concentration of 0.1% or 0.33% v/v.

3.3.2 Protein Extraction

Cells were disrupted by glass-bead agitation at 4°C in standard lysis buffer containing 50 mM Tris-acetate pH 7, 100 mM NaCl, 30 mM MgCl2, 20 mM iodoacetamide (IAM), and 1X protease inhibitor cocktail set I (Sigma, #539131). Cells intended for sucrose sedimentation were disrupted in standard lysis buffer with 1X protease inhibitor cocktail replaced by 1x complete mini EDTA-free protease inhibitor cocktail (Roche #04693159001). Extracts were clarified by centrifugation, and protein concentration was determined via Bradford Assay (Bio-Rad, #5000205).

3.3.3 Ribosome sucrose sedimentation

Yeast lysates were sedimented by ultracentrifugation for 120 min at 70,000 rpm (Beckman Optima Max-TL, TLA-110 rotor) at 4°C in a 50% sucrose cushion buffered in 50 mM Tris-acetate, pH 7.0, 150 mM NaCl, and 15 mM MgCl2. Ribosome pellet was resuspended in the same lysis buffer, and protein concentration was determined via Bradford Assay (Bio-Rad, #5000205) prior to western blot.

3.3.4 Western blot

Proteins were separated by standard 10-15% SDS-PAGE and transferred to PVDF membrane (ThermoFisher, #88518). Immunoblotting was performed using the antibodies in Table A4. Western blots were quantified using ImageJ Software [237], and Student's t-test was used to calculate statistically significant differences with a p-value cutoff of 0.05.

3.3.5 Dual luciferase reporter

Yeast strains transformed with Rluc-P2A-X-P2A-Fluc plasmids, where X represents a variable sequence, were grown to mid-log phase in SD complete medium. Cells were pelleted and resuspended in SD Methionine depleted (SD -Met) medium to induce plasmid expression for 60 minutes. Cells were then either left untreated or treated with 0.6 mM H_2O_2 or 4-NQO (1 µg/mL, 5 µg/mL) for an additional 30 minutes under agitation. Cells were then pelleted and disrupted by glass bead agitation at 4°C in 1x Passive Lysis Buffer provided in the Dual-Luciferase Reporter Assay System (Promega #E1910). Extracts were clarified by centrifugation, and protein concentration was determined by BCA assay (ThermoFisher #23225). Luminescence activities of Rluc and Fluc were collected for 3 ug of protein combined with respective substrates 10x diluted and were measured in a Spectra Max M3 (Molecular Devices) plate reader.

3.4 Conclusion

In my proteomics analysis, I discovered two ribosome sites that were modified by ubiquitin in response to H_2O_2 stress and were dependent on Hel2 (Figs 12-13). While previous studies have shown that Hel2-mediated ribosome ubiquitination was induced by 4-NQO oxidative stress [135], to my knowledge, this is the first time such Ub-modification was reported in response to peroxide stress. Based on my analysis of the dynamics of ribosomal protein ubiquitination induced by H_2O_2 and 4-NQO, I concluded that Hel2-dependent activity induced by peroxide occurred through a different mechanism than that induced by 4-NQO (Fig 15-16).

Further investigation revealed that ribosomal ubiquitination associated with quality control pathways, including the RQC and NGD, occurred specifically in response to nucleotide-damaging stress and not in peroxide conditions (Fig 15-16). Alternatively, the accumulation of K63 Ub definitive of the RTU occurred only in response to peroxide stress (Fig 16B). These findings indicate that the RQC and RTU pathways are induced in a stressor-specific manner and generate distinct ribosomal ubiquitin codes.

Finally, my findings suggest that overexpression of the RTU enzyme Rad6 hindered RQC-mediated clearance of 6xCGA stalled ribosomes in steady-state conditions. As this antagonism was not dependent on Rad6's ubiquitin conjugating activity, I proposed a model in which the intrinsic interactions between Rad6 and the ribosome alone are enough to prevent RQC activity in steady-state conditions. However, how the dynamics between Rad6 and the RQC are altered upon exposure to specific stressors is unknown.

4. Stressor-specific contributions of the RTU and RQC pathways to the broader regulation of translation and the cellular stress response

Chapter 4 is modified from a manuscript in preparation for publication. The pre-print version is available on BioRxiv [150]. The authors are Shannon E. Dougherty, Géssica C. Barros, Matthew W. Foster, Guoshou Teo, Hyungwon Choi, and Gustavo M. Silva. S.E.D. devised the project, completed data analysis, and wrote the manuscript under the supervision of G.M.S. S.E.D. and G.C.B. carried out experimental work.

While the investigation of ubiquitin-mediated mechanisms of translational control is important to understand the interruption of elongating ribosomes in stress conditions, their contributions to the regulation of total protein translation remain unclear. It is well-established that translation initiation, rather than elongation, is the prime target for the regulation of global protein synthesis [63, 238]. However, there is increasing evidence that ribosome stalling and collisions in elongation act as a feedback mechanism to trigger further downregulation of translation initiation [200, 202, 236]. As Ub-mediated translation regulation is the first line of defense for mediating halted ribosomes, it is logical that they would also function as a signal for control of upstream translation initiation. As such, it is crucial to understand the contributions of ubiquitin-mediated elongation control pathways, such as Ribosome-associated protein quality control (RQC) and Redox control of translation by ubiquitin (RTU), to the regulation of translation to fully dissect the complex nature of translational control in the cellular stress response.

In the following section (Section 4.1), I will review the Integrated stress response (ISR) as a key mechanism of translational reprogramming in cellular stress and its connection to the RQC and RTU pathways. In Section 4.2, I will investigate the dynamics of stressor-specific translation reprogramming and the stressor-specific influence of the RQC and RTU. Section 4.3 contains a detailed description of the methods used in this chapter's analysis, and Section 4.4 contains concluding remarks.

4.1 Review of Integrated stress response (ISR)

The Integrated stress response (ISR) is a stress-adaptive mechanism of translational reprogramming conserved in both yeast and mammals [70]. In yeast, the ISR was originally discovered as a response to amino acid starvation and thus was named the general amino acid control pathway (GAAC) [239, 240]. As the pathway was soon found to be activated by a multitude of cell stressors, including glucose starvation [241], ER (endoplasmic reticulum) stress [242], alkylating agents [202, 243], and oxidative stress [244, 245], it is now commonly referred to as the ISR. In the following section, I will review the mechanisms of the ISR pathway in *S. cerevisiae* and highlight the known links to both the RTU and RQC pathways.

4.1.1 Phosphorylation of eIF2α is the main driver of translation initiation inhibition and selective expression of stress response genes in the ISR

In response to various cellular stressors, the ISR pathway functions to suppress translation initiation and induce expression of selective stress response factors [70]. The central driver of this translation initiation suppression is the phosphorylation of the initiation factor eIF2α by the yeast kinase Gcn2 (Fig 21) [240]. eIF2α, in combination with eIF2β and eIF2γ, make up the eIF2 initiation complex (Fig 2A) [67]. As part of the initiation ternary complex, the eIF2 complex facilitates the binding of the initial methionine-charged tRNA (Met-tRNA$_i$) to the peptidyl tRNA binding site (P-site) of the small 40S ribosome through the hydrolysis of GTP to GDP (Fig 2C) [66]. Upon release from the 40S, the eIF2 complex must exchange its GDP for GTP in order to participate in another round of initiation [10]. In uninhibited initiation, the exchange of GDP for GTP is catalyzed by another initiation factor, eIF2B [67]. Upon phosphorylation of eIF2α (P-eIF2α), however, eIF2B is unable to mediate the recharging of the eIF2 complex with GTP, thus blocking new rounds of canonical (cap-dependent) translation initiation (Fig 2) [66, 240].

P-eIF2α slows the rate of canonical translation initiation, thereby suppressing global protein synthesis [70]. However, this slowed translation also promotes leaky scanning, in which ribosomes skip the first start codon and initiate translation at a downstream start codon [239, 240, 246]. It is through this mechanism of leaky scanning that essential stress response genes are expressed even when global translation is repressed [247, 248]. One of the most well-studied genes synthesized through the leaky scanning mechanisms of translation initiation is Gcn4 (ATF4 in mammals) (Fig 21) [40, 70, 249, 250]. The 5' untranslated region of the Gcn4 mRNA transcript contains four inhibitory upstream open reading frames (uORFS), which contain a start codon shortly followed by an in-frame stop codon (Fig 3) [70, 239]. In normal conditions, translation initiates at the inhibitory uORFs, but is quickly terminated, resulting in dissociation of the ribosome before the start codon of the main Gcn4 ORF is reached [236]. However, upon P-eIF2α, leaky scanning promotes translation of the main Gcn4 ORF, resulting in the translation of the otherwise suppressed gene (Fig 21)[40, 202, 251].

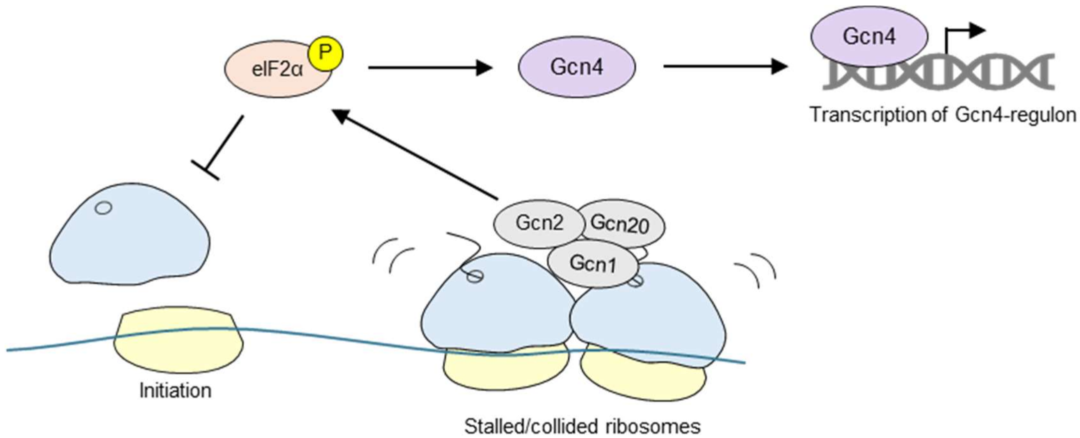

Figure 21: Diagram of Integrated stress response pathway (ISR). Cofactor Gcn1 binds to collided ribosome and along with Gcn20, promotes the Gcn2 kinase to phosphorylate initiation factor eIF2α. P-eIF2α inhibits translation initiation and promotes translation of the Gcn4 transcription factor. Gcn4 then promotes transcription of a set of stress response genes known as the Gcn4-regulon.

Expression of Gcn4 protein alone is not enough to rescue cells from stress conditions. Rather, Gcn4 acts as a transcription factor and is thought to regulate the expression of more than 500 mRNA transcripts [40, 243, 252]. Analysis of Gcn4 targets has revealed about 250 genes that are direct targets of Gcn4-induction upon amino acid starvation [251], now known as the Gcn4 regulon [200, 202]. Among the Gcn4 regulon are genes involved in amino acid biosynthesis, autophagy, and additional transcription factors [251].

While induction of the Gcn4 regulon has been well-studied in the context of amino acid starvation [239], Gcn4 is also known to be expressed in other stress conditions, including oxidative stress. Exposure to hydrogen peroxide (H_2O_2) stress was shown to induce phosphorylation of eIF2α and synthesis of Gcn4 independently of the Gcn2 kinase [54], but this response was not found to occur as a general oxidative stress response [40]. While 44 genes upregulated by Gcn4 in H_2O_2 stress were also found to be upregulated in amino acid starvation, a small number of peroxide-specific Gcn4 targets were also identified [40]. These findings suggest that Gcn4-controlled genes are not universally induced in all stress conditions but are uniquely induced in a stressor-specific manner.

In summary, the yeast ISR pathway inhibits canonical translation initiation through phosphorylation of eIF2α (P-eIF2α) by Gcn2. This also induces the expression of the Gcn4 transcription factor through leaky scanning translation initiation. However, it appears that the level of Gcn4 translation and expression of Gcn4-regulon genes are stressor-specific. As the ISR may be induced by ribosome collisions [200], it is critical to understand how regulation of translation elongation by the RQC and RTU contribute to overall translational reprogramming in specific stress conditions.

4.1.2 Regulation of Gcn2 by the RQC pathway

While P-eIF2α is the main suppressor of translation initiation in the ISR, it is the eIF2α kinase, Gcn2, that activates this suppression in response to stress in yeast [240]. Gcn2 was first identified to phosphorylate eIF2α in response to amino acid starvation and was hypothesized to be activated through binding of deacylated tRNAs [253, 254]. In addition to the deacylated tRNA-binding domain, Gcn2 contains a ribosome binding domain [255], identified to interact with the P stalk of ribosomes with empty acyl (A) tRNA binding sites [256, 257]. Several studies have shown the mammalian homolog of Gcn2 (GCN2) to be activated by stalled ribosomes independently of tRNA availability [231, 255, 256, 258, 259]. In yeast, the known Gcn2 cofactor, Gcn1, was found to interact with collided ribosomes (disomes) [260], suggesting the ribosome-centric model of Gcn2 activation found in mammalian cells is conserved in yeast. Further investigation of disome activation of Gcn2 in yeast has revealed that in addition to requiring Gcn1/Gcn20 cofactors, activation requires the ribosomal P-stalk [257].

As collided ribosomes are also targeted by the Ribosome-associated protein quality control pathway (RQC) [132, 200, 261], the Zaher lab has proposed a model in which the disome is a central nexus of both RQC and ISR activation in stress [202, 232]. In response to intermediate concentrations of MMS (0.33%-1%) stress proposed to induce ribosome collisions, the Zaher lab reported maximal levels of P-eIF2α and ubiquitinated uS3 [202]. Furthermore, they report saturation of P-eIF2α at lower levels of MMS in the absence of the E3 ligase, Hel2, suggesting that the ISR is activated upon a high-frequency of disomes [202]. However, while the oxidizing agent 4-NQO appeared to induce Hel2-dependent ubiquitination, it is unclear whether P-eIF2α was higher in *hel2*Δ [202]. Furthermore, RNA-seq analysis of the Gcn4 regulon suggested targets of Gcn4 regulation are upregulated in response to MMS stress and that this upregulation was enhanced upon deletion of *HEL2* [202]. As such, the Zaher lab proposed the RQC to antagonize disome activation of the ISR. Further investigation by the Zaher lab revealed that this antagonistic relationship was not due to direct competition by Hel2 for collided ribosomes but found Gcn4 to be highly expressed in response to MMS stress in the absence of Hel2 [232]. However, this upregulation did not appear to correlate with higher levels of P-eIF2α in *hel2*Δ [232], raising questions as to whether the induction of Gcn4 in the absence of Hel2 is mediated by Gcn2 phosphorylation of eIF2α or through an alternative mechanism.

4.1.3 P-eIF2α-independent induction of Gcn4 translation in the absence of the RTU pathway

Investigation into the impact of the Redox control of translation by ubiquitin pathway (RTU) on the ISR and expression of Gcn4 in H_2O_2 stress revealed that deletion of the E2 conjugase *RAD6* prevented phosphorylation of eIF2α but increased synthesis of Gcn4 [236]. While these results appear to contradict the established mechanism of Gcn4 induction by the ISR, it is not the first instance of P-eIF2α-independent Gcn4 translation. The leaky scanning that promotes the translation of Gcn4 is not only mediated through P-eIF2α but is known to be activation through depletion of 60S ribosomal subunits [262], depletion of the initiation factor eIF4E [85, 86], and through inhibition of Gcn4 degradation [87, 263, 264]. While the mechanism by which Gcn4 protein expression is heightened despite no increase of P- eIF2α in the absence of Rad6 remains unknown [236], it is clear that the peroxide-induced activity of the RTU acts as a feedback mechanism to control not only elongation but translation initiation.

4.2 Results

4.2.1 Enzymes of the RQC and RTU pathways contribute to global translation regulation in an oxidative stressor-specific manner

As suppression of global translation in response to stress is a crucial part of the cellular stress response, I first sought to establish the impact of the RQC and RTU on the rate of translation in specific oxidative stressors known to induce each pathway [116, 195, 202, 236]. To do so, we first established the rate of active translation in 0.6 mM H_2O_2 and a low (1 μg/mL) and high (5 μg/mL) concentration of 4-NQO [195] by measuring the incorporation of a methionine analog, homopropargylglycine (HPG)[5] (Fig 22A) [236]. Measurement of HPG incorporation showed that exposure to either H_2O_2 or 4-NQO led to a decrease in active translation in wild-type (WT) cells. Specifically, H_2O_2 treatment inhibited 90% of translation, while treatment with low (1 μg/mL) and high (5 μg/mL) 4-NQO inhibited 75% and over 95% of active translation, respectively (Fig 22A). It is logical that the level of translation inhibition in 4-NQO correlates with the intensity of the stress, with more translation inhibition in the high 4-NQO. However, this raises questions as to whether the differences observed between H_2O_2 and the low 4-NQO stress

[5] Experiment conducted by G.C.B

are due to differences in the intensity of oxidative stress experienced by the cell or due to the nature of the distinct oxidative stressors.

We then investigated whether the differences in translational suppression under H_2O_2 and 4-NQO were proportional to the intensity of oxidative stress in each examined condition. As oxidative stress is due to an overabundance of reactive oxygen species (ROS) [21], we utilized Tsa2, an antioxidant protein whose expression is known to be induced by ROS [265, 266], as a readout for oxidative stress intensity. The levels of Myc-tagged Tsa2 were measured upon exposure to H_2O_2 and 4-NQO by immunoblot[6] (Fig 22B). Tsa2-myc was found to be upregulated in H_2O_2 but not in either concentration of 4-NQO (Fig 22B), indicating that exposure to H_2O_2 generates more intense oxidative stress than even the high 4-NQO. These findings demonstrate that oxidative stress intensity does not correlate with the intensity of translation suppression (Fig 22A-B), suggesting that any differences are due to specific stressors.

[6] Experiment conducted by G.C.B

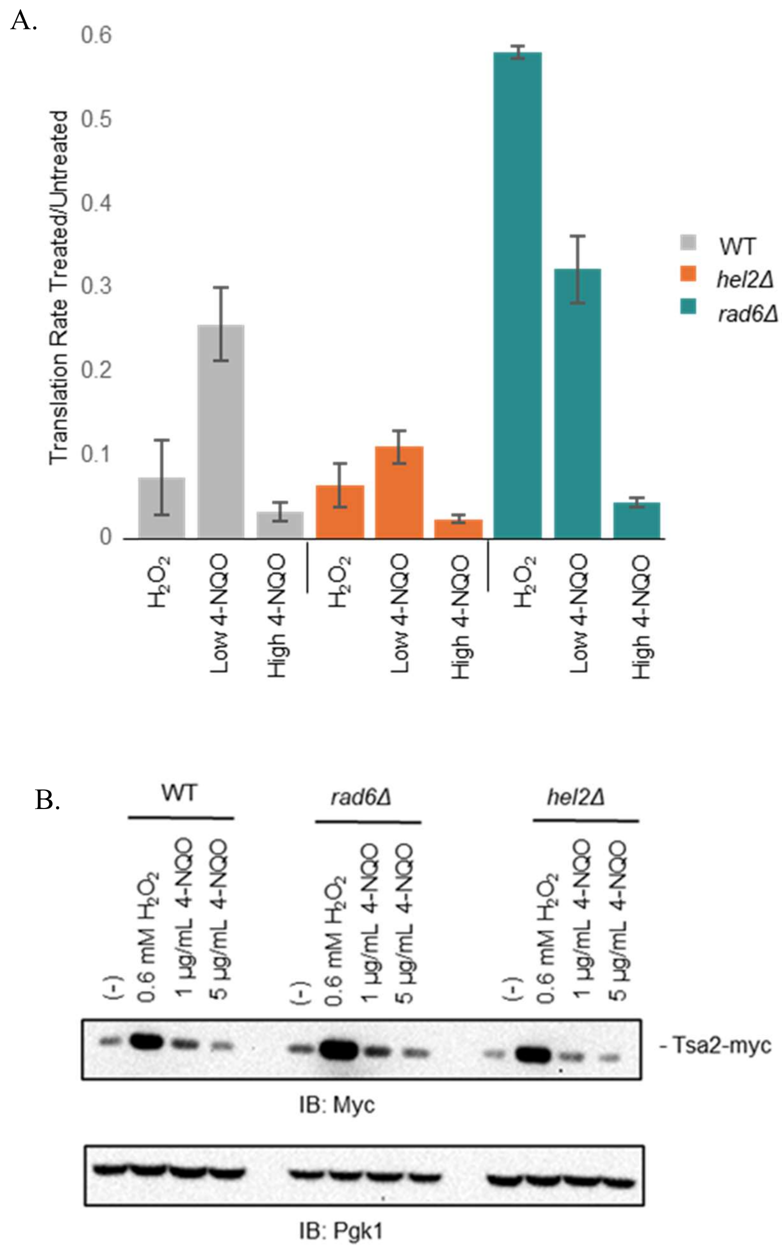

Figure 22: Translation suppression in oxidative conditions. A. Quantification of HPG incorporation during H_2O_2 (0.6 mM) and 4-NQO (1 µg/mL, 5 µg/mL) treatment normalized to untreated in WT, *hel2Δ*, and *rad6Δ*. B. Western blot for expression of Myc-tagged Tsa2 in untreated and H_2O_2 (0.6 mM) and 4-NQO (1 µg/mL, 5 µg/mL) treated WT, *rad6Δ*, and *hel2Δ* cells.

As I established that differences in translation rate were due to the differences between H_2O_2 and 4-NQO and not the intensity of oxidative stress, I hypothesized that the differences could be due to preferential induction of the RQC in 4-NQO and of the RTU in H_2O_2. To evaluate this hypothesis, we assessed the contribution of the RQC pathway to translation suppression upon exposure to the distinct oxidative stressors through HPG incorporation in *hel2*Δ. Translation suppression of *hel2*Δ did not significantly differ from WT upon exposure to H_2O_2 (Fig 22A). However, in low 4-NQO, active translation was further reduced from 75% inhibition in WT to 90% in *hel2*Δ (Fig 22A). These findings suggest that Hel2 hampers translation suppression specifically in response to 4-NQO stress and that translation is further repressed in its absence. This finding supports a model in which the accumulation of ribosome stalling and collisions in the absence of Hel2 promotes induction of the ISR and translation inhibition [202], but only upon exposure to nucleotide-damaging stressors. However, the impact of Hel2 on translation suppression is not observed in high levels of 4-NQO stress (Fig 22A), suggesting that there is a threshold of stress intensity in which Hel2 enables the cell to maintain active translation. Once the higher range of stress intensity is achieved, it appears that Hel2 is not sufficient to avoid exceeding the cellular limits for stress.

Next, to determine whether the RTU pathway had an H_2O_2-specific role in translation suppression, we measured HPG incorporation in the absence of Rad6. Consistent with previously reported findings [236], deletion of *RAD6* resulted in only 40% inhibition of translation in H_2O_2 compared to 90% in WT (Fig 22A). However, in the low concentration of 4-NQO, *rad6*Δ showed slightly higher, but statistically insignificant, levels of translation inhibition to WT, quantified as around 30% in *rad6*Δ to 25% measured for WT (Fig 22A). Finally, in high 4-NQO, translation inhibition was more than 95% for *rad6*Δ (Fig 22A). As exposure to high 4-NQO showed over

95% translation inhibition regardless of *HEL2* or *RAD6* deletion, it is likely that this level of stress overwhelms the cell's capacity to sustain any translation [267]. These findings show that Rad6 promotes translation inhibition in an H_2O_2-specific manner. Finally, analysis of active translation revealed distinct levels of suppression in response to H_2O_2 and 4-NQO stress that did not correlate with the level of ROS produced in each condition (Fig 22B), indicating that there is no universal translational control in response to oxidative stress.

Overall, these findings indicate that Hel2 and the induction of the RQC pathway are important for the broader cellular stress response in 4-NQO, while Rad6 and the RTU are important for the broader cellular stress response in H_2O_2. This supports a model of pathway competition wherein Rad6 and the RTU predominantly regulate translation elongation under peroxide stress, whereas the balance shifts towards Hel2 and RQC pathway regulation under 4-NQO stress. However, these pathways appear to have opposite effects on translation rate in their respective stressors, as Rad6 appears to promote translation suppression in H_2O_2 while Hel2 appears to maintain active translation in 4-NQO (Fig 22A). The mechanism by which they do so and the biological significance of their stressor-specific contributions to the broader cellular stress response remain unclear.

4.2.2 The RQC and RTU pathways influence translational reprogramming in a stressor-specific manner

To determine the biological significance of the stressor-specific influences of the RQC and RTU on global translation rates, I next sought to investigate their impact on the stressor-specific reprogramming of translation. To do so, I conducted a comparative analysis of gene expression from two published RNA-seq datasets [202, 236]. These datasets feature data collected from cells treated with MMS [202], an alkylating agent known to induce a similar response as 4-NQO [135], and from cells treated with H_2O_2 [236]. Analysis of the MMS dataset

[202] revealed that 121 genes of the Gcn4-regulon were upregulated by more than 50% in MMS (Fig 23A-B). Moreover, 75% of the transcripts induced by MMS stress were further induced in *hel2*Δ (Fig 23A), indicating that the cellular stress response is upregulated in the absence of Hel2. This finding is consistent with the further translation repression observed in *hel2Δ* in low 4-NQO stress (Fig 22A) and supports a model in which Hel2 and the RQC function delay activation of the cellular stress response in low-intensity stress.

Alternatively, analysis of the H_2O_2 RNA-seq dataset [236] revealed that only 4 genes of the Gcn4-regulon showed increased transcript levels in H_2O_2 stress in the wild-type strain (Fig 23A-B). Of these 4 genes, only 1, *CTT1*, a gene important for protection from hydrogen peroxide [268], was exclusive to H_2O_2 as the remaining 3 were also upregulated in MMS (Fig 23B). Evaluation of the Gcn4-regulon in *rad6*Δ revealed 29 genes to be upregulated by more than 50% of WT amounts. This number increased to 64 genes upon exposure of *rad6*Δ to H_2O_2 (Fig 23A), suggesting that the cellular response to H_2O_2 is elevated in the absence of Rad6. This finding contradicts previous data that showed less translation suppression in H_2O_2 in *rad6*Δ (Fig 22A) but supports a previously proposed model in which Gcn4 is upregulated in the absence of Rad6 independently of translation suppression [236].

In summary, comparative analysis of the previously published RNA-seq datasets revealed that the absence of Hel2 exacerbates selective expression of the Gcn4-regulon in MMS stress, suggesting that Hel2 functions to suppress the expression of selective stress response genes when the cell is exposed to nucleotide-damaging stress. Alternatively, the absence of Rad6 alone is enough to induce Gcn4-regulon expression, suggesting Rad6 plays an important role in mitigating stress, even in steady-state conditions. These findings support a model in which the RQC pathway acts to mitigate activation of the cellular translation response in low-intensity nucleotide-damaging stress while Rad6 performs a continuous role in mitigating ROS that is overwhelmed under peroxide stress. In terms of the broader cellular stress response, this model suggests that the RTU pathway acts as more of a preventative mechanism for cellular damage while the RQC acts as more of a failsafe mechanism after molecular damage occurs. However, this model is contrary to the expected results of ISR induction based on stressor-specific translation suppression (Fig 22A), which would suggest that *rad6Δ* would have less P-eIF2α than WT in H_2O_2 stress and, therefore, less upregulation of Gcn4. This contradiction raises questions as to whether the increased expression of the Gcn4 regulon in specific stress conditions is mediated by the ISR pathway.

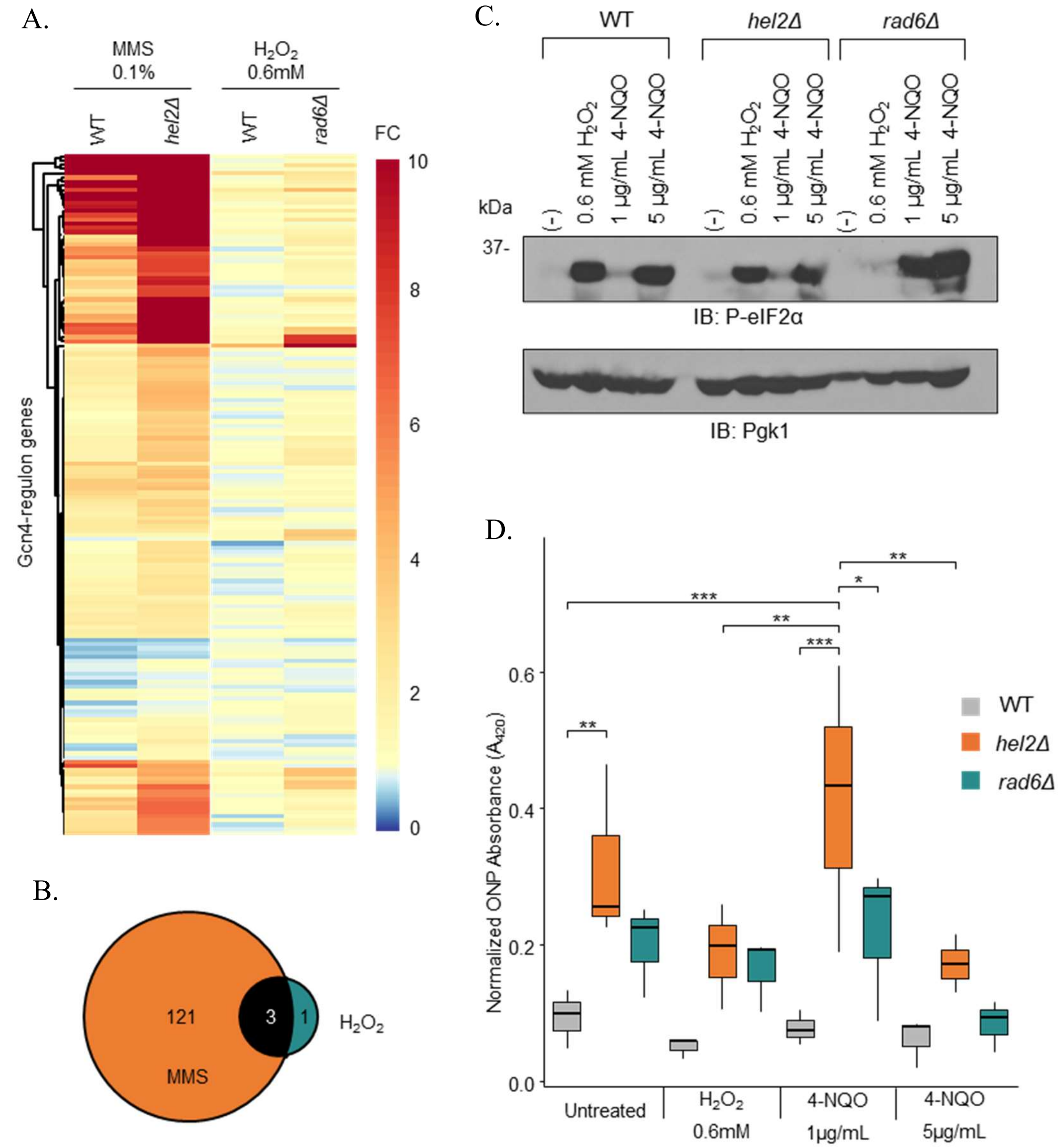

Figure 23: Induction of the ISR in oxidative stressors. A. Heatmap of RNA-seq meta-analysis of known GCN4-targeted stress response transcripts. Datasets from GSE150790 [202] and GSE226082 [236] were evaluated for differential expression of GCN4 target transcripts due to stress and pathway-specific induction. B. Venn diagram of more than 50% differentially expressed Gcn4-targeted genes in 0.6 mM H_2O_2 and 0.1% MMS compared to untreated. Datasets from GSE150790 [202] and GSE226082 [236]. C. Western blot of phosphorylated eIF2α in untreated and H_2O_2 (0.6 mM) and 4-NQO (1 µg/mL, 5 µg/mL) treated conditions for WT, *hel2Δ,* and *rad6Δ* cells. anti-Pgk1 was used as a loading control. D. Reporter assay for GCN4 activation by *GCN4-lacZ* fusion construct in WT, *hel2Δ,* and *rad6Δ*. ONPG absorption values detected at 420 nm were normalized to protein levels. Statistical significance was determined by pairwise student's t-test (* = $p < 0.05$, ** = $p < 0.005$, *** = $p < 0.0005$).

4.2.3 Stressor-specific contributions of the RQC and RTU to the ISR

To determine whether the stressor and pathway-specific induction of the Gcn4-regulon observed in the comparative analysis of the RNAseq datasets (Fig 23 A-B) was mediated by the ISR, I measured the levels of phosphorylated eIF2α (P-eIF2α) in response to stressor exposure in wild-type (WT) cells (Fig 23C, lanes 1-4). I observed a large increase of P-eIF2α in response to H_2O_2 and high 4-NQO (Fig 23C, lanes 2&4), but only a minor increase upon treatment in low 4-NQO (Fig 23C, lane 3). The amount of P-eIF2α measured in each stressor aligns with the level of translation suppression observed by HPG incorporation (Fig 22A), suggesting the ISR is largely responsible for the downregulation of global translation in response to both H_2O_2 and 4-NQO stress.

To determine the contribution of the RQC to ISR induction, I measured the level of P-eIF2α in response to the oxidative stressors in the absence of Hel2 (Fig 23C, lanes 4-8). The pattern of P-eIF2α in *hel2*Δ did not appear to differ from that observed in the wildtype strain (Fig 23C, lanes 1-4), suggesting that Hel2, and therefore the RQC, has minimal impact on ISR induction. This finding does not align with the further repression of translation observed in 4-NQO (Fig 22A) or with the increased expression of the Gcn4-regulon in MMS stress (Fig 23 A) upon *HEL2* deletion. However, similar levels of eIF2α phosphorylation between WT and *hel2*Δ strains upon treatment with low concentrations of MMS and 4-NQO have also been reported in the literature [202, 232]. It is plausible that in the absence of Hel2, the accumulation of uncleared disomes in low 4-NQO stress is severe enough to minimize active translation independent of the ISR pathway.

Next, I sought to dissect the contribution of the RTU to stressor-specific ISR induction by measuring the amount of P-eIF2α in the absence of Rad6 (Fig 23C, lanes 9-12). Consistent with published findings [236], P-eIF2α did not accumulate in response to H_2O_2 exposure in the absence of Rad6 (Fig 23C, lane 10). The lack of P-eIF2α in *rad6*Δ aligns with the higher rate of translation measured in H_2O_2 (Fig 22A) and indicates that Rad6 is crucial for ISR induction in the cellular response to peroxide stress. However, this finding does indicate that expression of the Gcn4-regulon in H_2O_2 stressed *rad6Δ* occurs through a P-eIF2α-independent mechanism [236]. Surprisingly, the deletion of *RAD6* resulted in the phosphorylation of eIF2α in low 4-NQO (Fig 23C, lane 11). As *rad6*Δ did not result in more translation inhibition in 4-NQO (Fig 22A), the function of this increase in P-eIF2α is unclear. Finally, exposure to the high 4-NQO stress appeared to induce similar levels of P-eIF2α regardless of *HEL2* or *RAD6* deletion (Fig 23C, lanes 4, 8, 12). This finding aligns with the suppression of active translation observed by HPG incorporation (Fig 22A) and suggests that the ISR becomes the prominent regulator of protein synthesis as stress levels intensify.

Overall, the measurement of P-eIF2α levels (Fig 23 C) revealed consistent trends with the inhibition of translation (Fig 22A) in wild-type cells across H_2O_2 and 4-NQO stressed conditions, indicating that the ISR is differentially induced based on stressor-specific conditions rather than the amount of ROS stress. While I did not observe the increase of phosphorylated eIF2α reported to occur upon deletion of *hel2*Δ [200] or upon exposure of *hel2*Δ to MMS stress [202], several pieces of published data also fail to show an increase of eIF2α phosphorylation in *hel2*Δ or in nucleotide-damaging stresses [202, 232]. The conflicting nature of my findings, in addition to those featured in the literature, highlights the sensitivity and complexity of the interplay between the RQC and the ISR pathways in stress and the need for further study. Finally, the meager amount of P-eIF2α detected in *rad6*Δ in H_2O_2 stress agreed with previously published findings (Fig 23C) [236]. However, I also observed an unexpected upregulation of P-eIF2α in *rad6*Δ upon low 4-NQO stress (Fig 23C). This finding suggests an inverse role for Rad6 in 4-NQO stress compared to its role in H_2O_2 and further supports the model in which Rad6 function is highly stressor-specific. However, neither 4-NQO stress in *hel2Δ* nor H_2O_2 stress in *rad6Δ* showed the increase of P-eIF2α expected from the analysis of Gcn4-regulon expression (Fig 23A). This finding calls into question whether the upregulation of genes within the Gcn4-regulon observed via RNA-seq (Fig 22A) is due to increased translation of Gcn4 in stress conditions, or through an alternative mechanism.

Finally, I sought to determine whether the upregulation of the genes within the Gcn4-regulon (Fig 23A) corresponded to increased levels of Gcn4. To do so, I measured the impact of the oxidative stressors on the translation of Gcn4 itself using an established Gcn4-lacZ reporter in wild-type (WT), *hel2Δ*, and *rad6Δ* strains [236, 269]. I first measured the amount of Gcn4 in untreated conditions to establish a baseline for each strain. Both *hel2*Δ and *rad6*Δ strains showed higher levels of Gcn4 than wild-type, quantified as more than 300% and 200% of WT Gcn4 levels, respectively (Fig 23D). While this finding aligns with expectations of increased Gcn4 upon deletion of *RAD6*, the amount of Gcn4 expressed in *hel2*Δ is unexpected in the absence of exposure to stress. However, this finding is in line with a model of ISR antagonism put forth by the Zaher lab [135].

To determine whether the amount of Gcn4 was stressor and pathway-specific, as predicted from the RNAseq data analysis, I measured the amount of Gcn4-lacZ in each strain upon treatment with H_2O_2 and 4-NQO. In H_2O_2, wild-type Gcn4 levels did not significantly differ from untreated conditions (Fig 23D). However, *hel2*Δ and *rad6*Δ strains both demonstrated about 200% of the amount of WT Gcn4 (Fig 23D). Despite expressing twice as much Gcn4 as WT, *hel2*Δ actually showed a decrease in Gcn4 in H_2O_2 stress compared to untreated amounts (Fig

23D), suggesting that Hel2 and subsequent activation of the RQC pathway are less essential in peroxide stress. Expression of Gcn4 in *rad6*Δ did not significantly change between untreated and H_2O_2 conditions (Fig 23D). This data is consistent with previous findings that the deletion of *RAD6* in steady-state conditions is enough to activate the cellular stress response [236].

While Gcn4 levels in wild-type and *rad6*Δ did not appear to significantly differ from untreated levels in low 4-NQO, Gcn4 in *hel2*Δ was quantified as over 400% of WT amounts (Fig 23D). The amount of Gcn4 measured in low 4-NQO for *hel2*Δ was higher than the amount measured in untreated *hel2*Δ, suggesting that Hel2 and subsequent RQC activity are important in the cellular response to low 4-NQO stress and not H_2O_2. In high 4-NQO, Gcn4 levels in wild-type and *rad6*Δ did not appear to differ significantly from those measured in WT untreated conditions (Fig 23D). Furthermore, *hel2*Δ showed only a modest increase of 150% compared to WT Gcn4 levels (Fig 23D). Compared to the effects of *hel2*Δ and *rad6*Δ on Gcn4 translation in steady-state conditions, deletion of *HEL2* and *RAD6* seemed to have less effect in high 4-NQO stress. This finding aligns with the substantial translation inhibition observed in 5 μg/mL 4-NQO regardless of gene deletion (Fig 22A) and suggests that even the translation of selective genes cannot be maintained at this stress intensity.

In summary, measurement of Gcn4 levels revealed that in the absence of Hel2, and subsequently the RQC, translation of Gcn4 is upregulated in response to the low concentration of 4-NQO but not in response to high 4-NQO (Fig 23D). This finding agrees with the Gcn4-regulon RNAseq data (Fig 23A) and indicates that expression of the Gcn4 regulon in 4-NQO is mediated by increased translation of Gcn4 independently of eIF2α phosphorylation (Fig 23C). Alternatively, Gcn4 was found to be similarly upregulated in untreated, H_2O_2, and low 4-NQO in *rad6*Δ (Fig 23D). While this finding seems to contradict the H_2O_2-specificity of RTU induction, Rad6 also serves a well-established function in DNA repair [270]. As 4-NQO specifically targets nucleotides, it is possible that the role of Rad6 in 4-NQO stress is distinct from its ribosome ubiquitinating activity observed in peroxide stress.

In all, these findings support a model in which Hel2 and the RQC oppose the activation of ISR in nucleotide-damaging stress but still induce selective translation of stress-response genes through an ISR-independent mechanism. This opposition appears to function as a first line of defense, as the RQC does not appear to be sufficient to prevent the cell's capacity from being overwhelmed by high-intensity stress. Additionally, Hel2 was observed to be even less crucial for Gcn4 translation in H_2O_2 stress than in untreated conditions (Fig 23D), suggesting that its opposition to the ISR pathway is stressor-specific. Alternatively, levels of translated Gcn4 in *rad6Δ* appeared to be similar regardless of stressor exposure, consistent with reports that the cellular stress response is already activated in the absence of Rad6 [236]. This further supports a preventative role for Rad6 in the broader cellular stress response.

4.3 Methods

4.3.1 Yeast strain generation, protein extraction, ribosome sucrose sedimentation, western blot

For yeast strain generation and growth conditions, refer to section 3.3.1. For yeast protein extraction, refer to section 3.3.2. 1X Phosphatase Inhibitor (Sigma-Aldrich #P5726) was added to the standard lysis buffer for samples probed for phosphorylated proteins by western blot. For ribosome sucrose sedimentation and western blot, refer to sections 3.3.3 and 3.3.4 respectively.

4.3.3 Translation rate assay

The indicated SUB280-derived yeast strains were grown to mid-log phase in SD complete medium and back diluted to OD600 0.1-0.2 in SD -Met medium. Cells were treated with 50 µM of HPG (L-Homopropargylglycine, Sigma, #900893) at OD600 0.4-0.5. Cells were collected by centrifugation after 15, 30 and 45 min of HPG incubation at 30°C with agitation. For stress treatment, cells were incubated with 0.6 mM H_2O_2, 1 µg/mL 4-NQO, or 5 µg/mL 4-NQO for 15 min prior to HPG incubation for the times listed above. Pelleted cells were fixed overnight in 70% ethanol at 4°C. HPG conjugation with Alexa Fluor 488 was done with the Click-iT HPG Alexa Fluor Protein Synthesis Assay (ThermoFisher #C10428) per the manufacturer's protocol. Alexa Fluor 488 fluorescent signal was measured in the BD FACS Symphony A1 flow cytometer using a 488 nm laser. FlowJo Software (Becton Dickinson) was used for single-cell population gates, histogram plots, and mean calculations.

4.3.4 Gcn4 target mRNA-seq analysis

RNA-seq data from WT and hel2Δ cells in the presence and absence of 0.1% MMS treatment (GSE150790) [202] and from WT and rad6Δ cells in the presence and absence of 0.6 mM H2O2 treatment (GSE226082) [236] were analyzed for differential expression of known targets of Gcn4 transcription regulation. Statistically significant differences in transcript expression were calculated in RStudio using a 2-way ANOVA and post hoc comparisons with multiple testing corrections with the Benjamini-Hochberg procedure.

4.3.5 Gcn4-lacZ reporter assay

GCN4-lacZ expressing yeast cells from the indicated SUB280-derived strains were grown to mid-log phase and disrupted by glass bead agitation at 4°C in buffer containing 1x PBS, 40 mM KCl, 10 mM MgCl2. Extracts were clarified by centrifugation, and protein concentration was quantified by BCA assay (ThermoFisher #23225). 120 ug of protein was combined with substrate containing 15mM ONPG (2-Nitrophenyl-β-D-galactopyranoside)(Goldbio, #N27510), 5mM DTT, 1x PBS, 40mM KCl, and 10mM MgCl2, and incubated for 60 min at 30°C. Absorbance was read at 420 nm in a Tecan Sunrise plate reader (Tecan # 30190079).

4.4 Conclusion

My investigation into the contributions of the RQC and RTU to the broader translation response to cellular stress exposure revealed that each pathway acts as a feedforward mechanism for the control of translation initiation by the ISR pathway. The RQC enzyme, Hel2, was observed to mitigate translation suppression and the translation of Gcn4 in 4-NQO, but not H_2O_2 stress (Fig 22-23). Although I did not observe increased phosphorylation of eIF2α in response to low 4-NQO in either WT or *hel2Δ* as reported in the literature [200, 202], this may be due to the different cellular effects of 4-NQO and MMS stress. While MMS and 4-NQO stresses have been similarly grouped due to their tendency to damage nucleotides [195, 202], it is also likely that each agent induces a highly specific cellular stress response. This likelihood is further underscored by my findings of the drastic differences between the cellular response to 4-NQO and H_2O_2 (Fig 22-23), indicating that response to oxidative stress is not universal.

In H_2O_2 stress, Rad6 was observed to be crucial for the phosphorylation of eIF2α (Fig 23C) but not for the translation of Gcn4 (Fig 23D). This agrees with previous findings [236] and suggests the impact of Rad6 on Gcn4 translation occurs through a P-eIF2α-independent mechanism. Upon low 4-NQO stress, Rad6 appeared to have the opposite effect on the phosphorylation of eIF2α, as P-eIF2α was upregulated in its absence (Fig 23C). However, this may be due to Rad6's role in DNA repair [270], rather than its role in translation regulation. In addition to its role in the RTU pathway, Rad6 promotes bypass of DNA damage and completion of DNA replication through ubiquitination of the DNA polymerase factor, PCNA [270, 271]. As nucleotide-damaging agents, both MMS and 4-NQO have been found to induce PCNA ubiquitination [272, 273]. In the absence of Rad6, the DNA damage from 4-NQO exposure may go unaddressed and could lead to activation of the ISR [274]. Even if this hypothesis is later found to be incorrect, it is apparent from these findings that Rad6's impact on ISR induction seems to vary in a stressor-specific manner.

Overall, these findings support a model in which RTU induction in peroxide stress serves as an early defense mechanism to shut down translation before damage can occur. Alternatively, the induction of the RQC appears to function in an attempt to mitigate the effects of already existing damage arising from treatment with nucleotide-damaging stressors.

5. Conclusion

5.1 Summary of Findings

Ubiquitination of the ribosome is a key feature of multiple translational control pathways, including Redox control of translation by ubiquitin (RTU) and Ribosome-associated protein quality control (RQC). However, how ribosomal Ub-modification occurs due to each pathway and its downstream implications in stress conditions previously remained unexplored. In this dissertation, I dissected the complex code of ribosomal ubiquitination and associated translational control pathways in response to oxidative stressors. I found site-specific Ub-modification of the ribosome to vary in abundance, E2-E3 dependency, stressor sensitivity, and importance for the broader cellular response to stress.

In Chapter 2, I developed and optimized a targeted mass spectrometry (MS)-based proteomics approach to detect and quantify site-specific ribosomal Ub-modification in response to hydrogen peroxide (H_2O_2) exposure. This analysis identified 11 sites that were significantly modified in response to stress. Further analysis revealed that ubiquitination of the two most abundant Ub-modified sites, uS5.K33 and uS10.K8, was largely mediated by the E3 ligase, Hel2. However, some Ub-modification of uS10.K8 was observed in the absence of Hel2, suggesting a novel role of uS10 ubiquitination outside of its established role in the RQC pathway. Additionally, the ubiquitination of four other ribosomal sites significantly increased in the absence of Hel2. Three of these sites are located near the region of deacylated-tRNA release and are ideal candidates for further investigation into how ribosomal K63 Ub mediates ribosome pausing in peroxide stress.

In Chapter 3, I explored the interplay between the RQC and RTU pathways in oxidative stress conditions at the level of ribosomal protein (RP) ubiquitination, the influence of pathway-specific enzymes, and stressor-specific pathway induction. Results from this analysis supported the novel, Hel2-independent mechanism of uS10 ubiquitination first elucidated in Chapter 1. Measurement of ubiquitination dynamics in two oxidative stressors revealed RTU-related K63 Ub accumulation to be a distinct response to peroxide stress. Conversely, ubiquitination of the known Hel2 target, uS3, was found to occur only in response to nucleotide-damaging stressors and not H_2O_2. Finally, overexpression of the RTU enzyme Rad6 was found to oppose RQC activity independent of its ability to ubiquitinate. The results of this analysis indicate a highly stressor-specific role for both the RTU and RQC-mediated ribosome ubiquitination.

Finally, in Chapter 4, I sought to further dissect the biological impact of the stressor-specific activation of each of the RQC and RTU pathways on the broader cellular stress response. I observed that cells lacking the RQC enzyme, Hel2, showed increased translation of the transcription factor, Gcn4, upon exposure to a low concentration of 4-NQO stress but reduced levels in H_2O_2 compared to untreated amounts. My findings support a model in which Hel2 and the RQC function to maintain active translation and delay activation of the broader cellular stress response as a first line of defense against low doses of nucleotide-damaging stress. However, when the system is overwhelmed, the activity of the RQC is not enough to prevent ISR activation. Additionally, cells lacking the RTU enzyme Rad6 appeared to show a decrease of P-eIF2α in H_2O_2 but an increase in 4-NQO compared to wild-type cells in each respective condition. My findings support a peroxide-specific role for Rad6 and the RTU in promoting ISR and translation inhibition. In response to nucleotide-damaging stress, however, I hypothesize that Rad6's function in DNA damage repair, rather than its role in K63 Ub of the ribosome, is crucial to maintain active translation.

5.2 Future Directions

While this work has made crucial strides in dissecting the complex code of ribosome ubiquitination and translational control in oxidative stress, many questions remain unanswered.

5.2.1 Elucidating the mechanistic details of how ribosomal K63 Ub pauses ribosomes in the RTU pathway

In this work, I discovered 5 ribosomal sites that were Ub-modified independently of the E3 ubiquitin ligase Hel2 in response to hydrogen peroxide (H_2O_2) stress, but it remains unclear which, if any, are required to trap ribosomes in the pretranslocation stage of elongation. As three of these sites (uL5.K35, uL5.K49, and eS25.K52) are all located near the tRNA exit (E-site) (Fig 1A-B, 13D), I predict that ubiquitination of these sites disrupts the release of deacylated-tRNA from the ribosome and halts translation elongation (Fig 3E). To evaluate this hypothesis, one could mutate these sites from lysine (K) to arginine (R) to prevent ubiquitination. If Ub-modification of these sites is crucial for trapping ribosomes in the pretranslocation state of elongation [56], one should observe a loss of ribosome pausing upon treatment with H_2O_2. To investigate whether Ub-modification of these sites disrupts tRNA release, as I hypothesize, one could employ single molecular fluorescence resonance energy transfer (FRET) to determine whether the site-specific K to R mutations alter the kinetics of tRNA release from the ribosome [74].

Identifying those ribosome sites that are ubiquitinated in response to H_2O_2 exposure would open new investigative avenues into the mechanisms by which ubiquitin induces ribosome pausing in the RTU pathway. Through site-specific mutations that prevent Ub-modification, the role of the RTU pathway can be more readily dissected from other translational control pathways, such as the RQC. Furthermore, as Rad6 performs numerous functions within the cell [139], mutating specific sites would also enable one to distinguish the impact of Rad6 on translation from its other functions. As such, continued investigation into the importance of each of the identified ribosome sites for the accumulation of K63 ubiquitination, interactions between the ribosome and various translation factors, and translational pausing, must be undertaken to decode the mechanistic details of the RTU response.

5.2.2 Dissecting the coordination of the RTU and RQC pathways and their contributions to the cellular response in oxidative stress conditions

This work has highlighted a novel role for site-specific ubiquitination of ribosomal protein uS10 from its established role as a target of Hel2 in the RQC pathway. While some studies have suggested the RQC to be induced in oxidative stress conditions, my observation of Hel2-independent uS10-Ub calls into question whether other reports of uS10 ubiquitination in oxidative stress are directly related to RQC pathway induction. My attempts to dissect the functions of the RTU and RQC pathways in two oxidative stressors highlight the complex and intertwined nature of ribosomal Ub-mediated translational control pathways. This complexity was further corroborated by my attempts to dissect the contributions of each pathway to broader translational control of stress. As far as we know, exposure to H_2O_2 stress does not lead to increased ubiquitination of uS3, recruitment of RQC factors to the ribosome, or clearance of 6xCGA stalled ribosomes. This suggests that the RTU is the predominant pathway activated in response to H_2O_2 stress. Meanwhile, as the RTU is not induced in 4-NQO, the RQC pathway appears to be the predominant pathway activated by nucleotide-damaging stress.

Investigation into the role of these stressor-specific pathways in the broader cellular stress response support a model in with the RTU pathway functions as a preventative mechanism to counter peroxide stress before cellular damage can occur. Alternatively, the RQC pathway appears to act as a first line of defense in response to nucleotide-damaging stress. In low intensity stress, the RQC seems to mitigate the effects of stress-induced damage and delay activation of the broader cellular stress response. However, RQC activity does not appear to be sufficient to counteract the effects of high-intensity stress in which the cell's capacity to maintain translation is exceeded.

While each the RTU and RQC have been discussed based on their role in the oxidative stress response [116, 135], it is clear from this study that these pathways are not equally susceptible to all oxidizing agents. Distinguishing the contexts in which the RTU and RQC pathways occur is critical to dissect the complex coordination of regulatory pathways that make up the cellular stress response. This could be done through further investigation into the activation of these pathways in alternative stress conditions, such as nucleotide-specific damaging agents like MMS [135, 202], superoxide generators such as xanthine oxidoreductase (XOR) [275], or ribosome stalling agents such as cycloheximide and anisomycin [231]. By examining the activity of the RTU and RQC, as well as the patterns of ribosome ubiquitination associated with each stress condition, we can better decipher the ribosome ubiquitin code and its implications for translational control and the broader cellular stress response.

5.3 Contributions to the field

In this work, I developed and optimized a novel MS-based approach to detect and quantify site-specific ribosomal ubiquitination. This method will be crucial to further dissect the dynamics of the ribosomal ubiquitin code in various stress conditions and will aid in the further dissection of RTU and RQC pathway induction. This method can be further adapted to investigate differences in site-specific Ub-modification in the absence of various enzymes, on different subcellular ribosome populations, and in different cell types. As the ribosome is highly conserved between *S. cerevisiae* and higher eukaryotes, this MS-based ubiquitinomics approach can be readily adapted to quantify ribosome ubiquitination in mammalian cells, thereby expanding the application of this method to the study of disease states and progression. With such high specificity and the ability to perform absolute quantification, this MS-based ubiquitinomics method could potentially be applied to diseased cells, providing specific targets for manipulation at the disease, or even patient-specific level.

Additionally, investigation into the role of RTU E2 conjugase, Rad6, revealed novel antagonism of RQC pathway activity and highlighted its importance for the cellular translational stress response in nucleotide-damaging stress. This finding highlights a new role for Rad6 that may be conserved in its human homolog, UBE2A [139]. As UBE2A deficiency, also known as Nascimento syndrome, is linked to congenital malformation [276], understanding how the deletion of *RAD6* affects cellular function in *S. cerevisiae* could provide crucial insights into cellular dysfunction associated with the disorder.

Appendix

A.1 Supplemental Tables

Table A1: Ribosome-target PRM (Rt-PRM) peptides and fold change (FC) of WT H_2O_2 Treated to Untreated

Universal Peptide Name	Sequence	Bio Precursor m/z	Heavy Precursor m/z	log2FC	P-value
uL2.K145	ASGNYVIIIGHNPDENK(GG)TR	738.0417+++	741.3778+++ (heavy)		
uL3.K153	K(GG)YASVVR	468.7667++	473.7708++ (heavy)	1.93	0.0971
uL3.K281	TSINHK(GG)IYR	415.8948+++	419.2309+++ (heavy)	1.99	0.0345
uL3.K287	VGK(GG)GDDEANGATSFDR	584.9310+++	588.2671+++ (heavy)	0.97	0.0240
uL3.K340	K(GG)SLYTNTSR	592.3069++	597.3111++ (heavy)	1.38	0.0124
uL5.K35	ASK(GG)VLEQLSGQTPVQSK	638.6812+++	641.3526+++ (heavy)	1.83	0.0081
uL5.K35.49	ASK(GG)VLEQLSGQTPVQSK(GG)AR				
uL5.K49	VLEQLSGQTPVQSK(GG)AR	619.0059+++	622.3420+++ (heavy)	1.16	0.0364
uL5.K75	GPK(GG)AEEILER	419.2262+++	422.5623+++ (heavy)	0.38	0.1137
eL6.K108	FNVEYFAK(GG)EK	463.5663+++	466.2377+++ (heavy)	0.45	0.4641
eL8.K213	AEDEAALAK(GG)LVSTIDANFADK				
eL13.K81	GFTLAEVK(GG)AAGLTAAYAR	642.0144+++	645.3505+++ (heavy)	0.83	0.2793
eL15.K33	QK(GG)NVIHR				
eL15.K83	GATYGK(GG)PTNQGVNELK	597.6392+++	600.3106+++ (heavy)	1.61	0.0240
eL15.K83.92	GATYGK(GG)PTNQGVNELK(GG)YQR				
eL15.K92	GATYGKPTNQGVNELK(GG)YQR	746.7136+++	750.0497+++ (heavy)	3.04	0.2229
uL15.K96	SASK(GG)ETAPVIDTLAAGYGK	665.0127+++	667.6841+++ (heavy)	1.06	0.1173
eL18.K31	LLVK(GG)LYTFLAR	484.2975+++	487.6336+++ (heavy)		

eL18.K98	IFEFPK(GG)TTVAALR	536.3032+++	539.6393+++ (heavy)	0.83	0.1778
eL18.K133	APK(GG)GQNTLILR	442.2614+++	445.5975+++ (heavy)	0.61	0.1869
eL20.K38	IFASNEVIAK(GG)SR	483.6001+++	486.9361+++ (heavy)	0.16	0.3719
eL20.K71	ASGEIVSINQINEAHPTK(GG)VK	750.4010+++	753.0724+++ (heavy)	0.84	0.1557
eL20.K131	VAEIEK(GG)TADVK	439.5734+++	442.2448+++ (heavy)	0.75	0.3114
eL20.K149	DLK(GG)FPLPHR	412.8998+++	416.2359+++ (heavy)	1.35	0.1505
eL22.K99	FVSTK(GG)TNEYR	453.5615+++	456.8976+++ (heavy)	1.29	0.0080
uL22.K89	SVK(GG)FVQGLLQNAAANAEAK	691.7078+++	694.3792+++ (heavy)	0.79	0.3466
uL23.K74	VIEQPITSETAMK(GG)K	563.6344+++	566.3058+++ (heavy)	0.02	0.9306
uL23.K100	AVK(GG)ELYEVDVLK	507.2837+++	509.9551+++ (heavy)	0.16	0.5739
uL29.K25	EQLASQLVDLK(GG)K	495.9472+++	498.6186+++ (heavy)	0.86	0.1145
eL30.K19	LALVIK(GG)SGK	521.8346++	525.8417++ (heavy)	1.09	0.2921
eL30.K5	APVK(GG)SQESINQK	481.5914+++	484.2628+++ (heavy)	0.82	0.0727
eL38.K61	GSSSLYTLVINDAGK(GG)AK	613.3267+++	615.9981+++ (heavy)	1.83	0.1441
P2.K61	GSLEEIIAEGQK(GG)K				
uS3.K45	VTPTK(GG)TEVIIR	457.6049+++	460.9410+++ (heavy)	-0.01	0.9632
uS3.K75	INELTLLVQK(GG)R	480.9559+++	484.2920+++ (heavy)	0.12	0.7328
uS3.K106	GLSAVAQAESMK(GG)FK	527.6082+++	530.2796+++ (heavy)	0.21	0.3924
uS3.K200	TGPK(GG)ALPDAVTIIEPK	588.6682+++	591.3396+++ (heavy)	0.2	0.3348
eS4.K155	YPDPNIK(GG)VNDTVK	539.6141+++	542.2855+++ (heavy)	0.23	0.2495
eS4.K168	IDLASGK(GG)ITDFIK	512.2874+++	514.9588+++ (heavy)	0.41	0.2925
eS4.K174	ITDFIK(GG)FDAGK	684.8615++	688.8686++ (heavy)	0.19	0.5829
uS5.K33	NTEEK(GG)GWVPVTK	501.2597+++	503.9311+++ (heavy)	1.3	0.0415
uS5.K119	TAK(GG)EVAGAIR	565.3198++	570.3240++ (heavy)	0.33	0.1656
eS6.K116	KGEQELEGLTDTTVPK(GG)R				

eS7a.K83	ELEK(GG)K				
eS7a.K84	K(GG)FQDR				
eS7a.K83.84	ELEK(GG)K(GG)FQDR				
eS7b.K84	K(GG)FPDR				
eS7b.K83.84	ELEK(GG)K(GG)FPDR	474.2442+++	477.5802+++ (heavy)		
eS7.K151	IQK(GG)VLLDSK	579.3481++	583.3552++ (heavy)	1.12	0.0958
eS7.K157	VLLDSK(GG)DVQQIDYK	593.3159+++	595.9873+++ (heavy)		
uS7.K212	GSSTSYAIK(GG)K	578.3039++	582.3110++ (heavy)	0.82	0.0462
uS8.K88	IGDIEK(GG)WTANLLPAR	604.3319+++	607.6679+++ (heavy)	3.07	0.0142
eS10.K25	KDFNQAK(GG)HEEIDTK				
eS10.K31	DFNQAK(GG)HEEIDTK	563.6007+++	566.2721+++ (heavy)	0.17	0.5754
eS10.K38	HEEIDTK(GG)NLYVIK	572.6369+++	575.3083+++ (heavy)	0.24	0.3907
eS10.K52	ALQSLTSK(GG)GYVK	470.2647+++	472.9361+++ (heavy)	-0.02	0.9214
uS10.K6	SDFQK(GG)EKVEEQEQQQQQIIK	868.7682+++	871.4396+++ (heavy)	4.13	0.0024
uS10.K6_1	SDFQK(GG)EK	498.2433++	502.2504++ (heavy)		
uS10.K6.K8	SDFQK(GG)EK(GG)VEEQEQQQQQIIK	906.7825+++	909.4539+++ (heavy)		
uS10.K8	EK(GG)VEEQEQQQQQIIK	667.0079+++	669.6793+++ (heavy)	2.86	0.0031
uS10.K21	VEEQEQQQQQIIK(GG)IR	671.0237+++	674.3598+++ (heavy)	0.12	0.5493
uS10.K32	VK(GG)QLENVSSNIVK	524.6299+++	527.3013+++ (heavy)	0.26	0.2718
uS10.K43	QLENVSSNIVK(GG)NAEQHNLVK	595.3160++++	597.3196++++ (heavy)	0.46	0.0579
uS10.K64	LPTK(GG)VLKISTR				
uS10.K101	YIDLEAPVQIVK(GG)R	553.3139+++	556.6500+++ (heavy)	0.52	0.0914
eS12.K85	LVEGLANDPENK(GG)VPLIK	655.0335+++	657.7049+++ (heavy)	-0.06	0.7958
eS12.K95	VADAK(GG)QLGEWAGLGK	552.9616+++	555.6330+++ (heavy)	-0.22	0.5494
eS12.K105	QLGEWAGLGK(GG)IDR	519.6108+++	522.9469+++ (heavy)	0.71	0.0777
eS12.K114	K(GG)VVGASVVVVK	400.2554+++	402.9268+++ (heavy)	0.64	0.5733

uS12.K56	GIVLEK(GG)LGIESK	467.2767+++	469.9481+++ (heavy)	1.98	0.0576
uS12.K114	AK(GG)GDIPGVR	513.7882++	518.7923++ (heavy)	1.67	0.0293
uS13.K96	QNDITDGK(GG)DYHTLANNVESK	792.7069+++	795.3783+++ (heavy)	0.51	0.1608
uS15.K43	K(GG)GLTPSQIGVLLR	499.3033+++	502.6394+++ (heavy)	0.41	0.3087
eS17.K23	YYPK(GG)LTLDFQTNKR	634.3354+++	637.6715+++ (heavy)		
eS17.K23.32	YYPK(GG)LTLDFQTNK(GG)R	672.3497+++	675.6858+++ (heavy)		
eS17.K81	K(GG)DQYVPEVSALDLSR	611.9829+++	615.3190+++ (heavy)	0.79	0.0979
eS17.K116	SLGLK(GG)LPLSVINVSAQR	637.0458+++	640.3819+++ (heavy)	2.43	0.0137
eS19.K119	IGIVEISPK(GG)GGR	447.2613+++	450.5973+++ (heavy)	1.78	0.0576
uS19.K24	GVDLEK(GG)LLEMSTEDFVK				
uS19.K64	AAK(GG)LAAPENEKPAPVR	592.6636+++	595.9997+++ (heavy)	0.95	0.1294
uS19.K64.72	AAK(GG)LAAPENEK(GG)PAPVR	630.6779+++	634.0140+++ (heavy)		
uS19.K72	LAAPENEK(GG)PAPVR	502.6072+++	505.9433+++ (heavy)	0.63	0.1738
eS21.K38	ADDHASVQINVAK(GG)VDEEGR	723.0173+++	726.3534+++ (heavy)	0.24	0.6164
eS25.K46	AQHAVILDQEK(GG)YDR	600.6393+++	603.9754+++ (heavy)	0.75	0.1040
eS25.K52	ILK(GG)EVPTYR	411.5714+++	414.9075+++ (heavy)	1.71	0.0217
eS25.K70	LK(GG)IGGSLAR				
eS28.K4	MDNK(GG)TPVTLAK	444.5711+++	447.2425+++ (heavy)		
eS31.K107	LAVLSYYK(GG)VDAEGK	557.2980+++	559.9694+++ (heavy)	1.14	0.0748
Ub.K6	MQIFVK(GG)TLTGK	460.5954+++	463.2668+++ (heavy)	2.38	0.0844
Ub.K6.11	MQIFVK(GG)TLTGK(GG)TLTGK				
Ub.K11	TLTGK(GG)TITLEVESSDTIDNVK	793.4147+++	796.0861+++ (heavy)	1.63	0.0620
Ub.K27	TITLEVESSDTIDNVK(GG)SK				
Ub.K29.33	SK(GG)IQDK(GG)EGIPPDQQR				
Ub.K29	SKIQDK(GG)EGIPPDQQR				
Ub.K33	IQDK(GG)EGIPPDQQR				

Ub.K48	LIFAGK(GG)QLEDGR	487.6001+++	490.9361+++ (heavy)	2.02	0.0022
Ub.K63	TLSDYNIQK(GG)ESTLHLVLR	748.7376+++	752.0737+++ (heavy)	2.98	0.0221
uL10.K132	AVNTGMEPGK(GG)TSFFQALGVPTK				
Ub.K27.29	TITLEVESSDTIDNVK(GG)SK(GG)IQDK				
uS3.K212	ALPDAVTIIEPK(GG)EEEPILAPSVK				
uL2.K92	ASLNVGNVLPLGSVPEGTIVSNVEEKPG DR				
uL11.K146	VDFK(GG)NPHDIIEGINAGEIEIPEN				
eL19.K186	RDALLK(GG)EDA				

Table A2: *Saccharomyces cerevisiae* strains used in this study

Yeast strain	Relevant genotype	Genetic background	Reference
SUB280	pUB39 *Ub*	MATa *lys2-801 leu2-3,112 ura3-52 his3-D200 trp1-1[am] ubi1-D1::TRP1 ubi2-D2::ura3 ubi3-Dub-2 ubi4-D2::LEU2* [pUB39 Ub, *LYS2*][pUB100, *HIS3*]	Finley *et al*., 1994
GMS131	*rad6::KanMX6*	SUB280	Silva *et al.,* 2015
GMS133	*bre1::KanMX6*	SUB280	Silva *et al.,* 2015
GMS135	*rad6::KanMX6 bre1::URA3*	SUB280	this study
GMS139	*hel2::KanMX6*	SUB280	Back *et al*., 2019
GMS676	*gcn1::GCN1-myc NatMX6*	SUB280	this study
GMS678	*gcn2::GCN2-myc NatMX6*	SUB280	this study
SUB62		MATa *his3-Δ200 leu2-3, 112 ura3-52 lys2-801 trp1-1*	Finley *et al*., 1994
GMS255	*rad6::NatMX6*	SUB62	this study
GMS256	*bre1::NatMX6*	SUB62	this study
GMS257	*ubp2::NatMX6*	SUB62	this study
GMS258	*hel2::NatMX6*	SUB62	this study
W303-1a		MATa *ade2 his3 leu2 trp1 ura3 can1*	
YMY46	*uS10-3HA::hisMX6*	W303-1a	Matsuo *et al.,* 2017
YSG039	*uS5-3HA::hisMX6*	W303-1a	Sugiyama *et al*., 2019

Table A3: Plasmids used in this study

Plasmid No.	Vector	Gene	Mutation	Tag	Reference
p025	pYES 2.0	-	-	-	Simões *et al.*, 2022
p055	p415 (Met25p)	-	-	-	
p057	p416	*GFP-FLAG-HIS3*	-	-	Matsuda *et al.*, 2013
p059	p416	*GFP-R(CGA)6-FLAG-HIS3*	-	-	Matsuo *et al.*, 2017
p028	pYES 2.0	*RAD6*	-	HA (C-term)	Simões *et al.*, 2022
p032	pYES 2.0	*RAD6*	C88S	HA (C-term)	Simões *et al.*, 2022
p110	pYES 2.0	*rad6(aa1-149)*	-	HA (C-term)	Simões *et al.*, 2022
p114	pYES 2.0	*RAD6*	D60L/E61L/E62L	HA (C-term)	Simões *et al.*, 2022
p116	pYES 2.0	*RAD6*	C88A	HA (C-term)	Simões *et al.*, 2022
p149	p180	*Gcn4-LacZ*			Gerashchenko *et al.*, 2012
p222	p416 (Met25p)	*Rluc-P2A-NoStall-P2A-Fluc*	-	-	Meydan *et al.*, 2023
p239	p415 (GPDp)	*GFP-NoStall-FLAG-HIS3*	-	-	this study
p240	p415 (GPDp)	*GFP-R(CGA)6-FLAG-HIS3*	-	-	this study
p250	p416 (Met25p)	*Rluc-P2A-6xGCA-P2A-Fluc*	-	-	Meydan *et al.*, 2023
p349	p415 (GPDp)	*HEL2*	-	FLAG (C-term)	this study
p350	p415 (GPDp)	*CUE3*	-	FLAG (C-term)	this study

Table A4: Reagents

Antibodies	Source	Catalog number
Anti-Ribosomal Protein S3 (D50G7)	Cell Signaling	9538S
Anti-eIF2α-phospho	Custom antibody made in the laboratory of Thomas Dever (NIH)	
Anti-K63 ubiquitin	Sigma-Aldrich	05-1308
Anti-Rad6	Abcam	ab31917
Anti-GFP	Santa Cruz Biotecnology	sc-9996
Anti-GAPDH	Abcam	ab9485
Anti-actin	Cell Signaling	4967
Anti-Pgk1	ThermoFisher Scientific	459250
Anti-Flag	Sigma-Aldrich	F3165
Anti-HA	ThermoFisher Scientific	715500
Anti-Myc	ThermoFisher Scientific	PA1981
Chemicals		
LB-medium	Sigma-Aldrich	L3022
Yeast nitrogen base	BD Difco	291940
D-Glucose	BD Difco	215510
Yeast nitrogen base	BD Difco	291940
Amino acid mix without Leu and Trp	Sigma-Aldrich	Y0750
Amino acid mix without Ura	Sigma-Aldrich	Y1501
Amino acid mix without His, Leu, Met, Trp, Ura	Sunrise Science Products	1095
L-leucine	Sigma-Aldrich	L800
Tryptophan	Sigma-Aldrich	T8941
Uracil	Sigma-Aldrich	U0750
L-Histidine	Sigma-Aldrich	H8000
Hydrogen peroxide	Sigma-Aldrich	216763
Methyl methanesulfonate (MMS)	Sigma-Aldrich	129925
4-nitroquinoline 1-oxide (4-NQO)	Sigma-Aldrich	N8141
L-Homopropargylglycine	Sigma-Aldrich	900893
ONPG (2-Nitrophenyl-β-D-galactopyranoside)	Goldbio	N27510
Iodoacetamide (IAM)	Sigma-Aldrich	I1149
Commercial assays		

Bradford Assay	Bio-Rad	5000205
BCA Assay	ThermoFisher Scientific	23225
Click-iT® HPG Alexa Fluor® Protein Synthesis Assay Kit	ThermoFisher Scientific	C10428
Dual Luciferase® Reporter Assay System	Promega	E1910
PTMScan HS Ubiquitin/SUMO Remnant Motif (K-ε-GG) Kit	Cell Signaling	59322
Other		
Protease Inhibitor Cocktail Set	Sigma-Aldrich	539131
Complete mini EDTA-free protease inhibitor cocktail	Roche	4693159001
Phosphatase Inhibitor	Sigma-Aldrich	P5726
T4 ligase	New England Biolabs	M0202L
HiFi DNA Assembly	New England Biolabs	E2621S
PVDF Transfer Membrane	ThemoFisher Scientific	88518
Sep-Pak C18 Cartridges	Waters	WAT051910
Bacteria strains		
E. coli strain NEB10-beta	New England Biolabs	C3019H
Software and algorithms		
FlowJo Version 10.8.1	Becton Dickinson	www.flowjo.com
Rstudio Version 1.3.1093	Rstudio, Inc., Boston, MA	
ImageJ Software		
ChimeraX Software Version 1.8	UCSF ChimeraX	www.cgl.ucsf.edu/chimerax/
Skyline Proteomics Software Version 24.1	MacCoss Lab Software	

A.2 Supplemental Figures

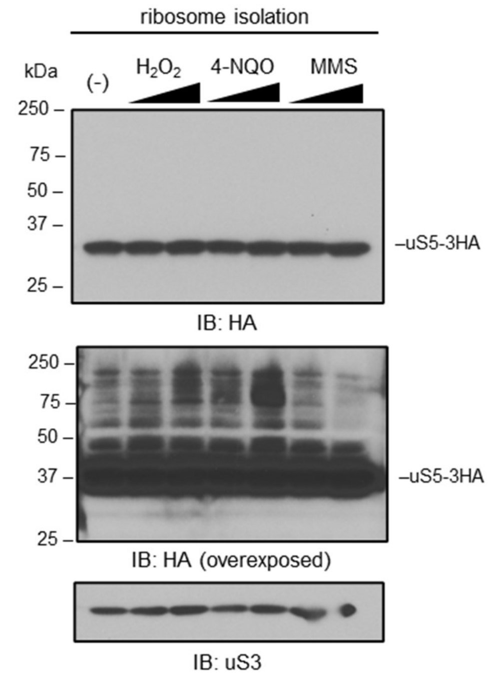

Figure A1: uS5-3HA immunoblot. Western blot of ribosomes isolated from untreated and H_2O_2 (0.6 mM, 5mM), 4-NQO (1 µg/mL, 5 µg/mL), and MMS (0.1%, 0.33%) treated cells with 3HA tagged uS5 probed with anti-HA. Anti-uS3 was used as a loading control.

References

1. Somero, G.N., *The cellular stress response and temperature: Function, regulation, and evolution.* Journal of Experimental Zoology Part A: Ecological and Integrative Physiology, 2020. **333**(6): p. 379-397.

2. Yuan, H.-X., Y. Xiong, and K.-L. Guan, *Nutrient Sensing, Metabolism, and Cell Growth Control.* Molecular Cell, 2013. **49**(3): p. 379-387.

3. Wellen, K.E. and C.B. Thompson, *Cellular Metabolic Stress: Considering How Cells Respond to Nutrient Excess.* Molecular Cell, 2010. **40**(2): p. 323-332.

4. Burg, M.B., J.D. Ferraris, and N.I. Dmitrieva, *Cellular Response to Hyperosmotic Stresses.* Physiological Reviews, 2007. **87**(4): p. 1441-1474.

5. Finan, J.D. and F. Guilak, *The effects of osmotic stress on the structure and function of the cell nucleus.* Journal of Cellular Biochemistry, 2010. **109**(3): p. 460-467.

6. van Agteren, J., et al., *A systematic review and meta-analysis of psychological interventions to improve mental wellbeing.* Nature Human Behaviour, 2021. **5**(5): p. 631-652.

7. Kültz, D., *MOLECULAR AND EVOLUTIONARY BASIS OF THE CELLULAR STRESS RESPONSE.* Annual Review of Physiology, 2005. **67**(Volume 67, 2005): p. 225-257.

8. Lamichhane, P.P. and P. Samir, *Cellular Stress: Modulator of Regulated Cell Death.* Biology, 2023. **12**(9): p. 1172.

9. Fulda, S., et al., *Cellular stress responses: cell survival and cell death.* Int J Cell Biol, 2010. **2010**: p. 214074.

10. Costa-Mattioli, M. and P. Walter, *The integrated stress response: From mechanism to disease.* Science, 2020. **368**(6489): p. eaat5314.

11. Robinson, A.M., *Let's Talk about Stress: History of Stress Research.* Review of General Psychology, 2018. **22**(3): p. 334-342.

12. Cuijpers, P., *Targets and outcomes of psychotherapies for mental disorders: an overview.* World Psychiatry, 2019. **18**(3): p. 276-285.

13. Burton, G.J. and E. Jauniaux, *Oxidative stress.* Best Practice & Research Clinical Obstetrics & Gynaecology, 2011. **25**(3): p. 287-299.

14. Lushchak, V.I., *Free radicals, reactive oxygen species, oxidative stress and its classification.* Chemico-Biological Interactions, 2014. **224**: p. 164-175.

15. Murphy, M.P., et al., *Guidelines for measuring reactive oxygen species and oxidative damage in cells and in vivo.* Nature Metabolism, 2022. **4**(6): p. 651-662.

16. Apel, K. and H. Hirt, *Reactive oxygen species: metabolism, oxidative stress, and signal transduction.* Annu Rev Plant Biol, 2004. **55**: p. 373-99.

17. Ray, P.D., B.W. Huang, and Y. Tsuji, *Reactive oxygen species (ROS) homeostasis and redox regulation in cellular signaling.* Cell Signal, 2012. **24**(5): p. 981-90.

18. He, L., et al., *Antioxidants Maintain Cellular Redox Homeostasis by Elimination of Reactive Oxygen Species.* Cellular Physiology and Biochemistry, 2017. **44**(2): p. 532-553.

19. Das, K. and A. Roychoudhury, *Reactive oxygen species (ROS) and response of antioxidants as ROS-scavengers during environmental stress in plants.* Frontiers in Environmental Science, 2014. **2**.

20. Palma, F.R., et al., *ROS production by mitochondria: function or dysfunction?* Oncogene, 2024. **43**(5): p. 295-303.

21. Pizzino, G., et al., *Oxidative Stress: Harms and Benefits for Human Health.* Oxid Med Cell Longev, 2017. **2017**: p. 8416763.

22. Schröder, P. and J. Krutmann, *Environmental Oxidative Stress – Environmental Sources of ROS*, in *Reactions, Processes: Oxidants and Antioxidant Defense Systems*, T. Grune, Editor. 2005, Springer Berlin Heidelberg: Berlin, Heidelberg. p. 19-31.

23. Betteridge, D.J., *What is oxidative stress?* Metabolism - Clinical and Experimental, 2000. **49**(2): p. 3-8.

24. Lobo, V., et al., *Free radicals, antioxidants and functional foods: Impact on human health.* Pharmacogn Rev, 2010. **4**(8): p. 118-26.

25. Avery, Simon V., *Molecular targets of oxidative stress.* Biochemical Journal, 2011. **434**(2): p. 201-210.

26. Srinivas, U.S., et al., *ROS and the DNA damage response in cancer.* Redox Biol, 2019. **25**: p. 101084.

27. Houldsworth, A., *Role of oxidative stress in neurodegenerative disorders: a review of reactive oxygen species and prevention by antioxidants.* Brain Communications, 2024. **6**(1): p. fcad356.

28. Liguori, I., et al., *Oxidative stress, aging, and diseases.* Clin Interv Aging, 2018. **13**: p. 757-772.

29. de Almeida, A., et al., *ROS: Basic Concepts, Sources, Cellular Signaling, and its Implications in Aging Pathways.* Oxid Med Cell Longev, 2022. **2022**: p. 1225578.

30. Rauf, A., et al., *Reactive oxygen species in biological systems: Pathways, associated diseases, and potential inhibitors—A review.* Food Science & Nutrition, 2024. **12**(2): p. 675-693.

31. Allen, R.G. and M. Tresini, *Oxidative stress and gene regulation.* Free Radical Biology and Medicine, 2000. **28**(3): p. 463-499.

32. Zhang, J., et al., *ROS and ROS-Mediated Cellular Signaling.* Oxidative Medicine and Cellular Longevity, 2016. **2016**(1): p. 4350965.

33. Lennicke, C. and H.M. Cochemé, *Redox metabolism: ROS as specific molecular regulators of cell signaling and function.* Molecular Cell, 2021. **81**(18): p. 3691-3707.

34. Buccitelli, C. and M. Selbach, *mRNAs, proteins and the emerging principles of gene expression control.* Nature Reviews Genetics, 2020. **21**(10): p. 630-644.

35. Morel, Y. and R. Barouki, *Repression of gene expression by oxidative stress.* Biochemical Journal, 1999. **342**(3): p. 481-496.

36. Baena-González, E., *Energy Signaling in the Regulation of Gene Expression during Stress.* Molecular Plant, 2010. **3**(2): p. 300-313.

37. Spriggs, K.A., M. Bushell, and A.E. Willis, *Translational Regulation of Gene Expression during Conditions of Cell Stress.* Molecular Cell, 2010. **40**(2): p. 228-237.

38. Scandalios, J., *Oxidative stress: molecular perception and transduction of signals triggering antioxidant gene defenses.* Brazilian journal of medical and biological research, 2005. **38**: p. 995-1014.

39. Espinosa-Diez, C., et al., *Antioxidant responses and cellular adjustments to oxidative stress.* Redox Biology, 2015. **6**: p. 183-197.

40. Mascarenhas, C., et al., *Gcn4 Is Required for the Response to Peroxide Stress in the Yeast Saccharomyces cerevisiae.* Molecular Biology of the Cell, 2008. **19**(7): p. 2995-3007.

41. Taymaz-Nikerel, H., A. Cankorur-Cetinkaya, and B. Kirdar, *Genome-Wide Transcriptional Response of Saccharomyces cerevisiae to Stress-Induced Perturbations.* Front Bioeng Biotechnol, 2016. **4**: p. 17.

42. de Nadal, E., G. Ammerer, and F. Posas, *Controlling gene expression in response to stress.* Nature Reviews Genetics, 2011. **12**(12): p. 833-845.

43. Gasch, A.P., et al., *Genomic Expression Programs in the Response of Yeast Cells to Environmental Changes.* Molecular Biology of the Cell, 2000. **11**(12): p. 4241-4257.

44. Costa, V., A. Quintanilha, and P. Moradas-Ferreira, *Protein oxidation, repair mechanisms and proteolysis in Saccharomyces cerevisiae.* IUBMB Life, 2007. **59**(4-5): p. 293-298.

45. Eleutherio, E., et al., *Oxidative stress and aging: Learning from yeast lessons.* Fungal Biology, 2018. **122**(6): p. 514-525.

46. Causton, H.C., et al., *Remodeling of Yeast Genome Expression in Response to Environmental Changes.* Molecular Biology of the Cell, 2001. **12**(2): p. 323-337.

47. Morano, K.A., C.M. Grant, and W.S. Moye-Rowley, *The Response to Heat Shock and Oxidative Stress in Saccharomyces cerevisiae.* Genetics, 2012. **190**(4): p. 1157-1195.

48. Vogel, C., G.M. Silva, and E.M. Marcotte, *Protein Expression Regulation under Oxidative Stress*.* Molecular & Cellular Proteomics, 2011. **10**(12): p. M111.009217.

49. Hershey, J.W., N. Sonenberg, and M.B. Mathews, *Principles of translational control: an overview.* Cold Spring Harb Perspect Biol, 2012. **4**(12).

50. Crawford, R.A. and G.D. Pavitt, *Translational regulation in response to stress in.* Yeast, 2019. **36**(1): p. 5-21.

51. Holcik, M. and N. Sonenberg, *Translational control in stress and apoptosis.* Nature Reviews Molecular Cell Biology, 2005. **6**(4): p. 318-327.

52. Advani, V.M. and P. Ivanov, *Translational Control under Stress: Reshaping the Translatome.* BioEssays, 2019. **41**(5): p. 1900009.

53. Barros, G.C., S. Guerrero, and G.M. Silva, *The central role of translation elongation in response to stress.* Biochemical Society Transactions, 2023. **51**(3): p. 959-969.

54. Shenton, D., et al., *Global Translational Responses to Oxidative Stress Impact upon Multiple Levels of Protein Synthesis*.* Journal of Biological Chemistry, 2006. **281**(39): p. 29011-29021.

55. Meng, E.C., et al., *UCSF ChimeraX: Tools for structure building and analysis.* Protein Science, 2023. **32**(11): p. e4792.

56. Zhou, Y., et al., *Structural impact of K63 ubiquitin on yeast translocating ribosomes under oxidative stress.* Proceedings of the National Academy of Sciences, 2020. **117**(36): p. 22157-22166.

57. Schuller, A.P. and R. Green, *Roadblocks and resolutions in eukaryotic translation.* Nature Reviews Molecular Cell Biology, 2018. **19**(8): p. 526-541.

58. Wilson, D.N. and J.H. Doudna Cate, *The structure and function of the eukaryotic ribosome.* Cold Spring Harb Perspect Biol, 2012. **4**(5).

59. Kressler, D., E. Hurt, and J. Baßler, *A Puzzle of Life: Crafting Ribosomal Subunits.* Trends in Biochemical Sciences, 2017. **42**(8): p. 640-654.

60. Weisser, M. and N. Ban, *Extensions, Extra Factors, and Extreme Complexity: Ribosomal Structures Provide Insights into Eukaryotic Translation.* Cold Spring Harb Perspect Biol, 2019. **11**(9).

61. Rodnina, M.V., et al., *Recognition and selection of tRNA in translation.* FEBS Letters, 2005. **579**(4): p. 938-942.

62. Graifer, D. and G. Karpova, *Interaction of tRNA with Eukaryotic Ribosome.* International Journal of Molecular Sciences, 2015. **16**(4): p. 7173-7194.

63. Jackson, R.J., C.U.T. Hellen, and T.V. Pestova, *The mechanism of eukaryotic translation initiation and principles of its regulation.* Nature Reviews Molecular Cell Biology, 2010. **11**(2): p. 113-127.

64. Dever, T.E., J.D. Dinman, and R. Green, *Translation Elongation and Recoding in Eukaryotes.* Cold Spring Harb Perspect Biol, 2018. **10**(8).

65. Hellen, C.U.T., *Translation Termination and Ribosome Recycling in Eukaryotes.* Cold Spring Harb Perspect Biol, 2018. **10**(10).

66. Brito Querido, J., I. Díaz-López, and V. Ramakrishnan, *The molecular basis of translation initiation and its regulation in eukaryotes.* Nature Reviews Molecular Cell Biology, 2024. **25**(3): p. 168-186.

67. Kimball, S.R., *Eukaryotic initiation factor eIF2.* The International Journal of Biochemistry & Cell Biology, 1999. **31**(1): p. 25-29.

68. Hinnebusch, A.G., *The Scanning Mechanism of Eukaryotic Translation Initiation.* Annual Review of Biochemistry, 2014. **83**(Volume 83, 2014): p. 779-812.

69. Richter, J.D. and N. Sonenberg, *Regulation of cap-dependent translation by eIF4E inhibitory proteins.* Nature, 2005. **433**(7025): p. 477-480.

70. Pakos-Zebrucka, K., et al., *The integrated stress response.* EMBO Rep, 2016. **17**(10): p. 1374-1395.

71. Lareau, L.F., et al., *Distinct stages of the translation elongation cycle revealed by sequencing ribosome-protected mRNA fragments.* eLife, 2014. **3**: p. e01257.

72. Behrmann, E., et al., *Structural Snapshots of Actively Translating Human Ribosomes.* Cell, 2015. **161**(4): p. 845-857.

73. Spahn, C.M., et al., *Domain movements of elongation factor eEF2 and the eukaryotic 80S ribosome facilitate tRNA translocation.* The EMBO journal, 2004. **23**(5): p. 1008-1019.

74. Chen, C., et al., *Allosteric vs. spontaneous exit-site (E-site) tRNA dissociation early in protein synthesis.* Proceedings of the National Academy of Sciences, 2011. **108**(41): p. 16980-16985.

75. Andersen, C.B.F., et al., *Structure of eEF3 and the mechanism of transfer RNA release from the E-site.* Nature, 2006. **443**(7112): p. 663-668.

76. Ranjan, N., et al., *Yeast translation elongation factor eEF3 promotes late stages of tRNA translocation.* The EMBO Journal, 2021. **40**(6): p. e106449.

77. Knight, J.R.P., et al., *Control of translation elongation in health and disease.* Disease Models & Mechanisms, 2020. **13**(3).

78. Williams, T.D. and A. Rousseau, *Translation regulation in response to stress.* The FEBS Journal, 2024. **n/a**(n/a).

79. Buskirk, A.R. and R. Green, *Ribosome pausing, arrest and rescue in bacteria and eukaryotes.* Philos Trans R Soc Lond B Biol Sci, 2017. **372**(1716).

80. Dougherty, S.E., et al., *Expanding Role of Ubiquitin in Translational Control.* Int J Mol Sci, 2020. **21**(3).

81. Inada, T. and R. Beckmann, *Mechanisms of Translation-coupled Quality Control.* Journal of Molecular Biology, 2024. **436**(6): p. 168496.

82. Jackson, R.J., C.U.T. Hellen, and T.V. Pestova, *Termination and post-termination events in eukaryotic translation*, in *Advances in Protein Chemistry and Structural Biology*, A. Marintchev, Editor. 2012, Academic Press. p. 45-93.

83. Song, H., et al., *The Crystal Structure of Human Eukaryotic Release Factor eRF1—Mechanism of Stop Codon Recognition and Peptidyl-tRNA Hydrolysis.* Cell, 2000. **100**(3): p. 311-321.

84. Sonenberg, N. and A.G. Hinnebusch, *Regulation of Translation Initiation in Eukaryotes: Mechanisms and Biological Targets.* Cell, 2009. **136**(4): p. 731-745.

85. Diamond, P.D., N.J. McGlincy, and N.T. Ingolia, *Depletion of cap-binding protein eIF4E dysregulates amino acid metabolic gene expression.* Molecular Cell, 2024. **84**(11): p. 2119-2134.e5.

86. Kim, K.Q., et al., *eIF4F complex dynamics are important for the activation of the integrated stress response.* Molecular Cell, 2024. **84**(11): p. 2135-2151.e7.

87. Váchová, L., et al., *Differential stability of Gcn4p controls its cell-specific activity in differentiated yeast colonies.* mBio, 2024. **15**(5): p. e00689-24.

88. Simsek, D. and M. Barna, *An emerging role for the ribosome as a nexus for post-translational modifications.* Current Opinion in Cell Biology, 2017. **45**: p. 92-101.

89. Komander, D. and M. Rape, *The Ubiquitin Code.* Annual Review of Biochemistry, 2012. **81**(Volume 81, 2012): p. 203-229.

90. Inada, T., *Quality controls induced by aberrant translation.* Nucleic Acids Research, 2020. **48**(3): p. 1084-1096.

91. Monem, P.C. and J.A. Arribere, *A ubiquitin language communicates ribosomal distress.* Seminars in Cell & Developmental Biology, 2024. **154**: p. 131-137.

92. Song, L. and Z.-Q. Luo, *Post-translational regulation of ubiquitin signaling.* Journal of Cell Biology, 2019. **218**(6): p. 1776-1786.

93. Hershko, A., et al., *Proposed role of ATP in protein breakdown: conjugation of protein with multiple chains of the polypeptide of ATP-dependent proteolysis.* Proceedings of the National Academy of Sciences, 1980. **77**(4): p. 1783-1786.

94. Li, W. and Y. Ye, *Polyubiquitin chains: functions, structures, and mechanisms.* Cellular and Molecular Life Sciences, 2008. **65**(15): p. 2397-2406.

95. Ye, Y., et al., *Ubiquitin chain conformation regulates recognition and activity of interacting proteins.* Nature, 2012. **492**(7428): p. 266-270.

96. Swatek, K.N. and D. Komander, *Ubiquitin modifications.* Cell Research, 2016. **26**(4): p. 399-422.

97. Akutsu, M., I. Dikic, and A. Bremm, *Ubiquitin chain diversity at a glance.* Journal of Cell Science, 2016. **129**(5): p. 875-880.

98. Dikic, I. and B.A. Schulman, *An expanded lexicon for the ubiquitin code.* Nature Reviews Molecular Cell Biology, 2023. **24**(4): p. 273-287.

99. Ohtake, F. and H. Tsuchiya, *The emerging complexity of ubiquitin architecture.* The Journal of Biochemistry, 2016. **161**(2): p. 125-133.

100. Pickart, C.M., *Targeting of substrates to the 26S proteasome.* The FASEB Journal, 1997. **11**(13): p. 1055-1066.

101. Peng, J., et al., *A proteomics approach to understanding protein ubiquitination.* Nature Biotechnology, 2003. **21**(8): p. 921-926.

102. Bard, J.A.M., et al., *Structure and Function of the 26S Proteasome.* Annual Review of Biochemistry, 2018. **87**(Volume 87, 2018): p. 697-724.

103. Kleiger, G. and T. Mayor, *Perilous journey: a tour of the ubiquitin–proteasome system.* Trends in Cell Biology, 2014. **24**(6): p. 352-359.

104. An, H. and J.W. Harper, *Ribosome abundance control via the ubiquitin–proteasome system and autophagy.* Journal of molecular biology, 2020. **432**(1): p. 170-184.

105. Shang, F. and A. Taylor, *Ubiquitin–proteasome pathway and cellular responses to oxidative stress.* Free Radical Biology and Medicine, 2011. **51**(1): p. 5-16.

106. Singh, G., S. Kumar, and R. Das, *Decoding the Assembly of Mixed and Branched Heterotypic Ubiquitin Chains.* Analytical Chemistry, 2023. **95**(26): p. 10061-10067.

107. Chen, Z.J. and L.J. Sun, *Nonproteolytic Functions of Ubiquitin in Cell Signaling.* Molecular Cell, 2009. **33**(3): p. 275-286.

108. Xu, P., et al., *Quantitative Proteomics Reveals the Function of Unconventional Ubiquitin Chains in Proteasomal Degradation.* Cell, 2009. **137**(1): p. 133-145.

109. Madiraju, C., et al., *K63 ubiquitination in immune signaling.* Trends Immunol, 2022. **43**(2): p. 148-162.

110. Erpapazoglou, Z., O. Walker, and R. Haguenauer-Tsapis, *Versatile roles of k63-linked ubiquitin chains in trafficking.* Cells, 2014. **3**(4): p. 1027-88.

111. Wang, G., et al., *K63-linked ubiquitination in kinase activation and cancer.* Frontiers in oncology, 2012. **2**: p. 5.

112. Grumati, P. and I. Dikic, *Ubiquitin signaling and autophagy.* Journal of Biological Chemistry, 2018. **293**(15): p. 5404-5413.

113. Martínez-Férriz, A., et al., *Ubiquitin-mediated mechanisms of translational control.* Seminars in Cell & Developmental Biology, 2022. **132**: p. 146-154.

114. Matsuo, Y. and T. Inada, *Co-Translational Quality Control Induced by Translational Arrest.* Biomolecules, 2023. **13**(2): p. 317.

115. Saito, K., W. Horikawa, and K. Ito, *Inhibiting K63 Polyubiquitination Abolishes No-Go Type Stalled Translation Surveillance in Saccharomyces cerevisiae.* PLOS Genetics, 2015. **11**(4): p. e1005197.

116. Silva, G.M., D. Finley, and C. Vogel, *K63 polyubiquitination is a new modulator of the oxidative stress response.* Nature Structural & Molecular Biology, 2015. **22**(2): p. 116-123.

117. McGrath, J.P., S. Jentsch, and A. Varshavsky, *UBA 1: an essential yeast gene encoding ubiquitin-activating enzyme.* The EMBO Journal, 1991. **10**(1): p. 227-236.

118. Damgaard, R.B., *The ubiquitin system: from cell signalling to disease biology and new therapeutic opportunities.* Cell Death & Differentiation, 2021. **28**(2): p. 423-426.

119. Finley, D., et al., *The Ubiquitin–Proteasome System of Saccharomyces cerevisiae.* Genetics, 2012. **192**(2): p. 319-360.

120. Yang, Q., et al., *E3 ubiquitin ligases: styles, structures and functions.* Mol Biomed, 2021. **2**(1): p. 23.

121. Stewart, M.D., et al., *E2 enzymes: more than just middle men.* Cell Research, 2016. **26**(4): p. 423-440.

122. Mevissen, T.E.T. and D. Komander, *Mechanisms of Deubiquitinase Specificity and Regulation.* Annual Review of Biochemistry, 2017. **86**(Volume 86, 2017): p. 159-192.

123. Hutchins, A.P., et al., *The Repertoires of Ubiquitinating and Deubiquitinating Enzymes in Eukaryotic Genomes.* Molecular Biology and Evolution, 2013. **30**(5): p. 1172-1187.

124. Amerik, A.Y., S.J. Li, and M. Hochstrasser, *Analysis of the deubiquitinating enzymes of the yeast Saccharomyces cerevisiae.* Biol Chem, 2000. **381**(9-10): p. 981-92.

125. Nijman, S.M.B., et al., *A Genomic and Functional Inventory of Deubiquitinating Enzymes.* Cell, 2005. **123**(5): p. 773-786.

126. Hewings, D.S., et al., *Activity-based probes for the ubiquitin conjugation–deconjugation machinery: new chemistries, new tools, and new insights.* The FEBS Journal, 2017. **284**(10): p. 1555-1576.

127. Joazeiro, C.A.P., *Mechanisms and functions of ribosome-associated protein quality control.* Nature Reviews Molecular Cell Biology, 2019. **20**(6): p. 368-383.

128. Shoemaker, C.J. and R. Green, *Translation drives mRNA quality control.* Nature Structural & Molecular Biology, 2012. **19**(6): p. 594-601.

129. Bao, C., et al., *mRNA stem-loops can pause the ribosome by hindering A-site tRNA binding.* eLife, 2020. **9**: p. e55799.

130. Tesina, P., et al., *Molecular mechanism of translational stalling by inhibitory codon combinations and poly(A) tracts.* The EMBO Journal, 2020. **39**(3): p. e103365.

131. Meydan, S. and N.R. Guydosh, *A cellular handbook for collided ribosomes: surveillance pathways and collision types.* Curr Genet, 2021. **67**(1): p. 19-26.

132. Ikeuchi, K., et al., *Collided ribosomes form a unique structural interface to induce Hel2-driven quality control pathways.* The EMBO Journal, 2019. **38**(5): p. e100276.

133. Filbeck, S., et al., *Ribosome-associated quality-control mechanisms from bacteria to humans.* Mol Cell, 2022. **82**(8): p. 1451-1466.

134. Park, J., et al., *The trinity of ribosome-associated quality control and stress signaling for proteostasis and neuronal physiology.* BMB Rep, 2021. **54**(9): p. 439-450.

135. Yan, L.L., et al., *Oxidation and alkylation stresses activate ribosome-quality control.* Nature Communications, 2019. **10**(1): p. 5611.

136. Simms, Carrie L., et al., *An Active Role for the Ribosome in Determining the Fate of Oxidized mRNA.* Cell Reports, 2014. **9**(4): p. 1256-1264.

137. Sheng, X., et al., *The ubiquitin codes in cellular stress responses.* Protein & Cell, 2024. **15**(3): p. 157-190.

138. Grice, G.L. and J.A. Nathan, *The recognition of ubiquitinated proteins by the proteasome.* Cellular and molecular life sciences, 2016. **73**: p. 3497-3506.

139. Simões, V., et al., *Redox-sensitive E2 Rad6 controls cellular response to oxidative stress via K63-linked ubiquitination of ribosomes.* Cell Reports, 2022. **39**(8).

140. Santos, C.M., et al., *Redox control of the deubiquitinating enzyme Ubp2 regulates translation during stress.* bioRxiv, 2024: p. 2024.04.30.591912.

141. Back, S., et al., *Site-Specific K63 Ubiquitinomics Provides Insights into Translation Regulation under Stress.* J Proteome Res, 2019. **18**(1): p. 309-318.

142. Spence, J., et al., *A ubiquitin mutant with specific defects in DNA repair and multiubiquitination.* Mol Cell Biol, 1995. **15**(3): p. 1265-73.

143. Cheng, Y., *Single-Particle Cryo-EM at Crystallographic Resolution.* Cell, 2015. **161**(3): p. 450-457.

144. Spence, J., et al., *Cell cycle-regulated modification of the ribosome by a variant multiubiquitin chain.* Cell, 2000. **102**(1): p. 67-76.

145. Svidritskiy, E., et al., *Structures of yeast 80S ribosome-tRNA complexes in the rotated and nonrotated conformations.* Structure, 2014. **22**(8): p. 1210-1218.

146. Cornish, P.V., et al., *Following movement of the L1 stalk between three functional states in single ribosomes.* Proc Natl Acad Sci U S A, 2009. **106**(8): p. 2571-6.

147. Fei, J., et al., *Coupling of ribosomal L1 stalk and tRNA dynamics during translation elongation.* Molecular cell, 2008. **30**(3): p. 348-359.

148. Naganuma, T., et al., *Structural basis for translation factor recruitment to the eukaryotic/archaeal ribosomes.* Journal of biological chemistry, 2010. **285**(7): p. 4747-4756.

149. Gonzalo, P. and J.P. Reboud, *The puzzling lateral flexible stalk of the ribosome.* Biology of the Cell, 2003. **95**(3-4): p. 179-193.

150. Dougherty, S.E., et al., *Context specific ubiquitin modification of ribosomes regulates translation under oxidative stress.* bioRxiv, 2024: p. 2024.05.02.592277.

151. Hershko, A., et al., *Components of ubiquitin-protein ligase system. Resolution, affinity purification, and role in protein breakdown.* Journal of Biological Chemistry, 1983. **258**(13): p. 8206-8214.

152. Pickart, C.M. and M.J. Eddins, *Ubiquitin: structures, functions, mechanisms.* Biochimica et Biophysica Acta (BBA) - Molecular Cell Research, 2004. **1695**(1): p. 55-72.

153. Varshavsky, A., *The early history of the ubiquitin field.* Protein Sci, 2006. **15**(3): p. 647-54.

154. Hershko, A., *The Ubiquitin System*, in *Ubiquitin and the Biology of the Cell*, J.-M. Peters, J.R. Harris, and D. Finley, Editors. 1998, Springer US: Boston, MA. p. 1-17.

155. Pickart, C.M., *Back to the Future with Ubiquitin.* Cell, 2004. **116**(2): p. 181-190.

156. Steger, M., Ö. Karayel, and V. Demichev, *Ubiquitinomics: History, methods, and applications in basic research and drug discovery.* PROTEOMICS, 2022. **22**(15-16): p. 2200074.

157. Sun, M. and X. Zhang, *Current methodologies in protein ubiquitination characterization: from ubiquitinated protein to ubiquitin chain architecture.* Cell & Bioscience, 2022. **12**(1): p. 126.

158. Aebersold, R. and M. Mann, *Mass spectrometry-based proteomics.* Nature, 2003. **422**(6928): p. 198-207.

159. Bantscheff, M., et al., *Quantitative mass spectrometry in proteomics: a critical review.* Analytical and Bioanalytical Chemistry, 2007. **389**(4): p. 1017-1031.

160. Griffiths, J., *A Brief History of Mass Spectrometry.* Analytical Chemistry, 2008. **80**(15): p. 5678-5683.

161. Coon, J.J., et al., *Tandem Mass Spectrometry for Peptide and Protein Sequence Analysis.* BioTechniques, 2005. **38**(4): p. 519-523.

162. Van Oudenhove, L. and B. Devreese, *A review on recent developments in mass spectrometry instrumentation and quantitative tools advancing bacterial proteomics.* Applied Microbiology and Biotechnology, 2013. **97**(11): p. 4749-4762.

163. Rozanova, S., et al., *Quantitative Mass Spectrometry-Based Proteomics: An Overview*, in *Quantitative Methods in Proteomics*, K. Marcus, M. Eisenacher, and B. Sitek, Editors. 2021, Springer US: New York, NY. p. 85-116.

164. Bustos, D., et al., *Characterizing ubiquitination sites by peptide-based immunoaffinity enrichment.* Mol Cell Proteomics, 2012. **11**(12): p. 1529-40.

165. Switzar, L., M. Giera, and W.M.A. Niessen, *Protein Digestion: An Overview of the Available Techniques and Recent Developments.* Journal of Proteome Research, 2013. **12**(3): p. 1067-1077.

166. Manadas, B., et al., *Peptide fractionation in proteomics approaches.* Expert Review of Proteomics, 2010. **7**(5): p. 655-663.

167. Vandermarliere, E., M. Mueller, and L. Martens, *Getting intimate with trypsin, the leading protease in proteomics.* Mass Spectrometry Reviews, 2013. **32**(6): p. 453-465.

168. Karpievitch, Y.V., et al., *Liquid Chromatography Mass Spectrometry-Based Proteomics: Biological and Technological Aspects.* Ann Appl Stat, 2010. **4**(4): p. 1797-1823.

169. Jennings, M.E., 2nd, et al., *Total Retention Liquid Chromatography-Mass Spectrometry to Achieve Maximum Protein Sequence Coverage.* Anal Chem, 2021. **93**(12): p. 5054-5060.

170. Moruz, L., et al., *Optimized Nonlinear Gradients for Reversed-Phase Liquid Chromatography in Shotgun Proteomics.* Analytical Chemistry, 2013. **85**(16): p. 7777-7785.

171. Shuken, S.R., *An Introduction to Mass Spectrometry-Based Proteomics.* Journal of Proteome Research, 2023. **22**(7): p. 2151-2171.

172. Han, X., A. Aslanian, and J.R. Yates, 3rd, *Mass spectrometry for proteomics.* Curr Opin Chem Biol, 2008. **12**(5): p. 483-90.

173. Jiang, Y., et al., *Comprehensive Overview of Bottom-Up Proteomics Using Mass Spectrometry.* ACS Measurement Science Au, 2024.

174. Haag, A.M., *Mass Analyzers and Mass Spectrometers*, in *Modern Proteomics – Sample Preparation, Analysis and Practical Applications*, H. Mirzaei and M. Carrasco, Editors. 2016, Springer International Publishing: Cham. p. 157-169.

175. Hughes, C., B. Ma, and G.A. Lajoie, *De Novo Sequencing Methods in Proteomics*, in *Proteome Bioinformatics*, S.J. Hubbard and A.R. Jones, Editors. 2010, Humana Press: Totowa, NJ. p. 105-121.

176. Kirkpatrick, D.S., C. Denison, and S.P. Gygi, *Weighing in on ubiquitin: the expanding role of mass-spectrometry-based proteomics.* Nature Cell Biology, 2005. **7**(8): p. 750-757.

177. Fulzele, A. and E.J. Bennett, *Ubiquitin diGLY Proteomics as an Approach to Identify and Quantify the Ubiquitin-Modified Proteome.* Methods Mol Biol, 2018. **1844**: p. 363-384.

178. Lai, Y.-H. and Y.-S. Wang, *Advances in high-resolution mass spectrometry techniques for analysis of high mass-to-charge ions.* Mass Spectrometry Reviews, 2023. **42**(6): p. 2426-2445.

179. Hjerpe, R., et al., *Efficient protection and isolation of ubiquitylated proteins using tandem ubiquitin-binding entities.* EMBO reports, 2009. **10**(11): p. 1250-1258-1258.

180. Zhang, Y., et al., *Protein analysis by shotgun/bottom-up proteomics.* Chem Rev, 2013. **113**(4): p. 2343-94.

181. Llácer, Jose L., et al., *Conformational Differences between Open and Closed States of the Eukaryotic Translation Initiation Complex.* Molecular Cell, 2015. **59**(3): p. 399-412.

182. Asano, K. and M.S. Sachs, *Translation factor control of ribosome conformation during start codon selection.* Genes Dev, 2007. **21**(11): p. 1280-7.

183. Peterson, A.C., et al., *Parallel reaction monitoring for high resolution and high mass accuracy quantitative, targeted proteomics.* Mol Cell Proteomics, 2012. **11**(11): p. 1475-88.

184. van Bentum, M. and M. Selbach, *An Introduction to Advanced Targeted Acquisition Methods.* Molecular & Cellular Proteomics, 2021. **20**.

185. Ordureau, A., et al., *Dynamics of PARKIN-Dependent Mitochondrial Ubiquitylation in Induced Neurons and Model Systems Revealed by Digital Snapshot Proteomics.* Mol Cell, 2018. **70**(2): p. 211-227.e8.

186. Plank, M.J., *Modern Data Acquisition Approaches in Proteomics Based on Dynamic Instrument Control.* Journal of Proteome Research, 2022. **21**(5): p. 1209-1217.

187. MacLean, B., et al., *Skyline: an open source document editor for creating and analyzing targeted proteomics experiments.* Bioinformatics, 2010. **26**(7): p. 966-968.

188. Manohar, S., et al., *Polyubiquitin Chains Linked by Lysine Residue 48 (K48) Selectively Target Oxidized Proteins In Vivo.* Antioxidants & Redox Signaling, 2019. **31**(15): p. 1133-1149.

189. Garshott, D.M., et al., *Distinct regulatory ribosomal ubiquitylation events are reversible and hierarchically organized.* eLife, 2020. **9**: p. e54023.

190. Matsuo, Y., et al., *Ubiquitination of stalled ribosome triggers ribosome-associated quality control.* Nature Communications, 2017. **8**(1): p. 159.

191. Mohan, S. and H.F. Noller, *Recurring RNA structural motifs underlie the mechanics of L1 stalk movement.* Nature Communications, 2017. **8**(1): p. 14285.

192. Higgins, R., et al., *The Unfolded Protein Response Triggers Site-Specific Regulatory Ubiquitylation of 40S Ribosomal Proteins.* Mol Cell, 2015. **59**(1): p. 35-49.

193. Ikeuchi, K., T. Izawa, and T. Inada, *Recent Progress on the Molecular Mechanism of Quality Controls Induced by Ribosome Stalling.* Front Genet, 2018. **9**: p. 743.

194. Garshott, D.M., et al., *iRQC, a surveillance pathway for 40S ribosomal quality control during mRNA translation initiation.* Cell Reports, 2021. **36**(9).

195. Yan, L.L. and H.S. Zaher, *Ubiquitin—a beacon for all during quality control on the ribosome.* The EMBO Journal, 2019. **38**(5): p. e101633.

196. Simms, C.L., L.L. Yan, and H.S. Zaher, *Ribosome Collision Is Critical for Quality Control during No-Go Decay.* Molecular Cell, 2017. **68**(2): p. 361-373.e5.

197. Winz, M.-L., et al., *Molecular interactions between Hel2 and RNA supporting ribosome-associated quality control.* Nature Communications, 2019. **10**(1): p. 563.

198. Sugiyama, T., et al., *Sequential Ubiquitination of Ribosomal Protein uS3 Triggers the Degradation of Non-functional 18S rRNA.* Cell Reports, 2019. **26**(12): p. 3400-3415.e7.

199. Juszkiewicz, S., et al., *ZNF598 Is a Quality Control Sensor of Collided Ribosomes.* Molecular Cell, 2018. **72**(3): p. 469-481.e7.

200. Meydan, S. and N.R. Guydosh, *Disome and Trisome Profiling Reveal Genome-wide Targets of Ribosome Quality Control.* Molecular Cell, 2020. **79**(4): p. 588-602.e6.

201. Brandman, O. and R.S. Hegde, *Ribosome-associated protein quality control.* Nature Structural & Molecular Biology, 2016. **23**(1): p. 7-15.

202. Yan, L.L. and H.S. Zaher, *Ribosome quality control antagonizes the activation of the integrated stress response on colliding ribosomes.* Molecular Cell, 2021. **81**(3): p. 614-628.e4.

203. Bengtson, M.H. and C.A.P. Joazeiro, *Role of a ribosome-associated E3 ubiquitin ligase in protein quality control.* Nature, 2010. **467**(7314): p. 470-473.

204. Lu, J. and C. Deutsch, *Electrostatics in the Ribosomal Tunnel Modulate Chain Elongation Rates.* Journal of Molecular Biology, 2008. **384**(1): p. 73-86.

205. Requião, R.D., et al., *Influence of nascent polypeptide positive charges on translation dynamics.* Biochemical Journal, 2020. **477**(15): p. 2921-2934.

206. Choe, Y.-J., et al., *Failure of RQC machinery causes protein aggregation and proteotoxic stress.* Nature, 2016. **531**(7593): p. 191-195.

207. Defenouillère, Q., et al., *Cdc48-associated complex bound to 60S particles is required for the clearance of aberrant translation products.* Proceedings of the National Academy of Sciences, 2013. **110**(13): p. 5046-5051.

208. Best, K., et al., *Structural basis for clearing of ribosome collisions by the RQT complex.* Nature Communications, 2023. **14**(1): p. 921.

209. Matsuo, Y., et al., *RQT complex dissociates ribosomes collided on endogenous RQC substrate SDD1.* Nature Structural & Molecular Biology, 2020. **27**(4): p. 323-332.

210. Yonashiro, R., et al., *The Rqc2/Tae2 subunit of the ribosome-associated quality control (RQC) complex marks ribosome-stalled nascent polypeptide chains for aggregation.* Elife, 2016. **5**: p. e11794.

211. Doamekpor, S.K., et al., *Structure and function of the yeast listerin (Ltn1) conserved N-terminal domain in binding to stalled 60S ribosomal subunits.* Proceedings of the National Academy of Sciences, 2016. **113**(29): p. E4151-E4160.

212. Sitron, C.S. and O. Brandman, *CAT tails drive degradation of stalled polypeptides on and off the ribosome.* Nature Structural & Molecular Biology, 2019. **26**(6): p. 450-459.

213. Osuna, B.A., et al., *In vitro analysis of RQC activities provides insights into the mechanism and function of CAT tailing.* eLife, 2017. **6**: p. e27949.

214. Sitron, C.S., et al., *Aggregation of CAT tails blocks their degradation and causes proteotoxicity in S. cerevisiae.* PLOS ONE, 2020. **15**(1): p. e0227841.

215. Verma, R., et al., *Cdc48/p97 promotes degradation of aberrant nascent polypeptides bound to the ribosome.* eLife, 2013. **2**: p. e00308.

216. Izawa, T., et al., *Cytosolic Protein Vms1 Links Ribosome Quality Control to Mitochondrial and Cellular Homeostasis.* Cell, 2017. **171**(4): p. 890-903.e18.

217. Nürenberg-Goloub, E. and R. Tampé, *Ribosome recycling in mRNA translation, quality control, and homeostasis.* 2020. **401**(1): p. 47-61.

218. Doma, M.K. and R. Parker, *Endonucleolytic cleavage of eukaryotic mRNAs with stalls in translation elongation.* Nature, 2006. **440**(7083): p. 561-564.

219. Harigaya, Y. and R. Parker, *No-go decay: a quality control mechanism for RNA in translation.* WIREs RNA, 2010. **1**(1): p. 132-141.

220. Powers, K.T., J.-Y.A. Szeto, and C. Schaffitzel, *New insights into no-go, non-stop and nonsense-mediated mRNA decay complexes.* Current Opinion in Structural Biology, 2020. **65**: p. 110-118.

221. Tomomatsu, S., et al., *Two modes of Cue2-mediated mRNA cleavage with distinct substrate recognition initiate no-go decay.* Nucleic Acids Research, 2023. **51**(1): p. 253-270.

222. Matsuki, Y., et al., *Ribosomal protein S7 ubiquitination during ER stress in yeast is associated with selective mRNA translation and stress outcome.* Scientific reports, 2020. **10**(1): p. 19669.

223. Buschauer, R., et al., *The Ccr4-Not complex monitors the translating ribosome for codon optimality.* Science, 2020. **368**(6488): p. eaay6912.

224. D'Orazio, K.N., et al., *The endonuclease Cue2 cleaves mRNAs at stalled ribosomes during No Go Decay.* eLife, 2019. **8**: p. e49117.

225. Veltri, A.J., et al., *Distinct elongation stalls during translation are linked with distinct pathways for mRNA degradation.* eLife, 2022. **11**: p. e76038.

226. Tsuboi, T., et al., *Dom34:Hbs1 Plays a General Role in Quality-Control Systems by Dissociation of a Stalled Ribosome at the 3′ End of Aberrant mRNA.* Molecular Cell, 2012. **46**(4): p. 518-529.

227. Cole, S.E., et al., *A Convergence of rRNA and mRNA Quality Control Pathways Revealed by Mechanistic Analysis of Nonfunctional rRNA Decay.* Molecular Cell, 2009. **34**(4): p. 440-450.

228. Li, S., et al., *Sensing of individual stalled 80S ribosomes by Fap1 for nonfunctional rRNA turnover.* Molecular Cell, 2022. **82**(18): p. 3424-3437.e8.

229. Ryder, L., et al., *Nitric oxide-induced ribosome collision activates ribosomal surveillance mechanisms.* Cell Death & Disease, 2023. **14**(7): p. 467.

230. Moon, S.L., et al., *Coupling of translation quality control and mRNA targeting to stress granules.* Journal of Cell Biology, 2020. **219**(8): p. e202004120.

231. Wu, C.C.-C., et al., *Ribosome Collisions Trigger General Stress Responses to Regulate Cell Fate.* Cell, 2020. **182**(2): p. 404-416.e14.

232. Nanjaraj Urs, A.N., et al., *Inability to rescue stalled ribosomes results in overactivation of the integrated stress response.* Journal of Biological Chemistry, 2024. **300**(5).

233. Yan, L.L. and H.S. Zaher, *How do cells cope with RNA damage and its consequences?* Journal of Biological Chemistry, 2019. **294**(41): p. 15158-15171.

234. Schmitt, K., A.-A. Kraft, and O. Valerius, *A Multi-Perspective Proximity View on the Dynamic Head Region of the Ribosomal 40S Subunit.* International Journal of Molecular Sciences, 2021. **22**(21): p. 11653.

235. Kim, K.Q. and H.S. Zaher, *Canary in a coal mine: collided ribosomes as sensors of cellular conditions.* Trends Biochem Sci, 2022. **47**(1): p. 82-97.

236. Meydan, S., et al., *The ubiquitin conjugase Rad6 mediates ribosome pausing during oxidative stress.* Cell Reports, 2023. **42**(11).

237. Schneider, C.A., W.S. Rasband, and K.W. Eliceiri, *NIH Image to ImageJ: 25 years of image analysis.* Nature Methods, 2012. **9**(7): p. 671-675.

238. Hinnebusch, A.G. and J.R. Lorsch, *The mechanism of eukaryotic translation initiation: new insights and challenges.* Cold Spring Harb Perspect Biol, 2012. **4**(10).

239. Hinnebusch, A.G., *TRANSLATIONAL REGULATION OF GCN4 AND THE GENERAL AMINO ACID CONTROL OF YEAST*.* Annual Review of Microbiology, 2005. **59**(Volume 59, 2005): p. 407-450.

240. Postnikoff, S.D.L., J.E. Johnson, and J.K. Tyler, *The integrated stress response in budding yeast lifespan extension.* Microb Cell, 2017. **4**(11): p. 368-375.

241. Yang, R., S.A. Wek, and R.C. Wek, *Glucose limitation induces GCN4 translation by activation of Gcn2 protein kinase.* Molecular and cellular biology, 2000.

242. Deloche, O., et al., *A membrane transport defect leads to a rapid attenuation of translation initiation in Saccharomyces cerevisiae.* Molecular cell, 2004. **13**(3): p. 357-366.

243. Natarajan, K., et al., *Transcriptional profiling shows that Gcn4p is a master regulator of gene expression during amino acid starvation in yeast.* Molecular and cellular biology, 2001.

244. Harding, H.P., et al., *An integrated stress response regulates amino acid metabolism and resistance to oxidative stress.* Molecular cell, 2003. **11**(3): p. 619-633.

245. Ryoo, H.D., *The integrated stress response in metabolic adaptation.* Journal of Biological Chemistry, 2024. **300**(4).

246. Singh, C.R., et al., *Eukaryotic translation initiation factor 5 is critical for integrity of the scanning preinitiation complex and accurate control of GCN4 translation.* Mol Cell Biol, 2005. **25**(13): p. 5480-91.

247. Gunišová, S. and L.S. Valášek, *Fail-safe mechanism of GCN4 translational control--uORF2 promotes reinitiation by analogous mechanism to uORF1 and thus secures its key role in GCN4 expression.* Nucleic Acids Res, 2014. **42**(9): p. 5880-93.

248. Kurihara, Y., *uORF Shuffling Fine-Tunes Gene Expression at a Deep Level of the Process.* Plants, 2020. **9**(5): p. 608.

249. Dey, S., et al., *Both transcriptional regulation and translational control of ATF4 are central to the integrated stress response.* Journal of Biological Chemistry, 2010. **285**(43): p. 33165-33174.

250. Neill, G. and G.R. Masson, *A stay of execution: ATF4 regulation and potential outcomes for the integrated stress response.* Front Mol Neurosci, 2023. **16**: p. 1112253.

251. Rawal, Y., et al., *Gcn4 Binding in Coding Regions Can Activate Internal and Canonical 5′ Promoters in Yeast.* Molecular Cell, 2018. **70**(2): p. 297-311.e4.

252. Jia, M.H., et al., *Global expression profiling of yeast treated with an inhibitor of amino acid biosynthesis, sulfometuron methyl.* Physiological Genomics, 2000. **3**(2): p. 83-92.

253. Masson, G.R., *Towards a model of GCN2 activation.* Biochem Soc Trans, 2019. **47**(5): p. 1481-1488.

254. Dong, J., et al., *Uncharged tRNA Activates GCN2 by Displacing the Protein Kinase Moiety from a Bipartite tRNA-Binding Domain.* Molecular Cell, 2000. **6**(2): p. 269-279.

255. Misra, J., et al., *Multiple mechanisms activate GCN2 eIF2 kinase in response to diverse stress conditions.* Nucleic Acids Research, 2024. **52**(4): p. 1830-1846.

256. Harding, H.P., et al., *The ribosomal P-stalk couples amino acid starvation to GCN2 activation in mammalian cells.* eLife, 2019. **8**: p. e50149.

257. Gupta, R. and A.G. Hinnebusch, *Differential requirements for P stalk components in activating yeast protein kinase Gcn2 by stalled ribosomes during stress.* Proceedings of the National Academy of Sciences, 2023. **120**(16): p. e2300521120.

258. Inglis, A.J., et al., *Activation of GCN2 by the ribosomal P-stalk.* Proc Natl Acad Sci U S A, 2019. **116**(11): p. 4946-4954.

259. Fedry, J., et al., *Visualization of translation reorganization upon persistent ribosome collision stress in mammalian cells.* Molecular Cell, 2024. **84**(6): p. 1078-1089.e4.

260. Pochopien, A.A., et al., *Structure of Gcn1 bound to stalled and colliding 80S ribosomes.* Proceedings of the National Academy of Sciences, 2021. **118**(14): p. e2022756118.

261. Matsuo, Y. and T. Inada, *The ribosome collision sensor Hel2 functions as preventive quality control in the secretory pathway.* Cell Reports, 2021. **34**(12).

262. Steffen, K.K., et al., *Yeast Life Span Extension by Depletion of 60S Ribosomal Subunits Is Mediated by Gcn4.* Cell, 2008. **133**(2): p. 292-302.

263. Shemer, R., et al., *Regulation of the Transcription Factor Gcn4 by Pho85 Cyclin Pcl5.* Molecular and Cellular Biology, 2002. **22**(15): p. 5395-5404.

264. Bömeke, K., et al., *Yeast Gcn4p Stabilization Is Initiated by the Dissociation of the Nuclear Pho85p/Pcl5p Complex.* Molecular Biology of the Cell, 2006. **17**(7): p. 2952-2962.

265. Wong, C.-M., et al., *Cooperation of Yeast Peroxiredoxins Tsa1p and Tsa2p in the Cellular Defense against Oxidative and Nitrosative Stress *.* Journal of Biological Chemistry, 2002. **277**(7): p. 5385-5394.

266. Wong, C.-M., et al., *Transcriptional regulation of yeast peroxiredoxin gene TSA2 through Hap1p, Rox1p, and Hap2/3/5p.* Free Radical Biology and Medicine, 2003. **34**(5): p. 585-597.

267. Galluzzi, L., T. Yamazaki, and G. Kroemer, *Linking cellular stress responses to systemic homeostasis.* Nat Rev Mol Cell Biol, 2018. **19**(11): p. 731-745.

268. Martins, D. and A.M. English, *Catalase activity is stimulated by H(2)O(2) in rich culture medium and is required for H(2)O(2) resistance and adaptation in yeast.* Redox Biol, 2014. **2**: p. 308-13.

269. Dever, T.E., *UsingGCN4as a Reporter of eIF2α Phosphorylation and Translational Regulation in Yeast.* Methods, 1997. **11**(4): p. 403-417.

270. Hoege, C., et al., *RAD6-dependent DNA repair is linked to modification of PCNA by ubiquitin and SUMO.* Nature, 2002. **419**(6903): p. 135-41.

271. Chatterjee, N. and W. Siede, *Replicating damaged DNA in eukaryotes.* Cold Spring Harb Perspect Biol, 2013. **5**(12): p. a019836.

272. Karras, G.I. and S. Jentsch, *The RAD6 DNA Damage Tolerance Pathway Operates Uncoupled from the Replication Fork and Is Functional Beyond S Phase.* Cell, 2010. **141**(2): p. 255-267.

273. Gallego-Sánchez, A., et al., *Reversal of PCNA Ubiquitylation by Ubp10 in Saccharomyces cerevisiae.* PLOS Genetics, 2012. **8**(7): p. e1002826.

274. Riepe, C., et al., *Double stranded DNA breaks and genome editing trigger loss of ribosomal protein RPS27A.* The FEBS Journal, 2022. **289**(11): p. 3101-3114.

275. Battelli, M.G., et al., *Xanthine Oxidoreductase-Derived Reactive Species: Physiological and Pathological Effects.* Oxid Med Cell Longev, 2016. **2016**: p. 3527579.

276. de Leeuw, N., et al., *UBE2A deficiency syndrome: Mild to severe intellectual disability accompanied by seizures, absent speech, urogenital, and skin anomalies in male patients.* Am J Med Genet A, 2010. **152a**(12): p. 3084-90.